ELECTRONIC AND SPECTRAL PROPERTIES OF PHOSPHONIUM YLIDES-BETAINES, DERIVATIVES OF 2-OXAZOLINE-5-ONE WITH CONJUGATED AND NON-CONJUGATED SUBSTITUENTS

Oleksandr Holovchenko[a], Antonina Naumenko[b], Roman Vydzhak[a], Esma Abdurakhmanova[a], Yaroslav Prostota[a], Oleksiy Kachkovsky[a] and Volodymyr Brovarets[a]*

The spectral and quantum-chemical studies of phosphonium ylides derivatives of 2-oxazoline-5-one with both conjugated and non-conjugated substituents were performed. It was found that considerable positive charge is located at phosphorus atom, whereas the substantial negative charge is fixed at sulphur atom. It has been found from the calculations and ^{13}C NMR spectral data that introducing of the non-conjugated and conjugated substituents in the position 2 of the oxazole cycle in thiaphosphonium ylides causes only small change in the molecular equilibrium geometry and in charge distribution in oxazole moiety, whereas spectral characteristics of substituted derivatives are very sensitive to the nature of the lowest electron transitions which reflects in changes of their absorption maxima.

* Corresponding Author
  Fax: +38044-573-25-52
  E-Mail: brovarets@bpci.kiev.ua
[a] Institute of Bioorganic Chemistry and Petrochemistry, National Academy of Sciences of Ukraine, 1 Murmanska Str., 02094 Kyiv, Ukraine
[b] Taras Shevchenko National University of Kyiv, 64/13 Volodymyrs'ka Str., 01601 Kyiv, Ukraine

INTRODUCTION

Phosphonium ylides of 2-oxazoline-5-one (PYOA) moiety are unique reagents in fine organic syntheses and enable ways to the broad range of novel stabilized compounds - all possible derivatives of azole.[1] So, it has resulted that the oxazole derivatives containing both positively charged PPh₃ group and, simultaneously, the exocyclic mono-coordinated oxygen or sulfur/selenium atom, bearing the negative charge formally; their general formulae can be presented by one neutral and two betainic structures: I-III,[2] as it is shown in Fig 1.
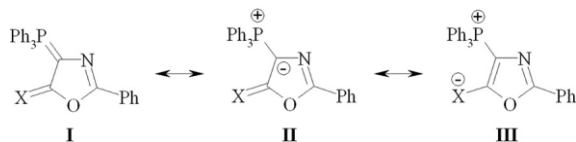
Figure 1. Canonical forms of PYOA.

The chemical constitution and some physical properties of 2-phenyl-2-oxazolin-5-one with X = O, S, Se were studied in details; so, it was shown that contribution of structure III with the separated charges decreases in the order, O > S > Se, whereas the dipole momentum increases regularly.

The ylide betaine molecules contain branched conjugated system and hence absorb the light in UV region at 340-370 nm. Earlier, it has been suggested that introduction of conjugated substituents at X causes an extension of the total π-electron system and should naturally be accompanied by a decrease in the gap energy resulting in a bathochromic shift of the absorbance band so that compounds become even colored.[3] On the other hand, the essential spectral effect can be reached upon introduction of highly polar substituents in the phenyl residue in 2-position of oxazole ring. Also, it is well known that an introduction of the mono-coordinated sulphur atom in the extensive π-electron system could promote the intersystem conversion from the singlet excited state to the triplet state, that is what happened upon going from the squaraine dyes to their thiaanalogues.[4] This paper incorporates the results of the spectral and quantum-chemical investigation of the electronic and spectral properties of phosphonium ylides and their sensitivity upon introduction of the simplest non-conjugated and conjugated substituents. A series of compounds, derivatives of phosphonium ylides of oxazole (**1**) has been studied (Figure 2). The reference virtual compound (**2**) was chosen as a model one for comparison with (**1**) in quantum-chemical calculations. Phosphonium ylides (**1**) were obtained from corresponding phosphonium salts (**4a-4l**).
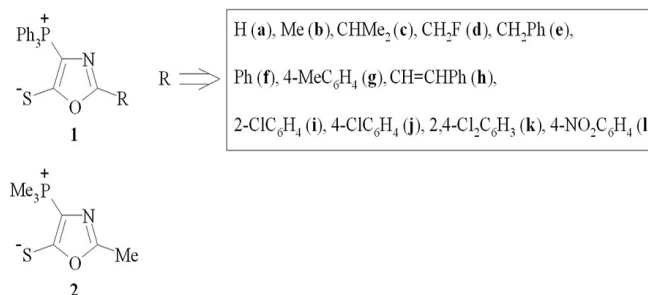
Figure 2. General structure of compound (**1**) and model reference molecule (**2**).

EXPERIMENTAL

^{1}H, ^{13}C, ^{31}P NMR spectra were obtained on a Bruker AVANCE DRX-500 spectrometer (TMS as internal reference or 85% phosphoric acid as external reference) in DMSO-d_6. IR spectra were recorded on a Vertex 70 spectrometer in KBr pellets.

GC-MS spectra were recorded on an LC-MS system - HPLC Agilent 1100 Series equipped with a diode array detector Agilent LC\MSD SL. Parameters of GC-MS analysis: Zorbax SB - C18 column (1.8 μm, 4.6 × 15 mm, PN 821975-932), solvent water – acetonitrile mixture (95 : 5), 0.1% of aqueous trifluoroacetic acid; eluent flow 3 mL min–1; injection volume 1 μL; UV detecting at 215, 254, 265 nm; chemical ionization at atmospheric pressure (APCI), scan range m/z 80 - 1000. UV-Vis absorption spectra were recorded on a Shimadzu UV-3100 spectrophotometer in toluene of spectral grade.

Elemental analysis was carried out in the Analytical Laboratory of the Institute of Bioorganic and Petrochemistry of the National Academy of Sciences of Ukraine by manual methods. The carbon and hydrogen contents were determined using the Pregl gravimetric method, while nitrogen was determined using the Duma's gasometrical micromethod. Sulfur was determined by the Scheininger titrimetric method, chlorine content was determined by the mercurometric method, phosphorus content was determined by the colorimetric method.[5] M. P. were determined on a Fisher–Johns apparatus and are uncorrected. Reactions and purity of the products were monitored by thin-layer chromatography on Silufol UV-254 plates using 9:1(v/v) chloroform–methanol as eluent. All reagents and solvents were purchased from Aldrich and used as received.

Quantum-Chemical Calculations

Optimized molecular geometry was performed by DFT/CAM-B3LYP//6-31(d,p) method. The electron transition characteristics were calculated by the non-empirical (TD/DFT/6-31G(d,p)/CAM-B3LYP) method using the package Gauss-03.[6] Certainly, there is not a perfect agreement of the calculated and experimental data but it is typical for such approach.[7-9] However the agreement is enough to analyze the nature of the electron transitions correctly.

Synthesis of 1-acylamino-2,2-dichloroethenyl triphenylphosphonium salts (general procedure)

Phosphonium salts (**4a-4l**) that are easily obtained from available N-(1,2,2,2-tetrachloroethyl)amides of carboxylic acids (**3a-3l**) were used in the synthesis of betaines (**1a-1l**).[10,11] To a solution of N-1,2,2,2-tetrachloroethylamides (0.01 mol) in 10 mL of dry benzene was added solution of triphenylphosphine (0.011 mol) in 5 mL of dry benzene. The mixture was heated at 70-80 °C for 2-3 h. Precipitates of compounds (**4a-4l**) were filtered, washed with THF, dried and analyzed without further purification. For the facilitation of identification chlorides (**4a-4c**), (**4f**), (**4g**) and (**4j**) were converted to corresponding perchlorates (**5a-5c**), (**5f**), (**5g**) and (**5j**) and analyzed without further purification. (Scheme 1).

Compounds (**4a**)-(**4l**) and (**5a-5c**), (**5f**), (**5g**) and (**5j**) are colourless crystalline substances soluble in methanol and sparingly soluble in water, THF, dichloromethane and benzene.
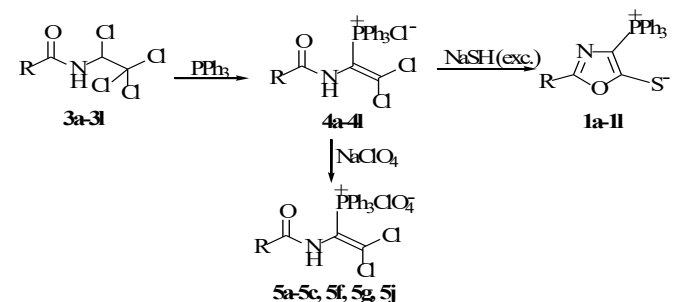
Scheme 1. Synthesis of 1-acylamino-2,2-dichloroethenyl triphenylphosphonium salts.

The structure and composition of phosphonium salts (**4a-4l** and **5a-5c**, **5f**, **5g** and **5j**) are in accordance with data of elemental analysis, ^{1}H, ^{13}C, ^{31}P NMR, IR spectroscopy and mass-spectrometry. Signals of NH proton in the ^{1}H NMR spectra of compounds **4d**, **4e**, **4h**, **4i**, **4k** and **4l** appeared as a singlet at 11.26 - 12.56 ppm, while the same signal of correspondent perchlorates (**5a-5c**, **5f**, **5g** and **5j**) ranging from 10.32 to 10.86 ppm. The signals of protons belong to CH_3 (**5b**), CH_2 and CH (**5c**) groups were shifted to the more strong field and appeared as singlet at 1.54 ppm (**5b**), 3.24 ppm, doublet at 4.54 ppm (splitted on F atom with coupling constant 46.2 Hz) in (**4d**) and multiplet ranging from 2.11 to 2.23 ppm in (**5c**).

Particular attention is to be paid to ^{13}C NMR data. The most typical resonances were signals of carbons in dichloroethenyl fragment appearing as doublets due to the interaction with the phosphorus nuclei. Thus, the signals of carbon nuclei (α-C) P–C=CCl_2 appeared in the range 119.5 - 121.5 ppm (with coupling constant 103.7 - 105.7 Hz), the signals of carbon nuclei (β-C) P–C=CCl_2 revealed in the range 142.5 - 145.5 ppm (coupling constant 27.4 - 31.4 Hz). The signals of phosphorus nuclei in ^{31}P NMR spectra of compounds **4d**, **4e**, **4h**, **4i**, **4k** and **4l** and **5a-5c**, **5f**, **5g** and **5j** were observed in the range of 23.7 - 24.7 ppm.

The intensive absorption bands of amide C=O bond appeared at 1659-1705 cm^{-1} in the IR spectra of compounds **4d**, **4e**, **4h**, **4i**, **4k** and **4l** and **5a-5c**, **5f**, **5g** and **5j**. Also, the broad intensive bands at 1102 – 1106 cm^{-1} correspond to perchlorate anion of **5a-5c**, **5f**, **5g** and **5j** were observed.

Synthesis of [2-R-4-(triphenylphosphoniumyl)-1,3-oxazol-5-yl]sulfanides

Dichloroenamides (**4a-4l**) reacted with an excess of sodium hydrosulfide in methanol stirred at ambient temperature for a 24 h giving betaines (**1a-1l**) which crystallized out from reaction mixtures in high yields. The conversion of phosphonic salts (**4a-4l**) to betaines (**1a-1l**) is monitored using ^{1}H, ^{13}C, ^{31}P NMR and IR spectroscopy. Thus, in the ^{1}H NMR spectra of (**1a-1l**) the NH proton

signal disappeared whereas the signal of CH$_3$ protons of **1d** revealed as singlet at 2.22 ppm, which indicated the formation of heterocyclic ring where a methyl group directly connected to cyclic fragment.[12] Signals of CH$_2$ groups in **1d** and **1e** and methine proton in **1c** shifted to more weak field and appeared as singlet at 3.94 ppm in **1e**, as a doublet splitted on interaction with F atom with coupling constant 48.0 Hz at 5.23 ppm in **1d** and multiplet ranged from 2.92 to 2.80 ppm in **1c**. The ^{13}C NMR spectra where signals of carbon nuclei of oxazole ring appeared as doublets due to the interaction with phosphorus nuclei are indicative for the confirmation of the ring formation. Thus, C(5) carbon atom signals were observed at 183.5 - 185.0 ppm (coupling constant 31.5 - 33.0 Hz), signals of C(4) carbon atoms appeared at 103.1 - 108.3 ppm (coupling constant 150.6 - 153.3 Hz), signals C(2) atoms of **1a-1c** and **1e-1l** were observed in range of 150.3 - 165.8 ppm (coupling constant 20.5 - 22.9 Hz), while that of **1d** as doublet (splitted on P atom with coupling constant 22.7 Hz and on F atom with coupling constant 18.3 Hz). The signals of phosphorus nuclei in the ^{31}P NMR spectra of **1a-1l** were observed at 12.4 - 13.1 ppm. On the other hand the absorption bands correspond to the carbonyl group in their IR spectra disappeared.

2,2-Dichloro-1-(2-fluoroacetamido)ethenyl]triphenylphos-phonium chloride (**4d**) *was* obtained from 2-fluoro-N-(1,2,2,2-tetrachloroethyl)acetamide (**3d**).[13] Yield 3.80 g (81 %); m.p. 194-196 °C. ^{1}H NMR (400 MHz, DMSO-d$_6$): δ = 11.24 (s, 1 H, NH), 7.99 - 7.88 (m, 9 H, PC$_6$H$_5$), 7.86 – 7.77 (m, 6 H, PC$_6$H$_5$), 4.54 (d, [2]*J*(F,C) = 46.2 Hz, 2 H, CH$_2$) ppm. ^{13}C NMR (100.6 MHz, DMSO-d$_6$): δ = 170.6 (d, [2]*J*(F,C) = 19.8 Hz, C=O), 145.4 (d, [2]*J*(P,C) = 29.3 Hz, C-β enamide), 136.0 (d, [4]*J*(P,C) = 2.9 Hz, C-4 PC$_6$H$_5$), 135.0 (d, [3]*J*(P,C) = 11.0 Hz, C-3, C-5 PC$_6$H$_5$), 130.8 (d, [2]*J*(P,C) = 13.2 Hz, C-2, C-6 PC$_6$H$_5$), 119.9 (d, [1]*J*(P,C) = 105.6 Hz, C-α enamide), 116.5 (d, [1]*J*(P,C) = 89.5 Hz, C-1 PC$_6$H$_5$), 79.8 (d, [1]*J*(F,C) = 181.9 Hz, CH$_2$) ppm. ^{31}P NMR (202.4 MHz, DMSO-d$_6$): δ = 24.4 ppm. IR (KBr): ν = 3054 (br), 2555 (br), 1705, 1554, 1513 1482, 1437, 1238, 1164, 1104, 1064, 964, 755, 722, 688, 520 cm^{-1}. LCMS: [M+H-M(An$^-$)]$^+$ = 432.0, 434.1. C$_{22}$H$_{18}$Cl$_3$FNOP (468.715): calcd. C 56.37, H 3.87, Cl 22.69, N 2.99, P 6.61; found C 56.16, H 4.14, Cl 22.83, N 3.20, P 6.47.

2,2-Dichloro-1-(2-phenylacetamido)ethenyl]triphenyl-phosphonium chloride (**4e**) was obtained from 2-phenyl-N-(1,2,2,2-tetrachloroethyl)acetamide (**3e**).[14] Yield 4.59 g (87 %); m.p. 205-207 °C. ^{1}H NMR (400 MHz, DMSO-d$_6$): δ = 11.72 (s, 1 H, NH), 7.99 - 7.88 (m, 9 H, PC$_6$H$_5$), 7.86 – 7.77 (m, 6 H, PC$_6$H$_5$), 7.25 – 7.16 (m, 3 H, C$_6$H$_5$), 6.97 – 6.87 (m, 2 H, C$_6$H$_5$), 3.24 (s, 2 H, CH$_2$) ppm. ^{13}C NMR (100.6 MHz, DMSO-d$_6$): δ = 171.6 (C=O), 144.1 (d, [2]*J*(P,C) = 30.4 Hz, C-β enamide), 135.8 (d, [4]*J*(P,C) = 3.0 Hz, C-4 PC$_6$H$_5$), 134.9 (d, [3]*J*(P,C) = 10.5 Hz, C-3, C-5 PC$_6$H$_5$), 134.5 (C$_6$H$_5$), 130.7 (d, [2]*J*(P,C) = 13.0 Hz, C-2, C-6 PC$_6$H$_5$), 129.7 (C$_6$H$_5$), 128.7 (C$_6$H$_5$), 127.1 (C$_6$H$_5$), 121.5 (d, [1]*J*(P,C) = 104.2 Hz, C-α enamide), 116.9 (d, [1]*J*(P,C) = 89.3 Hz, C-1 PC$_6$H$_5$), 41.2 (CH$_2$) ppm. ^{31}P NMR (202.4 MHz, DMSO-d$_6$): δ = 23.7 ppm. IR (KBr): ν = 3014 (br), 2686 (br), 1671, 1554, 1488, 1435, 1315, 1248, 1179, 1137, 1102, 959, 758, 721, 688, 556, 494 cm^{-1}. LCMS: [M+H-M(An$^-$)]$^+$ = 490.0, 492.0. C$_{28}$H$_{23}$Cl$_3$NOP (526.820): calcd. C 63.84, H 4.40, Cl 20.19, N 2.66, P 5.88; found C 63.61, H 4.55, Cl 20.33, N 2.89, P 5.79.

{2,2-Dichloro-1-[(2E)-3-phenylprop-2-enamido]ethenyl}-triphenylphosphonium chloride (**4h**) was obtained from (2E)-3-phenyl-N-(1,2,2,2-tetrachloroethyl)prop-2-enamide (**3h**).[15] Yield 3.81 g (71 %); m.p. 163-165 °C. ^{1}H NMR (400 MHz, DMSO-d$_6$): δ = 11.58 (s, 1 H, NH), 8.04 - 7.93 (m, 6 H, PC$_6$H$_5$), 7.92 – 7.84 (m, 3 H, PC$_6$H$_5$), 7.82 – 7.70 (m, 6 H, PC$_6$H$_5$), 7.51 – 7.45 (m, 2 H, C$_6$H$_5$), 7.43 – 7.34 (m, 3 H, C$_6$H$_5$), 7.28 (d,[3]*J*(H,H)= 15.9 Hz, 1 H, CH=CH), 6.46 (d,[3]*J*(H,H)= 15.9 Hz, 1 H, CH=CH) ppm. ^{13}C NMR (100.6 MHz, DMSO-d$_6$): δ = 166.1 (C=O), 143.9 (d, [2]*J*(P,C) = 31.4 Hz, C-β enamide), 142.5 (CH=CHC$_6$H$_5$), 135.7 (d, [4]*J*(P,C) = 2.5 Hz, C-4 PC$_6$H$_5$), 135.0 (d, [3]*J*(P,C) = 11.0 Hz, C-3, C-5 PC$_6$H$_5$), 134.4 (CH=CHC$_6$H$_5$), 130.8 (CH=CHC$_6$H$_5$), 130.6 (d, [2]*J*(P,C) = 13.0 Hz, C-2, C-6 PC$_6$H$_5$), 129.5 (CH=CHC$_6$H$_5$), 128.4 (CH=CHC$_6$H$_5$), 121.6 (d, [1]*J*(P,C) = 103.7 Hz, C-α enamide), 119.0 (CH=CHC$_6$H$_5$), 117.0 (d, [1]*J*(P,C) = 89.8 Hz, C-1 PC$_6$H$_5$) ppm. ^{31}P NMR (202.4 MHz, DMSO-d$_6$): δ = 24.0 ppm. IR (KBr): ν = 3417(br), 3055(br), 2794 (br), 1663, 1625, 1560, 1481, 1437, 1333, 1205, 1152, 1104, 953, 753, 725, 689, 522 cm^{-1}. LCMS: [M+H-M(An$^-$)]$^+$ = 502.0, 504.0. C$_{29}$H$_{23}$Cl$_3$NOP (538.831): calcd. C 64.64, H 4.30, Cl 19.74, N 2.60, P 5.75; found C 64.78, H 4.32, Cl 19.63, N 2.71, P 5.59.

{2,2-Dichloro-1-[(2-chlorophenyl)formamido]ethenyl}tri-phenylphosphonium chloride (**4i**) was obtained from 2-chloro-N-(1,2,2,2-tetrachloroethyl)benzamide (**3i**).[16,17] Yield 4.87 g (89 %); m.p. 192-195 °C. ^{1}H NMR (400 MHz, DMSO-d$_6$): δ = 11.51 (s, 1 H, NH), 8.05 - 7.90 (m, 9 H, PC$_6$H$_5$), 7.87 – 7.77 (m, 6 H, PC$_6$H$_5$), 7.49-7.43 (m, 2 H, 2-ClC$_6$H$_4$), 7.32-7.25 (m, 1 H, 2-ClC$_6$H$_4$), 6.75 (d,[3]*J*(H,H)= 7.8 Hz, 1 H, 2-ClC$_6$H$_4$) ppm. ^{13}C NMR (100.6 MHz, DMSO-d$_6$): δ = 166.6 (C=O), 145.5 (d, [2]*J*(P,C) = 28.9 Hz, C-β enamide), 135.9 (d, [4]*J*(P,C) = 3.0 Hz, C-4 PC$_6$H$_5$), 135.1 (d, [3]*J*(P,C) = 11.0 Hz, C-3, C-5 PC$_6$H$_5$), 133.2 (2-ClC$_6$H$_4$), 132.9 (2-ClC$_6$H$_4$), 131.0 (2-ClC$_6$H$_4$), 130.8 (d, [2]*J*(P,C) = 13.0 Hz, C-2, C-6 PC$_6$H$_5$), 130.8 (2-ClC$_6$H$_4$), 129.5 (2-ClC$_6$H$_4$), 127.4 (2-ClC$_6$H$_4$), 120.7 (d, [1]*J*(P,C) = 104.7 Hz, C-α enamide), 116.9 (d, [1]*J*(P,C) = 90.3 Hz, C-1 PC$_6$H$_5$) ppm. ^{31}P NMR (202.4 MHz, DMSO-d$_6$): δ = 24.3 ppm. IR (KBr): ν = 3500 (br), 3048 (br), 2708 (br), 1669, 1556, 1484, 1437, 1294, 1257, 1105, 954, 727, 689, 520, 495 cm^{-1}. LCMS: [M+H-M(An$^-$)]$^+$ = 512.1, 513.0. C$_{27}$H$_{20}$Cl$_4$NOP (547.238): calcd. C, calcd. H, calcd. C 59.26, H 3.68, Cl 25.91, N 2.56, P 5.66; found C 59.18, H 3.82, Cl 25.69, N 2.47, P 5.56.

{2,2-Dichloro-1-[(2,4-dichlorophenyl)formamido]ethe-nyl}triphenylphosphonium chloride (**4k**) was obtained from 2,4-dichloro-N-(1,2,2,2-tetrachloroethyl)benzamide (**3k**).[18] Yield 5.29 g (91 %); m.p. 189-191 °C. ^{1}H NMR (400 MHz, DMSO-d$_6$): δ = 12.02 (s, 1 H, NH), 8.02 - 7.98 (m, 6 H, PC$_6$H$_5$), 7.97 - 7.89 (m, 3 H, PC$_6$H$_5$), 7.87 – 7.76 (m, 6 H, PC$_6$H$_5$), 7.66 (d,[4]*J*(H,H)= 1.4 Hz, 1 H, 2,4-Cl$_2$C$_6$H$_3$), 7.42 (dd,[3]*J*(H,H)= 8.4 Hz, [4]*J*(H,H)= 1.4 Hz, 1 H, 2,4-Cl$_2$C$_6$H$_4$), 6.87 (d,[3]*J*(H,H)= 8.4 Hz, 1 H, 2,4-Cl$_2$C$_6$H$_3$) ppm. ^{13}C NMR (100.6 MHz, DMSO-d$_6$): δ = 165.7 (C=O), 145.4 (d, [2]*J*(P,C) = 28.9 Hz, C-β enamide), 136.8 (2,4-Cl$_2$C$_6$H$_3$), 135.9 (d, [4]*J*(P,C) = 2.5 Hz, C-4 PC$_6$H$_5$), 135.1 (d, [3]*J*(P,C) = 11.0 Hz, C-3, C-5 PC$_6$H$_5$), 132.5 (2,4-Cl$_2$C$_6$H$_3$), 131.9 (2,4-Cl$_2$C$_6$H$_3$), 131.0 (2,4-Cl$_2$C$_6$H$_3$), 130.8 (d, [2]*J*(P,C) = 13.0 Hz, C-2, C-6 PC$_6$H$_5$), 130.4 (2,4-Cl$_2$C$_6$H$_3$), 127.6 (2,4-Cl$_2$C$_6$H$_3$), 120.7 (d, [1]*J*(P,C) = 104.7 Hz, C-α enamide), 116.8 (d, [1]*J*(P,C) = 89.8 Hz, C-1 PC$_6$H$_5$) ppm.

^{31}P NMR (202.4 MHz, DMSO-d$_6$): δ = 24.1 ppm. IR (KBr): ν = 3458 (br), 3036 (br), 2713 (br), 1670, 1583, 1550, 1438, 1249, 1192, 1107, 958, 903, 854, 798, 763, 727, 690, 582, 562, 528, 450 cm^{-1}. LCMS: [M+H-M(An$^-$)]$^+$ = 512.1, 513.0. C$_{27}$H$_{19}$Cl$_5$NOP (581.683): calcd. C, calcd. H, calcd. C 55.75, H 3.29, Cl 30.47, N 2.41, P 5.32; found C 55.58, H 3.42, Cl 30.69, N 2.63, P 5.17.

{2,2-Dichloro-1-[(4-nitrophenyl)formamido]ethenyl}tri-phenylphosphonium chloride (**4l**) was obtained from 4-nitro-N-(1,2,2,2-tetrachloroethyl)benzamide (**3l**).[17] Yield 5.12 g (92 %); m.p. 206-208 °C. ^{1}H NMR (400 MHz, DMSO-d$_6$): δ = 12.56 (s, 1 H, NH), 8.21 (d,^{3}J(H,H)= 8.4 Hz, 2 H, 4-NO$_2$C$_6$H$_4$), 8.13 - 7.96 (m, 8 H, PC$_6$H$_5$, 4-NO$_2$C$_6$H$_4$), 7.91 – 7.82 (m, 3 H, PC$_6$H$_5$), 7.81 – 7.69 (m, 6 H, PC$_6$H$_5$), ppm. ^{13}C NMR (100.6 MHz, DMSO-d$_6$): δ = 165.5 (C=O), 150.2 (4-NO$_2$C$_6$H$_4$), 144.7 (d, ^{2}J(P,C) = 29.4 Hz, C-β enamide), 137.0 (4-NO$_2$C$_6$H$_4$), 135.8 (d, ^{4}J(P,C) = 2.5 Hz, C-4 PC$_6$H$_5$), 135.1 (d, ^{3}J(P,C) = 10.5 Hz, C-3, C-5 PC$_6$H$_5$), 130.6 (d, ^{2}J(P,C) = 13.5 Hz, C-2, C-6 PC$_6$H$_5$), 129.8 (4-NO$_2$C$_6$H$_4$), 124.0 (4-NO$_2$C$_6$H$_4$), 121.4 (d, ^{1}J(P,C) = 105.2 Hz, C-α enamide), 116.7 (d, ^{1}J(P,C) = 88.8 Hz, C-1 PC$_6$H$_5$) ppm. ^{31}P NMR (202.4 MHz, DMSO-d$_6$): δ = 24.2 ppm. IR (KBr): ν = 3437 (br), 3054 (br), 1669, 1563, 1517, 1476, 1438, 1345, 1278, 1105, 952, 755, 723, 689, 520, 498 cm^{-1}. LCMS: [M+H-M(An$^-$)]$^+$ = 521.1, 523.0. C$_{27}$H$_{20}$Cl$_3$N$_2$O$_3$P (557.791): calcd. C, calcd. H, calcd. C 58.14, H 3.61, Cl 19.07, N 5.02, P 5.55; found C 58.31, H 3.48, Cl 19.01, N 5.33, P 5.31.

(2,2-Dichloro-1-formamidoethenyl)triphenylphosphonium perchlorate (**5a**) Yield 3.65 g (73 %); m.p. 202-204 °C. ^{1}H NMR (400 MHz, DMSO-d$_6$): δ = 10.32 (s, 1 H, NH), 8.06 - 7.75 (m, 16 H, CH, PC$_6$H$_5$), ppm. ^{13}C NMR (100.6 MHz, DMSO-d$_6$): δ = 162.1 (C=O), 145.0 (d, ^{2}J(P,C) = 27.4 Hz, C-β enamide), 136.0 (C-4 PC$_6$H$_5$), 134.9 (d, ^{3}J(P,C) = 11.0 Hz, C-3, C-5 PC$_6$H$_5$), 130.8 (d, ^{2}J(P,C) = 13.0 Hz, C-2, C-6 PC$_6$H$_5$), 119.8 (d, ^{1}J(P,C) = 105.7 Hz, C-α enamide), 116.6 (d, ^{1}J(P,C) = 89.3 Hz, C-1 PC$_6$H$_5$) ppm. ^{31}P NMR (202.4 MHz, DMSO-d$_6$): δ = 24.2 ppm. IR (KBr): ν = 3222 (br), 1698, 1553, 1480, 1437, 1106 (br), 954, 861, 750, 724, 688, 621, 547, 522, 498, 471 cm^{-1}. LCMS: [M+H-M(An$^-$)]$^+$ = 400.0, 402.0. C$_{21}$H$_{17}$Cl$_3$NO$_5$P (500.695): calcd. C 50.37, H 3.42, Cl 21.24, N 2.80, P 6.19; found C 50.61, H 3.21, Cl 21.33, N 3.05, P 6.12.

(2,2-Dichloro-1-acetamidoethenyl)triphenylphosphonium perchlorate (**5b**) Yield 4.02 g (78 %); m.p. 208-210 °C (205-205 °C).[19] ^{1}H NMR (400 MHz, DMSO-d$_6$): δ = 10.32 (s, 1 H, NH), 7.99 - 7.92 (m, 3 H, PC$_6$H$_5$), 7.91 – 7.79 (m, 12 H, PC$_6$H$_5$), 1.54 (s, 3 H, CH$_3$) ppm. ^{13}C NMR (100.6 MHz, DMSO-d$_6$): δ = 170.6 (C=O), 143.9 (d, ^{2}J(P,C) = 30.8 Hz, C-β enamide), 135.8 (d, ^{4}J(P,C) = 2.9 Hz, C-4 PC$_6$H$_5$), 135.0 (d, ^{3}J(P,C) = 11.0 Hz, C-3, C-5 PC$_6$H$_5$), 130.7 (d, ^{2}J(P,C) = 13.2 Hz, C-2, C-6 PC$_6$H$_5$), 121.6 (d, ^{1}J(P,C) = 104.5 Hz, C-α enamide), 117.0 (d, ^{1}J(P,C) = 89.5 Hz, C-1 PC$_6$H$_5$) ppm. ^{31}P NMR (202.4 MHz, DMSO-d$_6$): δ = 24.5 ppm. IR (KBr): ν = 3500 (br), 1666 (br), 1556, 1440, 1277, 1190, 1106 (br), 980, 751, 727, 689, 623, 521, 499 cm^{-1}. LCMS: [M+H-M(An$^-$)]$^+$ = 414.0, 416.0. C$_{22}$H$_{19}$Cl$_3$NO$_5$P (514.722): calcd. C 51.34, H 3.72, Cl 20.66, N 2.72, P 6.02; found C 51.18, H 3.85, Cl 20.81, N 3.01, P 6.21.

2,2-Dichloro-1-(2-methylpropanamido) ethenyl]triphenyl-phosphonium perchlorate (**5c**) Yield 3.84 g (71 %); m.p. 204-206 °C. ^{1}H NMR (400 MHz, DMSO-d$_6$): δ = 10.69 (s, 1

H, NH), 7.98 - 7.87 (m, 9 H, PC$_6$H$_5$), 7.85 – 7.76 (m, 6 H, PC$_6$H$_5$), 2.23 – 2.11 (m, 1 H, CH), 0.68 (d, 3J(H,H) = 4 Hz, 6 H, 2 CH$_3$) ppm. ^{13}C NMR (100.6 MHz, DMSO-d$_6$): δ = 177.4 (C=O), 144.1 (d, ^{2}J(P,C) = 30.4 Hz, C-β enamide), 135.8 (d, ^{4}J(P,C) = 2.5 Hz, C-4 PC$_6$H$_5$), 135.0 (d, ^{3}J(P,C) = 10.5 Hz, C-3, C-5 PC$_6$H$_5$), 130.1 (d, ^{2}J(P,C) = 13.0 Hz, C-2, C-6 PC$_6$H$_5$), 121.3 (d, ^{1}J(P,C) = 105.2 Hz, C-α enamide), 116.9 (d, ^{1}J(P,C) = 89.8 Hz, C-1 PC$_6$H$_5$), 34.1 (CH), 18.9 (CH$_3$) ppm. ^{31}P NMR (202.4 MHz, DMSO-d$_6$): δ = 24.1 ppm. IR (KBr): ν = 3269 (br), 1682 (br), 1558, 1483, 1440, 1217, 1191, 1103 (br), 997, 970, 935, 756, 718, 689, 624, 525, 514, 493 cm^{-1}. LCMS: [M+H-M(An$^-$)]$^+$ = 442.0, 444.0. C$_{24}$H$_{23}$Cl$_3$NO$_5$P (542.775): calcd. C 53.11, H 4.27, Cl 19.60, N 2.58, P 5.71; found C 53.38, H 4.41, Cl 19.48, N 2.81, P 5.59.

2,2-Dichloro-1-(phenylformamido)ethenyl]triphenylphos-phonium perchlorate (**5f**) Yield 4.90 g (85 %); m.p. 228-230 °C. ^{1}H NMR (400 MHz, DMSO-d$_6$): δ = 10.73 (s, 1 H, NH), 7.99 - 7.86 (m, 9 H, PC$_6$H$_5$), 7.83 – 7.75 (m, 6 H, PC$_6$H$_5$), 7.57 (t,^{3}J(H,H)= 7.0 Hz, 1 H, C$_6$H$_5$), 7.51 (d,^{3}J(H,H)= 7.5 Hz, 2 H, C$_6$H$_5$), 7.46 – 7.40 (m, 2 H, C$_6$H$_5$) ppm. ^{13}C NMR (100.6 MHz, DMSO-d$_6$): δ = 167.6 (C=O), 145.0 (d, ^{2}J(P,C) = 29.4 Hz, C-β enamide), 136.0 (d, ^{4}J(P,C) = 3.0 Hz, C-4 PC$_6$H$_5$), 134.9 (d, ^{3}J(P,C) = 11.0 Hz, C-3, C-5 PC$_6$H$_5$), 133.5 (C$_6$H$_5$), 131.7 (C$_6$H$_5$), 130.8 (d, ^{2}J(P,C) = 13.0 Hz, C-2, C-6 PC$_6$H$_5$), 129.2 (C$_6$H$_5$), 127.9 (C$_6$H$_5$), 121.3 (d, ^{1}J(P,C) = 104.7 Hz, C-α enamide), 116.8 (d, ^{1}J(P,C) = 89.8 Hz, C-1 PC$_6$H$_5$) ppm. ^{31}P NMR (202.4 MHz, DMSO-d$_6$): δ = 24.7 ppm. IR (KBr): ν = 3239 (br), 1659, 1564, 1506, 1469, 1449, 1275, 1104 (br), 996, 961, 751, 717, 687, 622, 522 cm^{-1}. LCMS: [M+H-M(An$^-$)]$^+$ = 476.1, 478.0. C$_{27}$H$_{21}$Cl$_3$NO$_5$P (576.791): calcd. C 56.22, H 3.67, Cl 18.44, N 2.43, P 5.37; found C 56.38, H 3.78, Cl 18.29, N 2.61, P 5.19.

{2,2-Dichloro-1-[(4-methylphenyl)formamido]ethenyl}-triphenylphosphonium perchlorate (**5g**). Yield 4.84 g (84 %); m.p. 232-234 °C. ^{1}H NMR (400 MHz, DMSO-d$_6$): δ = 10.65 (s, 1 H, NH), 8.01 - 7.85 (m, 9 H, PC$_6$H$_5$), 7.83 – 7.73 (m, 6 H, PC$_6$H$_5$), 7.42 (d,^{3}J(H,H)= 7.5 Hz, 2 H, 4-CH$_3$C$_6$H$_4$), 7.24 (d,^{3}J(H,H)= 7.5 Hz, 2 H, 4-CH$_3$C$_6$H$_4$), 2.32 (s, 3 H, CH$_3$) ppm. ^{13}C NMR (100.6 MHz, DMSO-d$_6$): δ = 167.0 (C=O), 144.8 (d, ^{2}J(P,C) = 29.9 Hz, C-β enamide), 143.6 (4-CH$_3$C$_6$H$_4$), 135.9 (d, ^{4}J(P,C) = 2.5 Hz, C-4 PC$_6$H$_5$), 134.9 (d, ^{3}J(P,C) = 11.0 Hz, C-3, C-5 PC$_6$H$_5$), 130.7 (d, ^{2}J(P,C) = 13.0 Hz, C-2, C-6 PC$_6$H$_5$), 129.6 (4-CH$_3$C$_6$H$_4$), 128.9 (4-CH$_3$C$_6$H$_4$), 127.8 (4-CH$_3$C$_6$H$_4$), 121.4 (d, ^{1}J(P,C) = 105.2 Hz, C-α enamide), 116.8 (d, ^{1}J(P,C) = 88.8 Hz, C-1 PC$_6$H$_5$), 21.5 (CH$_3$) ppm. ^{31}P NMR (202.4 MHz, DMSO-d$_6$): δ = 24.6 ppm. IR (KBr): ν = 3202 (br), 1660, 1559, 1480, 1439, 1277, 1192, 1105 (br), 962, 750, 723, 689, 621, 521 cm^{-1}. LCMS: [M+H-M(An$^-$)]$^+$ = 490.0, 492.0. C$_{28}$H$_{23}$Cl$_3$NO$_5$P (590.818): calcd. C 56.92, H 3.92, Cl 18.00, N 2.37, P 5.24; found C 60.18, H 4.17, Cl 17.87, N 2.43, P 5.13.

{2,2-Dichloro-1-[(4-chlorophenyl)formamido]ethenyl}tri-phenylphosphonium perchlorate (j). Yield 4.84 g (89 %); m.p. 225-227 °C. ^{1}H NMR (400 MHz, DMSO-d$_6$): δ = 10.86 (s, 1 H, NH), 8.02 - 7.86 (m, 9 H, PC$_6$H$_5$), 7.85 – 7.75 (m, 6 H, PC$_6$H$_5$), 7.55 (s, 4 H, 4-ClC$_6$H$_4$) ppm. ^{13}C NMR (100.6 MHz, DMSO-d$_6$): δ = 166.1 (C=O), 145.2 (d, ^{2}J(P,C) = 29.4 Hz, C-β enamide), 138.2 (4-ClC$_6$H$_4$), 136.0 (d, ^{4}J(P,C) = 2.5 Hz, C-4 PC$_6$H$_5$), 134.9 (d, ^{3}J(P,C) = 11.0 Hz, C-3, C-5 PC$_6$H$_5$), 130.8 (d, ^{2}J(P,C) = 13.0 Hz, C-2, C-6 PC$_6$H$_5$), 130.3 (4-ClC$_6$H$_4$), 129.6 (4-ClC$_6$H$_4$), 128.3 (4-ClC$_6$H$_4$), 120.9 (d,

^1J(P,C) = 105.7 Hz, C-α enamide), 116.6 (d, ^1J(P,C) = 89.8 Hz, C-1 PC$_6$H$_5$) ppm. ^{31}P NMR (202.4 MHz, DMSO-d$_6$): δ = 24.7 ppm. IR (KBr): ν = 3271 (br), 1670, 1556, 1464, 1440, 1269, 1194, 1102 (br), 964, 755, 724, 690, 622, 527 cm^{-1}. LCMS: [M+H-M(An$^-$)]$^+$ = 512.0, 513.0. C$_{27}$H$_{20}$Cl$_4$NO$_5$P (611.236): calcd. C 53.05, H 3.30, Cl 23.20, N 2.29, P 5.07; found C 53.21, H 3.49, Cl 23.08, N 2.33, P 5.01.

Synthesis of [2-*R*-4-(Triphenylphosphoniumyl)-1,3-oxazol-5-yl]sulfanides (1a)-(1l) (General Procedure)

To a solution of 1-acylamino-2,2-dichloroethenyltriphenylphosphonium chlorides (0.01 mol) in 10 mL of methanol, a solution of NaSH (0.035 mol) in 50 mL of methanol was added. The mixture kept at 20-25 °C for 24 h. The residue formed was filtered, washed with water and dried in vaccuo over phosphorus pentoxide in vacuum desiccator. Analytically pure samples were obtained after recrystallization from methanol.

[4-(Triphenylphosphoniumyl)-1,3-oxazol-5-yl]sulfanide (**1a**) was obtained from (2,2-dichloro-1-formamido)-ethenyltriphenylphosphonium chloride (**4a**). Yield 3.21 g (89 %); m.p. 192 - 194 °C. ^{1}H NMR (400 MHz, DMSO-d$_6$): δ = 8.01 (d, ^4J(P,H) = 2.0 Hz, 1 H, 2-H oxazole), 7.82 - 7.75 (m, 3 H, PC$_6$H$_5$), 7.74 - 7.62 (m, 12 H, PC$_6$H$_5$) ppm. ^{13}C NMR (100.6 MHz, DMSO-d$_6$): δ = 183.5 (d, ^2J(P,C) = 32.9 Hz, C-5 oxazole), 150.3 (d, ^3J(P,C) = 21.9 Hz, C-2 oxazole), 134.5 (d, ^3J(P,C) = 10.5 Hz, C-3, C-5 PC$_6$H$_5$), 134.4 (C-4 PC$_6$H$_5$), 130.0 (d, ^2J(P,C) = 13.0 Hz, C-2, C-6 PC$_6$H$_5$), 120.8 (d, ^1J(P,C) = 92.4 Hz, C-1 PC$_6$H$_5$), 103.5 (d, ^1J(P,C) = 152.7 Hz, C-4 oxazole) ppm. ^{31}P NMR (202.4 MHz, DMSO-d$_6$): δ = 13.1 ppm. IR (KBr): ν = 1437, 1396 (br), 1110, 1047, 722, 689, 573, 517 cm^{-1}. LCMS: [M+H]$^+$ = 362.2. C$_{21}$H$_{16}$NOPS (361.398): calcd. C 69.79, H 4.46, N 3.88, P 8.57, S 8.87; found C 69.96, H 4.67, N 4.03, P 8.65, S 8.62.

[2-Methyl-4-(triphenylphosphoniumyl)-1,3-oxazol-5-yl]-sulfanide (**1b**) was obtained from (1-acetamido-2,2-dichloroethenyl)triphenylphosphonium chloride (**4b**). Yield 3.42 g (91 %); m.p. 219 - 220 °C (184-186 °C).[10] ^{1}H NMR (400 MHz, DMSO-d$_6$): δ = 7.82 - 7.60 (m, 15 H, PC$_6$H$_5$), 2.22 (s, 3 H, CH3) ppm. ^{13}C NMR (100.6 MHz, DMSO-d$_6$): δ = 183.6 (d, ^2J(P,C) = 32.3 Hz, C-5 oxazole), 158.6 (d, ^3J(P,C) = 22.7 Hz, C-2 oxazole), 134.5 (d, ^3J(P,C) = 10.3 Hz, C-3, C-5 PC$_6$H$_5$), 134.3 (d, ^4J(P,C) = 2.9 Hz, C-4 PC$_6$H$_5$), 129.9 (d, ^2J(P,C) = 13.2 Hz, C-2, C-6 PC$_6$H$_5$), 121.1 (d, ^1J(P,C) = 93.9 Hz, C-1 PC$_6$H$_5$), 103.4 (d, ^1J(P,C) = 153.3 Hz, C-4 oxazole) ppm. ^{31}P NMR (202.4 MHz, DMSO-d$_6$): δ = 12.4 ppm. IR (KBr): ν = 1599, 1438, 1397 (br), 1109,1074, 1030, 756, 690, 560, 517, 497 cm^{-1}. LCMS: [M+H]$^+$ = 376.2. C$_{22}$H$_{18}$NOPS (375.424): calcd. C 70.38, H 4.83, N 3.73, P 8.25, S 8.54; found C 70.12, H 4.98, N 3.98, P 8.37, S 8.67.

[2-(Propan-2-yl)-4-(triphenylphosphoniumyl)-1,3-oxazol-5-yl]sulfanide (**1c**) was obtained from [2,2-dichloro-1-(2-methylpropanamido)ethenyl]triphenylphosphonium chloride (**4c**). Yield 3.68 g (91 %); m.p. 182 - 184 °C. ^{1}H NMR (400 MHz, DMSO-d$_6$): δ = 7.81 - 7.57 (m, 15 H, PC$_6$H$_5$), 2.92 - 2.80 (m, 1 H, CH), 1.22 - 1.12 (6 H, CH3) ppm. ^{13}C NMR (100.6 MHz, DMSO-d$_6$): δ = 183.5 (d, ^2J(P,C) = 33.0 Hz, C-5 oxazole), 165.8 (d, ^3J(P,C) = 20.5 Hz, C-2 oxazole), 134.5 (d, ^3J(P,C) = 10.3 Hz, C-3, C-5 PC$_6$H$_5$), 134.3 (d, ^4J(P,C) =

2.2 Hz, C-4 PC$_6$H$_5$), 129.9 (d, ^2J(P,C) = 12.5 Hz, C-2, C-6 PC$_6$H$_5$), 121.2 (d, ^1J(P,C) = 93.9 Hz, C-1 PC$_6$H$_5$), 103.1 (d, ^1J(P,C) = 153.3 Hz, C-4 oxazole), 28.4 (CH), 20.6 (CH$_3$) ppm. ^{31}P NMR (202.4 MHz, DMSO-d$_6$): δ = 12.1 ppm. IR (KBr): ν = 1438, 1407 (br), 1109, 994, 722, 690, 559, 518 cm^{-1}. LCMS: [M+H]$^+$ = 404.2. C$_{24}$H$_{22}$NOPS (403.477): calcd. C 71.44, H 5.50, N 3.47, P 7.68, S 7.95; found C 71.15, H 5.74, N 3.68, P 7.42, S 8.17.

[2-Flouromethyl-4-(triphenylphosphoniumyl)-1,3-oxazol-5-yl]sulfanide (**1d**) was obtained from [2,2-dichloro-1-(2-fluoroacetamido)ethenyl]triphenylphosphonium chloride (**4d**). Yield 3.22 g (82 %); m.p. 150 - 154 °C. ^{1}H NMR (400 MHz, DMSO-d$_6$): δ = 7.82 - 7.76 (m, 3 H, PC$_6$H$_5$), 7.75 - 7.62 (m, 12 H, PC$_6$H$_5$), 5.23 (d, 2J(F,H) = 48.0 Hz, 2 H, CH$_2$F) ppm. ^{13}C NMR (100.6 MHz, DMSO-d$_6$): δ = 185.0 (d, ^2J(P,C) = 31.5 Hz, C-5 oxazole), 155.9 (dd, ^3J(P,C) = 22.7 Hz, ^2J(F,C) = 18.3 Hz C-2 oxazole), 134.6 (C-4 PC$_6$H$_5$), 134.5 (d, ^3J(P,C) = 11.0 Hz, C-3, C-5 PC$_6$H$_5$), 130.1 (d, ^2J(P,C) = 13.2 Hz, C-2, C-6 PC$_6$H$_5$), 120.5 (d, ^1J(P,C) = 94.6 Hz, C-1 PC$_6$H$_5$), 105.4 (d, ^1J(P,C) = 152.6 Hz, C-4 oxazole), 76.0 (d, ^1J(F,C) =163.6 Hz, CH$_2$F) ppm. ^{31}P NMR (202.4 MHz, DMSO-d$_6$): δ = 13.0 ppm. IR (KBr): ν = 1437, 1402 (br), 1109, 963, 723, 688, 565, 520 cm^{-1}. C$_{22}$H$_{17}$FNOPS (393.415): calcd. C 67.16, H 4.36, N 3.56, P 7.87, S 8.15; found C 67.44, H 4.71, N 3.78, P 7.96, S 8.03.

[2-Benzyl-4-(triphenylphosphoniumyl)-1,3-oxazol-5-yl]-sulfanide (**1e**) was obtained from [2,2-dichloro-1-(2-phenylacetamido)ethenyl]triphenylphosphonium chloride (**4e**). Yield 3.91 g (87 %); m.p. 192 - 194 °C. ^{1}H NMR (400 MHz, DMSO-d$_6$): δ = 7.81 - 7.59 (m, 15 H, PC$_6$H$_5$), 7.35 - 7.19 (m, 5 H, C$_6$H$_5$), 3.94 (s, 2 H, CH$_2$) ppm. ^{13}C NMR (100.6 MHz, DMSO-d$_6$): δ = 184.0 (d, ^2J(P,C) = 32.3 Hz, C-5 oxazole), 160.2 (d, ^3J(P,C) = 22.0 Hz, C-2 oxazole),136.4 (C$_6$H$_5$) 134.5 (d, ^3J(P,C) = 11.0 Hz, C-3, C-5 PC$_6$H$_5$), 134.3 (d, ^4J(P,C) = 2.2 Hz, C-4 PC$_6$H$_5$), 130.0 (d, ^2J(P,C) = 12.5 Hz, C-2, C-6 PC$_6$H$_5$), 129.2 (C$_6$H$_5$), 129.1 (C$_6$H$_5$), 127.3 (C$_6$H$_5$), 121.0 (d, ^1J(P,C) = 93.9 Hz, C-1 PC$_6$H$_5$), 103.6 (d, ^1J(P,C) = 152.6 Hz, C-4 oxazole), 34.6 (CH$_2$) ppm. ^{31}P NMR (202.4 MHz, DMSO-d$_6$): δ = 12.4 ppm. IR (KBr): ν =1577, 1435, 1410 (br), 1108, 995, 732, 723, 564, 521, 503 cm^{-1}. LCMS: [M+H]$^+$ = 452.2. C$_{28}$H$_{22}$NOPS (451.520): calcd. C 74.48, H 4.91, N 3.10, P 6.86, S 7.10; found C 74.11, H 4.78, N 3.22, P 6.59, S 6.97.

[2-Phenyl-4-(triphenylphosphoniumyl)-1,3-oxazol-5-yl]-sulfanide (**1f**) was obtained from [2,2-dichloro-1-(phenylformamido)ethenyl]triphenylphosphonium chloride (**4f**). Yield 4.06g (93%); m.p. 189 - 191 °C (183-185 °C, 188-189 °C).[10,11] ^{1}H NMR (400 MHz, DMSO-d$_6$): δ = 7.87 - 7.74 (m, 11 H, PC$_6$H$_5$), 7.72 - 7.62 (m, 6 H, PC$_6$H$_5$, C$_6$H$_5$), 7.51 - 7.35 (m, 3 H, C$_6$H$_5$) ppm. ^{13}C NMR (100.6 MHz, DMSO-d$_6$): δ = 183.9 (d, ^2J(P,C) = 32.9 Hz, C-5 oxazole), 158.2 (d, ^3J(P,C) = 21.9 Hz, C-2 oxazole), 134.6 (d, ^3J(P,C) = 10.5 Hz, C-3, C-5 PC$_6$H$_5$), 134.5 (C-4 PC$_6$H$_5$), 130.0 (d, ^2J(P,C) = 13.0 Hz, C-2, C-6 PC$_6$H$_5$), 130.0 (C$_6$H$_5$), 129.5 (C$_6$H$_5$), 129.1 (C$_6$H$_5$), 127.3 (C$_6$H$_5$),125.4 (C$_6$H$_5$), 120.8 (d, ^1J(P,C) = 93.7 Hz, C-1 PC$_6$H$_5$), 106.2 (d, ^1J(P,C) = 152.1 Hz, C-4 oxazole) ppm. ^{31}P NMR (202.4 MHz, DMSO-d$_6$): δ = 12.6 ppm. IR (KBr): ν =1437, 1404 (br),1225, 1108, 1080, 981, 754, 711, 617, 564, 582, 517 cm^{-1}. LCMS: [M+H]$^+$ = 438.2. C$_{27}$H$_{20}$NOPS (437.494): calcd. C 74.12, H 4.61, N 3.20, P 7.08, S 7.33; found C 74.47, H 4.48, N 3.41, P 6.83, S 7.09.

[2-(4-Methylphenyl)-4-(triphenylphosphoniumyl)-1,3-oxazol-5-yl]sulfanide (**1g**) was obtained from {2,2-dichloro-1-[(4-methylphenyl)formamido]ethenyl}triphenylphosphonium chloride (**4g**). Yield 4.28 g (95 %); m.p. 197 - 198 °C (194-197 °C).[6] ^{1}H NMR (400 MHz, DMSO-d_6): δ = 7.85 - 7.73 (m, 9 H, PC$_6$H$_5$), 7.73 - 7.62 (m, 8 H, PC$_6$H$_5$, 4-CH$_3$C$_6$H$_4$), 7.26 (d, ^{3}J(H,H) = 7.9 Hz, 2 H, 4-CH$_3$C$_6$H$_4$), 2.32 (s, 3 H, CH$_3$) ppm. ^{13}C NMR (100.6 MHz, DMSO-d_6): δ = 183.6 (d, ^{2}J(P,C) = 32.9 Hz, C-5 oxazole), 158.5 (d, ^{3}J(P,C) = 21.9 Hz, C-2 oxazole), 139.8 (4-CH$_3$C$_6$H$_4$), 134.6 (d, ^{3}J(P,C) = 10.5 Hz, C-3, C-5 PC$_6$H$_5$), 134.5 (d, ^{2}J(P,C) = 3.0 Hz, C-4 PC$_6$H$_5$), 130.0 (4-CH$_3$C$_6$H$_4$), 130.0 (d, ^{2}J(P,C) = 13.0 Hz, C-2, C-6 PC$_6$H$_5$), 125.4 (4-CH$_3$C$_6$H$_4$), 124.8 (4-CH$_3$C$_6$H$_4$), 120.8 (d, ^{1}J(P,C) = 93.7 Hz, C-1 PC$_6$H$_5$), 105.9 (d, ^{1}J(P,C) = 152.1 Hz, C-4 oxazole) ppm. ^{31}P NMR (202.4 MHz, DMSO-d_6): δ = 12.5 ppm. IR (KBr): ν =1437, 1392 (br), 1111, 1078, 972, 819, 754, 720, 699, 686, 646, 567, 518 cm^{-1}. LCMS: [M+H]$^+$ = 452.0. C$_{28}$H$_{22}$NOPS (451.520): calcd. C 74.48, H 4.91, N 3.10, P 6.86, S 7.10; found C 74.56, H 4.69, N 3.34, P 6.51, S 7.19.

{2-[(E)-2-Phenylethenyl]-4-(triphenylphosphoniumyl)-1,3-oxazol-5-yl]sulfanide (**1h**) was obtained from {2,2-dichloro-1-[(2E)-3-phenylprop-2-enamido]ethenyl}triphenylphosphonium chloride (**4h**). Yield 4.12 g (89 %); m.p. 200 - 202 °C. ^{1}H NMR (400 MHz, DMSO-d_6): δ = 7.90 - 7.60 (m, 17 H, PC$_6$H$_5$, C$_6$H$_5$), 7.44 - 7.27 (m, 3 H, C$_6$H$_5$), 7.20 (d, ^{3}J(H,H) = 16.3 Hz, 1 H, CH=CH), 6.89 (d, ^{3}J(H,H) = 16.3 Hz, 1 H, CH=CH) ppm. ^{13}C NMR (100.6 MHz, DMSO-d_6): δ = 183.8 (d, ^{2}J(P,C) = 32.9 Hz, C-5 oxazole), 158.8 (d, ^{3}J(P,C) = 22.4 Hz, C-2 oxazole), 136.2 (CH=CHC$_6$H$_5$), 134.5 (d, ^{3}J(P,C) = 10.5 Hz, C-3, C-5 PC$_6$H$_5$), 134.5 (C-4 PC$_6$H$_5$), 133.3 (CH=CHC$_6$H$_5$), 130.0 (d, ^{2}J(P,C) = 13.0 Hz, C-2, C-6 PC$_6$H$_5$), 129.3 (CH=CHC$_6$H$_5$), 129.1 (CH=CHC$_6$H$_5$), 127.5 (CH=CHC$_6$H$_5$), 120.7 (d, ^{1}J(P,C) = 93.7 Hz, C-1 PC$_6$H$_5$), 114.0 (CH=CHC$_6$H$_5$), 106.8 (d, ^{1}J(P,C) = 152.1 Hz, C-4 oxazole) ppm. ^{31}P NMR (202.4 MHz, DMSO-d_6): δ = 12.7 ppm. IR (KBr): ν =1437, 1389 (br), 1218, 1109, 753, 723, 685, 560, 518, 499 cm^{-1}. LCMS: [M+H]$^+$ = 464.0. C$_{29}$H$_{22}$NOPS (463.531): calcd. C 75.14, H 4.78, N 3.02, P 6.68, S 6.92; found 74.93, H 4.91, N 3.29, P 6.81, S 7.06.

[2-(2-Chlorophenyl)-4-(triphenylphosphoniumyl)-1,3-oxazol-5-yl]sulfanide (**1i**) was obtained from {2,2-dichloro-1-[(2-chlorophenyl)formamido]ethenyl}triphenylphosphonium chloride (**4i**). Yield 3.97 g (84 %); m.p. 211 - 213 °C. ^{1}H NMR (400 MHz, DMSO-d_6): δ = 7.90 - 7.75 (m, 10 H, PC$_6$H$_5$), 7.73 - 7.62 (m, 6 H, PC$_6$H$_5$, 2-ClC$_6$H$_4$), 7.57-7.51 (m, 1 H, 2-ClC$_6$H$_4$), 7.48-7.38 (m, 2 H, 2-ClC$_6$H$_4$) ppm. ^{13}C NMR (100.6 MHz, DMSO-d_6): δ = 183.9 (d, ^{2}J(P,C) = 32.4 Hz, C-5 oxazole), 155.6 (d, ^{3}J(P,C) = 22.9 Hz, C-2 oxazole), 134.6 (d, ^{3}J(P,C) = 10.5 Hz, C-3, C-5 PC$_6$H$_5$), 134.6 (C-4 PC$_6$H$_5$), 131.7 (2-ClC$_6$H$_4$), 131.2 (2-ClC$_6$H$_4$), 130.7 (2-ClC$_6$H$_4$), 130.1 (2-ClC$_6$H$_4$), 130.0 (d, ^{2}J(P,C) = 13.0 Hz, C-2, C-6 PC$_6$H$_5$), 128.0 (2-ClC$_6$H$_4$), 125.7 (2-ClC$_6$H$_4$), 120.7 (d, ^{1}J(P,C) = 93.7 Hz, C-1 PC$_6$H$_5$), 106.5 (d, ^{1}J(P,C) = 152.1 Hz, C-4 oxazole) ppm. ^{31}P NMR (202.4 MHz, DMSO-d_6): δ = 12.4 ppm. IR (KBr): ν =1471, 1437, 1392 (br), 1220, 1109, 980, 770, 758, 741, 719, 686 (br), 657, 589, 563, 538, 514 cm^{-1}. LCMS: [M]$^+$ = 472.2, 473.2. C$_{27}$H$_{19}$ClNOPS (471.938): calcd. C 68.71, H 4.06, N 2.97, P 6.56, S 6.79, Cl 7.51; found C 68.79, H 4.28, N 3.24, P 6.51, S 6.63, Cl 7.49.

[2-(4-Chlorophenyl)-4-(triphenylphosphoniumyl)-1,3-oxazol-5-yl]sulfanide (**1j**) was obtained from {2,2-dichloro-1-[(4-chlorophenyl)formamido]ethenyl}triphenylphosphonium chloride (**4j**). Yield 4.53 g (96 %); m.p. 222 - 223 °C (216-218 °C).[5] ^{1}H NMR (400 MHz, DMSO-d_6): δ = 7.84 - 7.62 (m, 17 H, PC$_6$H$_5$, 4-ClC$_6$H$_4$), 7.74 - 7.50 (d, ^{3}J(H,H) =8.8 Hz, 2 H, 2-ClC$_6$H$_4$) ppm. ^{13}C NMR (100.6 MHz, DMSO-d_6): δ = 184.1 (d, ^{2}J(P,C) = 32.3 Hz, C-5 oxazole), 157.3 (d, ^{3}J(P,C) = 22.0 Hz, C-2 oxazole), 134.6 (d, ^{3}J(P,C) = 11.0 Hz, C-3, C-5 PC$_6$H$_5$), 134.6 (C-4 PC$_6$H$_5$),134.5 (4-ClC$_6$H$_4$), 130.0 (d, ^{2}J(P,C) = 12.5 Hz, C-2, C-6 PC$_6$H$_5$), 129.6 (4-ClC$_6$H$_4$),127.1 (4-ClC$_6$H$_4$), 126.1 (4-ClC$_6$H$_4$), 120.6 (d, ^{1}J(P,C) = 93.9 Hz, C-1 PC$_6$H$_5$), 106.5 (d, ^{1}J(P,C) = 151.9 Hz, C-4 oxazole) ppm. ^{31}P NMR (202.4 MHz, DMSO-d_6): δ = 12.7 ppm. IR (KBr): ν =1482, 1438, 1384 (br), 1219, 1111, 1077, 834, 752, 721, 686 (br), 603, 563, 539, 520 cm^{-1}. LCMS: [M]$^+$ = 472.2, 473.2. C$_{27}$H$_{19}$ClNOPS (471.938): calcd. C 68.71, H 4.06, N 2.97, P 6.56, S 6.79, Cl 7.51; found C 69.03, H 3.85, N 3.19, P 6.68, S 6.87, Cl 7.74.

[2-(2,4-Dichlorophenyl)-4-(triphenylphosphoniumyl)-1,3-oxazol-5-yl]sulfanide (**1k**) was obtained from {2,2-dichloro-1-[(2,4-dichlorophenyl)formamido]ethenyl}triphenylphosphonium chloride (**4k**). Yield 4.81 g (95 %); m.p. 178 - 179 °C. ^{1}H NMR (400 MHz, DMSO-d_6): δ = 7.87 - 7.73 (m, 10 H, PC$_6$H$_5$), 7.72 - 7.63 (m, 7 H, PC$_6$H$_5$, 2,4-Cl$_2$C$_6$H$_3$), 7.50 (d, ^{3}J(H,H) = 8.3 Hz, 1 H, 2,4-Cl$_2$C$_6$H$_3$) ppm. ^{13}C NMR (100.6 MHz, DMSO-d_6): δ = 184.0 (d, ^{2}J(P,C) = 32.3 Hz, C-5 oxazole), 154.7 (d, ^{3}J(P,C) = 22.7 Hz, C-2 oxazole), 134.7 (2,4-Cl$_2$C$_6$H$_3$),134.6 (d, ^{4}J(P,C) = 2.9 Hz, C-4 PC$_6$H$_5$), 134.6 (d, ^{3}J(P,C) = 10.3 Hz, C-3, C-5 PC$_6$H$_5$), 131.6 (2,4-Cl$_2$C$_6$H$_3$), 131.2 (2,4-Cl$_2$C$_6$H$_3$), 131.1 (2,4-Cl$_2$C$_6$H$_3$), 130.0 (d, ^{2}J(P,C) = 13.0 Hz, C-2, C-6 PC$_6$H$_5$), 128.3 (2,4-Cl$_2$C$_6$H$_3$), 124.5 (2,4-Cl$_2$C$_6$H$_3$), 120.6 (d, ^{1}J(P,C) = 93.9 Hz, C-1 PC$_6$H$_5$), 107.0 (d, ^{1}J(P,C) = 151.9 Hz, C-4 oxazole) ppm. ^{31}P NMR (202.4 MHz, DMSO-d_6): δ = 12.5 ppm. IR (KBr): ν =1468, 1437, 1395 (br), 1221, 1108, 1082, 975, 841, 753, 718, 685 (br), 623, 611, 543, 514 cm^{-1}. LCMS: [M]$^+$ = 506.2, 507.2. C$_{27}$H$_{18}$Cl$_2$NOPS (506.383): calcd. C 64.04, H 3.58, N 2.77, P 6.12, S 6.33, Cl 14.00; found C 64.29, H 3.41, N 2.94, P 6.21, S 6.51, Cl 14.39.

[2-(4-Nitrophenyl)-4-(triphenylphosphoniumyl)-1,3-oxazol-5-yl]sulfanide (**1l**) was obtained from {2,2-dichloro-1-[(4-nitrophenyl)formamido] ethenyl} triphenylphosphonium chloride (**4**). Yield 4.62 g (96 %); m.p. 207 - 208 °C. ^{1}H NMR (400 MHz, DMSO-d_6): δ = 8.29 (d, ^{3}J(H,H) = 8.4 Hz, 2 H, 4-NO$_2$C$_6$H$_4$), 7.94 (d, ^{3}J(H,H) = 8.4 Hz, 2 H, 4-NO$_2$C$_6$H$_4$), 7.90 - 7.66 (m, 15 H, PC$_6$H$_5$) ppm. ^{13}C NMR (100.6 MHz, DMSO-d_6): δ = 185.0 (d, ^{2}J(P,C) = 32.4 Hz, C-5 oxazole), 156.4 (d, ^{3}J(P,C) = 21.9 Hz, C-2 oxazole), 147.6 (4-NO$_2$C$_6$H$_4$), 134.7 (C-4 PC$_6$H$_5$), 134.6 (d, ^{3}J(P,C) = 11.0 Hz, C-3, C-5 PC$_6$H$_5$), 132.3 (4-NO$_2$C$_6$H$_4$), 130.1 (d, ^{2}J(P,C) = 13.0 Hz, C-2, C-6 PC$_6$H$_5$),126.1 (4-NO$_2$C$_6$H$_4$), 125.0 (4-NO$_2$C$_6$H$_4$), 120.3 (d, ^{1}J(P,C) = 94.2 Hz, C-1 PC$_6$H$_5$), 108.3 (d, ^{1}J(P,C) = 150.6 Hz, C-4 oxazole) ppm. ^{31}P NMR (202.4 MHz, DMSO-d_6): δ = 12.8 ppm. IR (KBr): ν =1595, 1511, 1489, 1389, 1213, 1108, 722, 695 (br), 660, 563, 540, 520 cm^{-1}. LCMS: [M+H]$^+$ = 483.2. C$_{27}$H$_{19}$N$_2$O$_3$PS (482.491): calcd. C 67.21, H 3.97, N 5.81, P 6.42, S 6.65; found C 67.39, H 4.35, N 6.02, P 6.68, S 6.83.

RESULTS AND DISCUSSION

Effect of substituent at 2-position of oxazole ring-

Optimized Molecular Geometry

The optimized molecules of PYOA with the different substituents in the 2-position are shown in Figure 3. One can see that the non-variable core molecular part (including oxazole cycle and phenyl substituent in position 2 and the amino group in position 5) are situated in the same plane, i.e. this molecular fragment is planar with maximum conjugation between oxazole and both substituents. The thickness of π-electron systems is ≈1.4 Å.

The variable substituents in positions 4 differ essentially by their spatial constitution. In the reference molecule, R = Me, the methyl group (Figure 3, a) has the spherical structure with radius ≈1.8 Å. The CN group is situated in the same plane with the molecular core and conjugate with them; its thickness is also ≈1.4 Å, while the total length is ≈1.6 Å. Other substituents that are bonded with oxazole cycle by tri-coordinated atom (S or P) and are of propeller-type, hence can rotate around S–C or P–C bond.

Additionally, the phenyl group at sulfur or phosphorus atom can rotate practically freely; its extension is approximately following: $6.5 \times 6.5 \times 1.4$ Å^3.

It was found that the introducing of the Cl atoms as well as NO$_2$ groups has not disturbed the planar constitution. The planar spatial position of the conjugated molecular fragments is obtained upon optimization of the stilbene-like molecule (**1h**) (Figure 3, c), whereas three phenyl substituents at the phosphorus atoms form propeller-like space structure, and the torsion angles between P–Ph bonds

and oxazole cycle plane are following: 22°, 97° and -38°, every phenyl ring is twisted relatively to P–oxazole bond at 71°, 167° and -40°, correspondingly. As regard to the optimized bonds, their values for the (**1f**) are presented in Figure 4.

The calculated bond lengths are close to the experimental values (within ±0.02 Å). The lengths of two C–O and two C–N bonds are not equivalent. The carbon-phosphorus bond to phosphorus atom with oxazole cycle (1.740 Å) is somewhat shorter than the bonds linked that phosphorus atom with the phenyl substituents (1.816 Å), as experimentally confirmed. The exocyclic C–S bond connecting the oxazole with the single-coordinated sulphur atom is longer (1.671 Å) in comparison, for example, with the calculated C = S bond in thioacetone (1.622 Å).

In the other PYOA derivatives, the bond lengths in PYOA core are negligibly modified, with the exception of PYOA – R length i.e., 1.492 Å (R = Me), 1.466 Å (**1f**), 1.465 Å (**1i**), 1.467 Å (**1j**) and 1.457 Å (**1l**). The bonds in 5-membered oxazole cycle are close to aromatic bonds excepting the comparative short double C=N bond (≈1.29 Å) (Figure 4). The calculations give the theoretical aromatic C–C bond length for phenyl substituents in (**1f**) and (**1h**). C–C bond lengths in the open chain of the stilbene (**1h**) are substantially alternated viz., 1.448, 1.339 and 1.465 Å, exactly as in the ordinary polyenes. It is also to be mentioned that the aromatic bonds in the phenyl substituents at the phosphorus are slightly distorted from standard values of 1.40 Å. It can be assumed that in the PYOA molecule (**1**) two main conjugated systems exist: π-electron system of the planar oxazole moiety with its conjugated substituents R and the π-electron system of the three phenyl residues at the phosphorus atom forms propeller-like structure. Both conjugated systems are interconnected by the phosphorus atom. Other bonds in PYOA contained the non-conjugated substituents were not analyzed in this study.


a	b	c

● - C, ● - N, ● - O, ● - P, ● - S
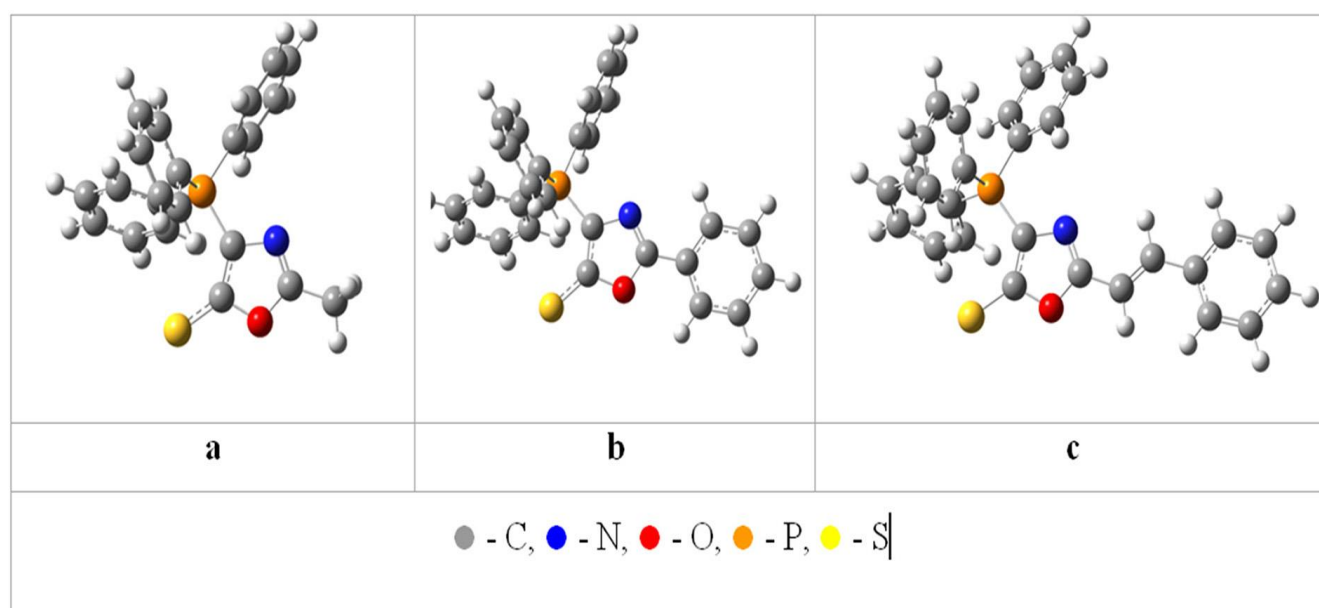
Figure 3. Optimized molecular geometry: a = **1b**, b = **1f**, c = **1h**.
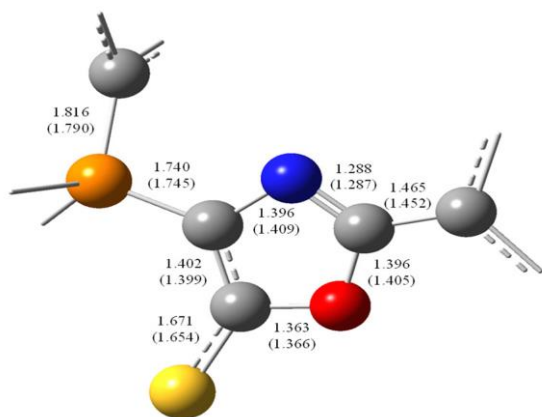
Figure 4. Optimized bond lengths in (**1f**), bond lengths obtained

Atomic charges

At first, it should be pointed that the DFT calculations indicated considerable polarization of C–H bonds, for example, in the phenyl substituents, as well as in the open polyenic chain in the stilbene (**1h**) and consequently these carbon atoms bear the negative charges. The charges on the hydrogen atoms are not shown in Figure 5, only the charges on carbon atoms and heteroatoms are shown.
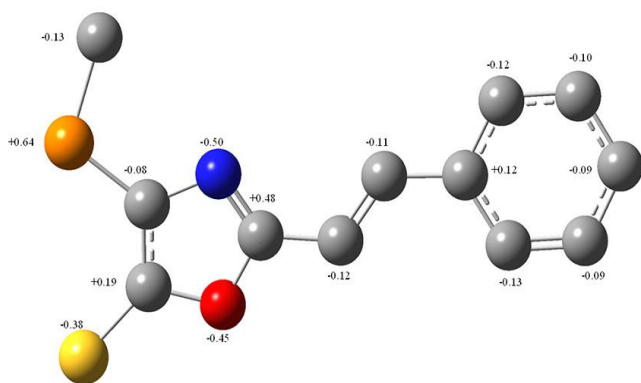
Figure 5. Charges on carbon atoms and heteroatoms in (**1h**).by X-spectroscopy are in brackets (ref. 2)

One can see that the charges at the carbon atoms of the exocyclic phenyl ring are in a narrow range, -0.09-013. Practically the same charges are obtained for the carbon atoms in three phenyl substituents at the phosphorus atom.

The atomic charges of the carbon atoms in the oxazole cycle depend appreciably on the adjacent heteroatoms because of the high polarization of the C–N and C–O bonds; the maximum positive charge is seen to be present at C-2 connected with the conjugated substituent, while the positive charge at the position 5 is appreciably lower, evidently, because of the opposite polarization C–S bond. Also, the carbon atom bonded to the phosphorus atom of the low electronegativity bear the small negative charges because of the considerable opposite polarization of the C–P bond directed to the carbon atom.

The calculation showed the presence of appreciable negative charge at the double-coordinated oxygen atom. An

excess of electron density is obtained for the double-coordinated nitrogen atoms and mono-coordinated sulphur atom also. It is obvious that the maximum deficit of the electron density (Figure 5) is obtained, from the calculation, for the tetra-coordinated phosphorus atom with the minimum electronegativity.

The calculations also give the negligible influence of the substituents (Cl, NO_2) and/or lengthening of the open conjugated chain on the charge distribution in oxazole cycle, only atomic charges at the carbon atoms bonded with such substituents are affected. Thus, introduction of the chlorine atom in *o*-position increases slightly the negative charge from -0.12 to -0.15 (while q[Cl] = +0.03), the calculated effect of *p*-Cl atom differs somewhat: q[C] = -0.09, q[Cl] = +0.03. At the same time, the effect of high acceptor group is appreciably greater q[C] = +0.24, q[N] = +0.10 and q[O] = -0.40.

To summarise, the negligible influence of the non-conjugated and conjugated substituents on the atomic charges in PYOA moiety is seen in figure 6a where the charges at the carbon atoms and heteroatoms upon variation of the residue R are presented. The quantum-chemical conclusion about the negligible influence of the non-conjugated and conjugated substituents on the atomic charges on PYOA moiety is experimentally confirmed by ^{13}C NMR spectroscopy data. The measured signals for three carbon atoms are given in the figure 6b.

The atomic charges in the benzene cycle depend weakly on the carbon atom position, except the carbon atom bonded with PYOA cycle (Figure 6). The calculated data are in good agreement with the experimental results obtained by ^{13}C NMR spectroscopy (Table 1). For comparison, the signals for benzene ring in non-conjugated residue CH_2Ph (compound **1e**) are also presented.

The measured values δ for the carbon atoms in the corresponding positions coincide practically for both conjugated phenyl substituent (compound **1f**), and non-conjugated benzyl substituent (compound **1l**), except the atom in the benzene ring connected with the rest of molecule. Introducing of one chlorine atom (compound **1i**) or two atoms (compound **1k**) makes the substituent unsymmetrical, the charges on the atoms C-2 and C-5 become different (Table 1), which also confirmed experimentally. The maximum change of the charge occurs for the atom in *para*-position upon introducing of the high acceptor nitro group in the molecule (compound **1l**). The calculation gives the considerable atomic charge: +0.235. The signal δ (C-4) is appreciably shifted in the weak field at 147.6 ppm. Regarding carbon atoms in the open chain of the molecule (**1h**), the atomic charges (Figure 5) are close: -0.12 and -0.11. However, the ^{13}C NMR data show the appreciable difference in the chemical shifts: δ(α) = 136.2 ppm and δ(β) = 114.0 ppm.

It is to be noted the first carbon atom is bonded with the phenyl substituent while the second atom is bond with the highly electron-donating oxazole cycle. The disagreement between the calculated and experimental data likely relates with the quantum-chemical method used in this work probably because of the influence of the nearest neighbour atoms is not take into consideration.
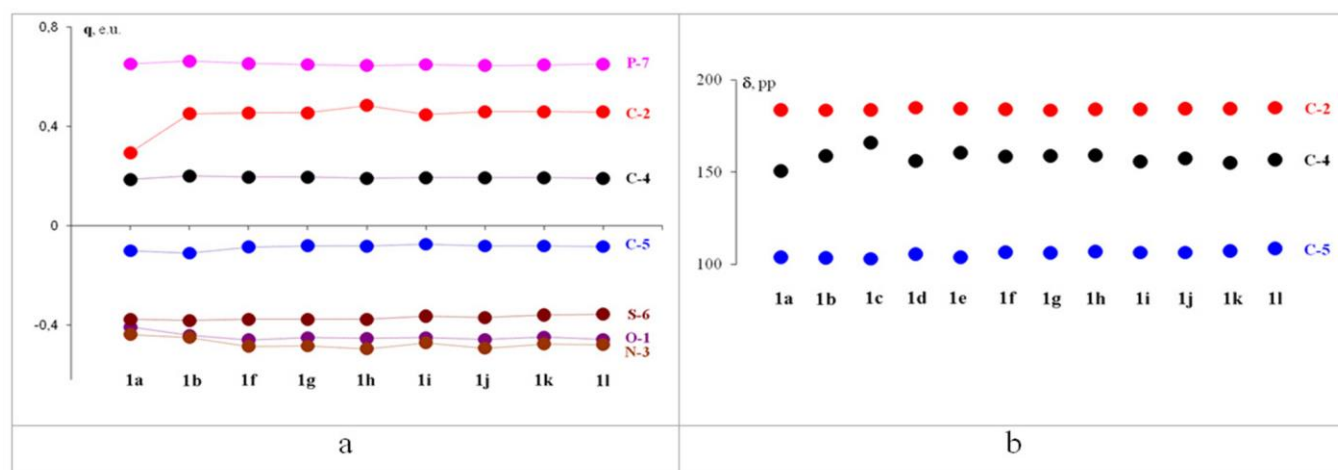
Figure 6. (a) Calculated charges at carbon atoms and heteroatoms and (b) ^{13}C NMR signals within **PYOA** moiety.

Summarizing, both non-conjugated and conjugated substituents R affect comparatively weak on the equilibrium molecular geometry and charge distribution in PYOA moiety, i.e. the electron structure in the ground state is weakly sensitive to the nature of exocyclic substituents. It is supposed that the excited state should be more perceptible.

Delocalized and local MOs

The influence of the substituents is more clearly recognized in the shape of molecular orbitals and, hence, in nature of the lowest electron transitions involved the frontier and nearest MOs. It is noted that the three phenyl substituents at the phosphorus atom do not conjugate with the oxazole cycle and their π-orbitals should generate own conjugated systems. Therefore, let us first compare the MOs in the simplest molecule (**1b**) and the reference molecule (**2**). After this, we have considered the influence of the phenyl substituent (**1f**) and the lengthening of the chain, and finally the effects of the introduction of chlorine atoms and the nitro group have been analyzed.

MOs and electron transitions in PYOA and reference compound (2)

The shape of the frontier and some nearest MOs of the molecules studied are shown in figure 7. According to the obtained data, there are three types of orbitals:

(a) MOs delocalized within the planar molecular fragment, we have named them as delocalized MOs (Deloc. MO),

(b) lone electron pair (LEP or n-MO) located only on the sulphur atom. It lies in the PYOA plane and hence is perpendicular to the π-orbitals of the main conjugated system and

(c) orbitals localized in three phenyl substituents on the phosphorus atoms, named as local MOs (Loc MO). They appear only in compounds containing P$^+$Ph$_3$ substituent and are absent in the model molecule (**2**).

These MOs generate the lowest electron transitions of following different types.

- π → π transitions; we should differ two types of such transitions:

  (i)   Π (Del) → π* (Del), the transition between the HOMO and lowest occupied delocalized π-orbital;

  (ii)   π (Del) → π* (Loc), transitions from the delocalized occupied MOs to the lowest vacant local MO.

- n → π* -transitions: n → π* (Del) and n → π* (Loc).

The calculated characteristics of the lowest transitions of different types are collected in Table 2.

Table 1. ^{13}C NMR signals, δ, of carbon atoms in benzene ring.

Molecule	C-1*, ppm	C-2, ppm	C-3, ppm	C-4, ppm	C-5, ppm	C-6, ppm
1e	136.4	129.1	129.2	127.3	129.2	129.1
1f	130.0	129.5	125.4	127.5	125.4	129.5
1g	124.6	130.0	125.5	139.8	125.5	130.0
1h	133.3	129.3	127.5	129.1	127.5	129.3
1i	130.7	131.2	130.1	131.7	125.7	128.0
1j	126.1	129.6	127.1	134.5	127.1	129.6
1k	124.5	131.6	131.2	134.7	128.8	131.1
1l	132.3	125.0	126.1	147.6	126.1	125.0

*C-1 is carbon atom bonded with oxazole cycle.
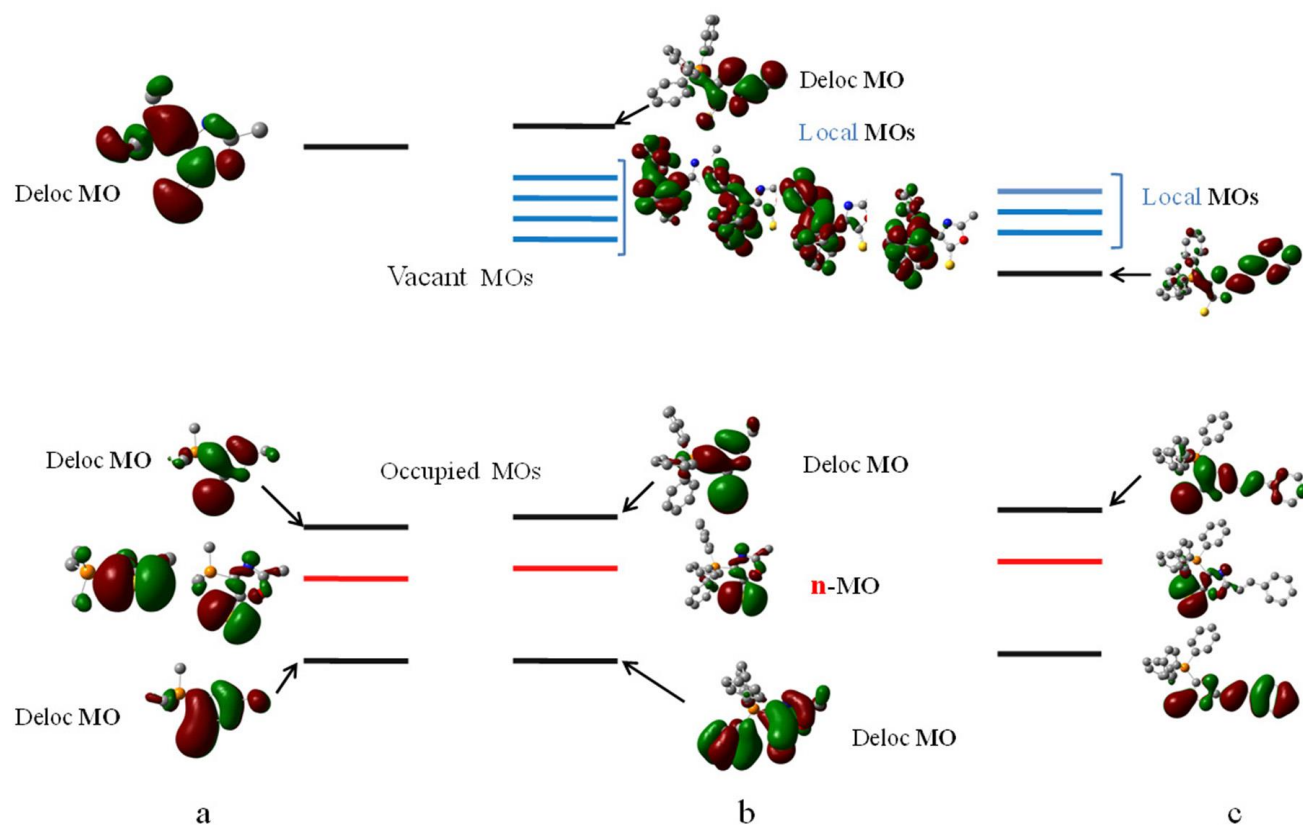
Figure 7. Energy levels of molecules (a) = (**2**), (b) = (**1b**), (c) = (**1h**).

In the reference model molecule (**2**) only π (Del) $\rightarrow \pi^*$ (Del) and n $\rightarrow \pi^*$ (Del) transitions exist (Figure 7, a). The calculation showed that the transition involved LEP orbital has the minimum energy, its oscillator strength, f_1, is negligible, so as the n- and π-MOs are situated in the perpendicular plane and, hence, are not overlap. In contrast, the oscillator strength of the transition between the totally delocalized frontier MOs, f_2, is comparatively large, mainly because of the high overlapping of both the orbitals.

The molecule PYOA (with the non-conjugated substituent R), as seen in Figure 7 b, additionally processes local vacant levels, disposed below the delocalized level, LUMO+4. As a result, the transitions from delocalized HOMO to MOs, located at the phenyl substituents at the phosphorus atom, have the lowest energies. As the overlapping between HOMO and local MOs is practically absent, the oscillator strength of these transitions is negligible (table 2). Therefore, such electron transitions should not manifest themselves in the absorption spectra. Also, the transitions started from n-MO are not observed spectrally as their oscillator strengths are very small.

Only the transitions involving delocalized HOMO and high situated delocalized LUMO+4 has comparatively large oscillator strength, f_{11} (see Table 2). Thus, we can postulate that the band maximum observed in the absorption spectra (Figure 8) at λ_{max} = 337 nm corresponds to the $S_0 \rightarrow S_{11}$ transition of the π (Del) $\rightarrow \pi^*$(Del) type. Similar nature of the lowest electron transitions take place in other PYOA derivatives with non-conjugated substituents: (**1c-1e**).

MOs and electron transitions in PYOA derivatives with conjugated substituents

The MO shapes in PYOA containing the π-enhanced substituents (**1h**) are presented in Figure 7,c, while the MO shapes PYOA containing phenyl groups at phosphorus atom are similar. The calculated characteristics of the some lowest transitions are collected in Table 2.

It should be noted that the introduction of any conjugated substituent is appropriately accompanied by the substantial enhancement of π-electron system and hence, increases the number of π-levels close to energy gap. As it has been shown above, based on quantum-chemical optimization of the molecular geometry, the introduced fragment lies in the plane of the PYOA core. Indeed, the calculations show that the HOMO in both molecules is totally delocalized along whole planar π-system. Among the vacant orbitals, only LUMO+4 in compound **1f** is delocalized in the planar molecular part, when the corresponding level is situated on the local levels. However, in contrast to the PYOA containing the non-conjugated residues, the vacant delocalized MO in the phenyl substituted derivative (compound **1f**) has lower energy, so that the energy of the π (Del) $\rightarrow \pi^*$(Del) transition with the large oscillator strength ($S_0 \rightarrow S_6$) is lower than energy of the corresponding transition ($S_0 \rightarrow S_{11}$) in PYOA when R=CH$_3$ (cf. calculated data in Table 2). Although, the calculations predict that two local π (Del) $\rightarrow \pi^*$(Loc) transitions and three n- π^* transitions should have the lower energies (Table 2) both have the negligible oscillator strength and hence were not appear in the absorption spectra.

Table 2. Calculated wavelengths (λ) and oscillator strength (f) of compounds (**1**) and (**2**).

Compound	Transition	Type	λ, nm	f	Main configuration
1a	$S_0 \to S_{1,2}$	π (Del) → π*(Loc)	345, 331, 317	<0.01	|HOMO → LUMO+0,1,2>
	$S_0 \to S_{3,4}$	n → π*(Loc)	313, 294	<0.01	|HOMO-1 → LUMO+0,1>
	$S_0 \to S_{5,6,7}$	π (Del) → π*(Loc)	278	<0.01	|HOMO → LUMO+3>
	$S_0 \to S_8$	π (Del) → π*(Del)	262	0.0637	|HOMO → LUMO +4>
1b	$S_0 \to S_{1,2}$	π (Del) → π*(Loc)	380, 365	<0.01	|HOMO → LUMO+0,1>
	$S_0 \to S_{3,4}$	n → π*(Loc)	322, 315	<0.01	|HOMO-1 → LUMO+0,1>
	$S_0 \to S_{5,6,7}$	π (Del) → π*(Loc)	311, 293, 283	<0.01	|HOMO → LUMO+2,3>
	$S_0 \to S_8$	π (Del) → π*(Del)	278	0.0767	|HOMO → LUMO +4>
1f	$S_0 \to S_{1,2}$	π (Del) → π*(Loc)	372, 354	<0.01	|HOMO → LUMO+0,1>
	$S_0 \to S_{3,4,5}$	n → π*(Loc)	318, 311, 307	<0.01	|HOMO-1 → LUMO+0,1,2>
	$S_0 \to S_6$	π (Del) → π*(Del)	302	0.4368	|HOMO → → LUMO +4>
1h	$S_0 \to S_1$	π (Del) → π*(Loc)	359	0.0603	|HOMO → LUMO+1>
	$S_0 \to S_2$	π (Del) → π*(Del)	351	0.6712	|HOMO → LUMO>
	$S_0 \to S_{3,4}$	π (Del)) → π*(Loc)	342, 334	<0.01	|HOMO-1 → LUMO+2,3>
	$S_0 \to S_5$	n → π*(Loc)	315	<0.01	|HOMO-1 → LUMO>
1i	$S_0 \to S_{1,2,3}$	π (Del) → π*(Loc)	365, 344, 321	<0.01	|HOMO → LUMO+0.1,2>
	$S_0 \to S_4$	π (Del) → π*(Del)	316	0.4730	|HOMO → LUMO+3>
	$S_0 \to S_5$	n → π*(Loc)	315	<0.01	|HOMO-1 → LUMO>
1k	$S_0 \to S_{1,2}$	π (Del) → π*(Loc)	360, 344	<0.01	|HOMO → LUMO+0,1>
	$S_0 \to S_3$	π (Del) → π*(Del)	326	0.4336	|HOMO → LUMO+3>
	$S_0 \to S_4$	π (Del) → π*(Loc)	323	0.1597	|HOMO → LUMO+2>
	$S_0 \to S_5$	n → π*(Loc)	316	<0.01	|HOMO-1 → LUMO>
1l	$S_0 \to S_1$	π (Del) → π*(Del)	374	0.5648	|HOMO → LUMO>
	$S_0 \to S_2$	π (Del) → π*(Loc)	345	0.0018	|HOMO → LUMO+1>
	$S_0 \to S_3$	n → π*(Del)	326	<0.01	|HOMO-1 → LUMO>
2	$S_0 \to S_1$	n → π*	285	0.0001	|HOMO-1 → LUMO>
	$S_0 \to S_2$	π → π*	277	0.1793	|HOMO → LUMO>

Table 3. Effects of substituents in PYOA compounds (**1**) on absorption spectra.

Compound	Δλ, nm	Δλ₁*, nm	Δλ₁calc, nm	Δλ₂**, nm	Δλ₂calc, nm
1b	337	-			
1c	336	-1			
1d	332	-5			
1e	338	+1			
1f	351	+14	+24		
1g	350	+13		-1	
1h	401	+64	+73	+50	+49
1i	355	+18	+38	+4	+14
1j	360	+23	+43	+9	+19
1k	365	+28	+48	+14	+24
1l	440	+103	+162	+89	+72

The experimental spectrum of (**1**) (R = Ph) is presented in Figure 8 and the Table 3.

Further increasing of the conjugated chain length (upon introducing of the vinyl-phenyl substituent in (**1h**), as seen figure 7 c, causes a decrease of delocalized level energy, so its LUMO becomes delocalized. As a result, the transition energy of π (Del) → π*(Del) decreases and becomes like the second electron transition. Noteworthy, this transition with large oscillator strength should manifest itself as an intensive band shifted bathochromically to nearly 73 nm in the absorption spectra, in compare with the PYOA with the simplest non-conjugated substituent (compound **1b**) and on 49 nm, in compare with compound (**1f**): this is "pure"

spectral effect of lengthening of the chromophore. Other transitions have small-scale oscillator strengths. The experimental spectrum of the compound (**1f**) is presented in figure 8 and table 3 is in good agreement with the calculated data.

MOs and electron transitions in PYOA with the substituted phenyl derivatives

The MO shapes in PYOA containing substituted residues (**1i**, **1k**, **1l**) are practically the same as in compound (**1f**) and compound (**1h**), represented in figure 7 c, while the calculated characteristics of the some lowest transitions are collected in Table 2.

In this series, the vacant delocalized levels shifts regularly down, so that **PYOA** with the *p*-nitrophenyl residue has both frontier MOs delocalized along whole planar conjugated system which follows from calculations. It should be noted that view of the higher occupied MOs remains nearly similar, only the region of the delocalization becomes wider. Usually, the delocalization region of corresponding vacant delocalized MO also increases. The widening of π-system leads to the decreasing of the energy of the π(Del) → π*(Del) transition with the large oscillator strength which is connected with the intensive spectral band. The calculations predict the regular bathochromic shift of this band in absorption spectra so that the lowest electron transition in the nitro derivative should be π(Del) → π*(Del) transition type. As a general rule, the n→ π* transition for all molecules (Table 2) is not the lowest transition.

The experimental spectra of the compounds containing substituents (Cl or NO_2) in side benzene ring are presented in Figure 8 and Table 3. The nitro group shifted the absorption maximum on 103 nm, as it has seen from absorption spectra of the compound **1b**, and on 89 nm, for **1f** (Figure 8; Table 2). The calculated effects differ somewhat. These spectral effects of the influence of the substituents on the value of absorption maxima are most demonstrative.
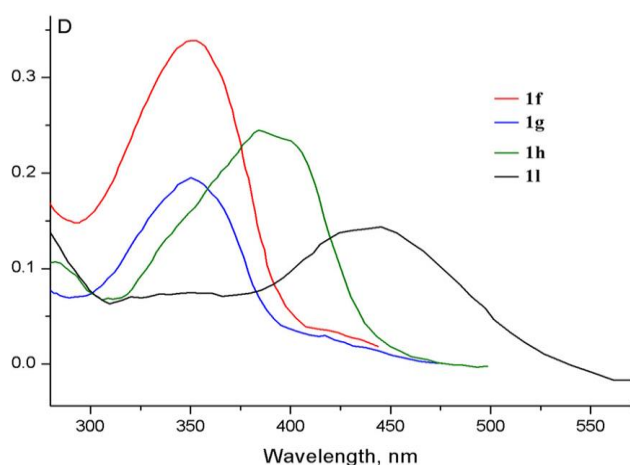
Figure 8. Absorption spectra (**1f**), (**1g**), (**1h**) and (**1l**) in toluene ($C_M = 1 \cdot 10^{-5}$).

CONCLUSION

The study has shown that introducing of the non-conjugated and conjugated substituents in the position 2 of the oxazole cycle in thiaphosphonium ylides cause only small change in the molecular equilibrium geometry and in charge distribution in oxazole moiety, whereas spectral characteristics of substituted derivatives are very sensitive to the nature of the lowest electron transitions which reflects in changes of their absorption maxima.

REFERENCES

[1]Johnson, A.W., *Ylides and Imines of Phosphorus*, John Wiley & Suns, Inc.: New York, **1993**, 1-99.

[2]Van Meervelt, L., Schuerman, G.S., Brovarets, V.S., Mishchenko, N.I., Romanenko, E.A., Drach, B.S., *Tetrahedron*, **1995**, *51*, 1471. DOI: 10.1016/0040-4020(94)01041-W

[3]Valeur, B., *Molecular Fluorescence. Principles and Applications.* Wiley-VCH Verlag GmbH. Weinheim **2001**, 381. DOI: 10.1002/3527600248

[4]Webster, S., Peceli, D., Hu, H., Padilha, L. A., Przhonska, O. V., Masunov, A. E., Gerasov, A. O., Kachkovski, A. D., Slominsky, Yu. L., Tolmachev, A. I., Kurdyukov, V. V., Viniychuk, O. O., Barrasso, E., Lepkowicz, R., Hagan, D. J., Van Stryland, E. W., *J. Phys. Chem. Lett.,* **2010**, *1*, 2354. DOI:10.1021/jz100381v

[5]Klimova, V. A., *Basic Micromethods for the Analysis of Organic Compounds [in Russian]*, Khimiya, Moscow, **1975**.

[6]M. J. Frisch, G. W. Trucks, H. B. Schlegel, G. E. Scuseria,M. A. Robb, J. R. Cheeseman, J. A. Jr Montgomery, T. Vreven, K. N. Kudin, J. C. Burant, M. Millam, S. S. Iyengar, J. Tomasi, V. Barone, B. Mennucci, M. Cossi, G. Scalmani, N. Rega, G. A. Petersson, H. Nakatsuji, M. Hada, M. Ehara, K. Toyota, R.Fukuda, J. Hasegawa, M. Ishida., T. Nakajima, Y. Honda, O.Kitao, H. Nakai, M. Klene, X. Li, J. E. Knox, H. P. Hratchian, J. B. Cross, C. Adamo, J. Jaramillo, R. Gomperts, R. E. Stratmann, O. Yazyev, A. J. Austin, R. Cammi, C. Pomelli, J. W. Ochterski, P. Y. Ayala, K. Morokuma, G. A. Voth, P. Salvador, J.J Dannenberg, V. G. Zakrzewski, S. Dapprich, A. D. Daniels, M. C. Strain, O. Farkas, D. K. Malick, A. D. Rabuck, K.Raghavachari, J. B. Foresman, J. V. Ortiz, Q. Cui, A. G. Baboul, S. Clifford, J. Cioslowski, B. B. Stefanov, G. Liu, A. Liashenko, P. Piskorz, I. Komaromi, R. L. Martin, D. J. Fox, T.Keith, M. A. Al-Laham, C. Y. Peng, A. Nanayakkara, M.Challacombe, P. M. W. Gill, B. Johnson, W. Chen, M. W. Wong, C. Gonzalez, J. A. Pople, *GAUSSIAN03; revision B.05, Gaussian, Inc., Pittsburgh PA,* **2003**.

[7]Fabian, J., *Dyes & Pigments,* **2009,** *84,* 36. DOI: 10.1016/j.dyepig.2009.06.008

[8]Karaca, S., Elmaci, N., *Comput. Theor. Chem.,* **2011,** *964*, 160. DOI:10.1016/j.comptc.2010.12.016

[9]Jacquemin, D., Zhao, Ya., Valero, R., Adamo, C., Ciofini, I., Truhlar, D. G., *J. Chem. Theor. Comput.,* **2012,** *8,* 1255. DOI:10.1021/ct200721d

[10]Lobanov, O. P., Martynyuk, A. P., Drach, B. S., *J. Gen. Chem. USSR (Engl)*, **1980**, *50*, 1816.

[11]Brovarets, V. S., Lobanov, O. P., Drach, B. S., *J. Gen. Chem. USSR (Engl),* **1983**, *53*, 574.

[12]Drach, B. S., Sviridov, E. P., Kisilenko, A. A., Kirsanov, A.V., *J. Org. Chem. USSR (Engl.)* **1973**, *9*, 1842.

[13]Pianka, M., Polton, D. J., *J. Sci. Food Agric*., **1965**, *16*, 330. DOI:10.1002/jsfa.2740160607

[14]Drach, B. S., Sinitsa, A. D., Kirsanov, A. V., *J. Gen. Chem. USSR (Engl),* **1970**, *40*, 1917.

[15]Liu, J., He, K.-L., Li, X., Li, R.-J., Liu, C.-L., Zhong, W., Li, S., *Curr. Med. Chem.*, **2012**, *19*, 6072. DOI: 10.2174/092986712804485971

[16]Guirado, A., Andreu, R., Cereso, A., Galves, J., *Tetrahedron,* **2001**, *57*, 4925. DOI:10.1016/S0040-4020(01)00434-3

[17]Kasper, F., Bottger, H., *Zeitsch. Chem.,* **1987**, *27*, 70. DOI:10.1002/zfch.19870270215

[18]Hudson, H. R., Mavrommatis, Ch. N., Pianka, M., *Phosp. Sulf. and Silicon*, **1996**, *108*, 141. DOI:10.1080/10426509608029647

[19]Drach, B. S., Sviridov, E. P., Kirsanov, A. V., *J. Gen. Chem. USSR (Engl),* **1975**, *45*, 10.

HYPERTENSION: AN OVERVIEW

Aditya Dixit [a]* and Prashant Kumar Dhakad[a]

Hypertension is a serious challenge worldwide. It is one of the most prevalent conditions seen today by researchers in both developed and underdeveloped countries. Depending upon progression of systolic and diastolic blood pressure it is classified into prehypertension, stage 1 and 2 hypertension. Modification in the lifestyle is an initial stage but pharmacological treatment is necessary when it become difficult to control it. In regular practice, drug therapy is being selected from diuretics, β-blockers, calcium channel blockers and renin angiotensin system inhibitors either alone or in combination for both initial and maintenance therapy. Choice of drug depends upon favorable effects in specific clinical setting. This article is all about the reasons and treatments of hypertension. The article elaborates the common reasons which lead to raise the blood pressure in a normal individual. It also reviews the studies related to the effect of different factors of our daily life on the blood pressure.

* Corresponding Authors
      Tel.: +919258474535
      E-Mail: adixit70@gmail.com
[a]   Department of Pharmacy, School of Medical & Allied Sciences, Galgotias University, Yamuna Expressway, Gautam Budh Nagar, U.P., India.

Introduction

The heart pumps blood through the blood vessels, the blood is pushed against the walls of the blood vessels. This creates a pressure, called as blood pressure. Body requires this pressure to move the blood throughout in itself. So that every part of body can get the oxygen it needs. Healthy arteries are elastic and they stretch to allow more blood to push through them. Their stretch depends on how hard the blood is pushed against the artery walls. It's important that the blood pressure be within a healthy range to remain healthy.

A device called sphygmomanometer is used to measure blood pressure. Blood pressure is recorded as two numbers. Systolic blood pressure ("upper" number) tells about the pressure exerted by blood against artery walls while the heart is pumping blood. The diastolic blood pressure (the "lower" number) tells about the pressure exerted by blood against artery walls while the heart is resting between beats. Blood pressure is measured in units of mm of Hg. For example, a blood pressure reading might be 120/80 mm Hg. A healthy blood pressure is under 120/80 mm Hg. A blood pressure reading of 120-139 systolic or 80-89 diastolic is defined as "prehypertension." This means that the blood pressure is not high enough to be called high blood pressure (hypertension), but that it is higher than normal. If systolic blood pressure is 140 or greater, or diastolic blood pressure is 90 or greater, it's high blood pressure (Table 1).

Factors affecting blood pressure

Hypertension has been emerged as a challenge worldwide irrespective of developing and developed nations.[1] It is responsible for the death of 1 billion individuals, and approximately 7.1 million per year.[2] Its recognition is for cardiovascular disease (CVD), cerebrovascular disease and end-stage renal disease. A significant relationship between hypertension and risk factors such as age, body mass index, smoking and physical inactivity are reported by many studies. Chronic disease conditions including hypertension include physical inactivity as a major factor.[3]

Hypertension is a different kind of medical condition. In almost 90 % of patients it results from unknown factors (essential or primary hypertension) and only 10 % of patients have a specific cause of their hypertension (secondary hypertension). While essential hypertension cannot be cured, it can be controlled. Although it has frequently been indicated that the causes of essential hypertension are not known, this is only partially true because we have little information on genetic variations or genes that are over-expressed or under-expressed as well as the intermediary phenotypes that they regulate to cause high BP.[4] A number of factors increase BP, including physical activity, obesity, insulin resistance, high alcohol intake, high salt intake, ageing, sedentary lifestyle, stress, low potassium intake and low calcium intake.[5,6]

Table 1. Threshold values.

Blood Pressure Category	Systolic (mm Hg)		Diastolic (mm Hg)
Normal	<120	and	< 80
Prehypertension	120-139	or	80-89
Hypertension (Stage 1)	140-159	or	90-99
Hypertension (Stage 2)	=>160	or	=>100
Hypertensive crisis (Emergency)	>180	or	>110

Physical activity

Lack of physical activity lead to many chronic conditions and hypertension is one of them.[7] Commonly the people do not control blood pressure adequately, which contribute towards excessive cardiovascular mortality & morbidity. Risk of hypertention can be prevented and the best way to do this is life style modification. Hypertension can be controlled by doing physical activities. Many studies are finding the support in this way. An article (effect of exercise

on blood pressure control in hypertensive patients) reported that exercise can be a cornerstone therapy for the prevention, treatment, and control of hypertension.[8]

A review of 15 studies supported that exercise is an important practice to treat the moderate elevations in blood pressure.[9] An article used data of National Health and Nutritional Examination Survey III, found that patients who followed the advice to engage in physical activity to treat hypertension had systolic blood pressure that was on average of approximately equal to 3-4 mm Hg lower than those who did not follow them.[10]

Regular exercise reduces systolic blood pressure in prehypertensive as well as hypertensive people.[11] Systematic review of randomized controlled trials shows that blood pressure reductions were followed by weight loss, modification in diet and increased physical activity.[12]

Diet and exercise, alone or combination, were reported as an effective tool in reducing the blood pressure in subjects with moderate hypertension, with same effect of drug therapy in patients with higher BP level.[13] A research on Japanese-American people in Hawaii stated the beneficial outcomes of physical activity, body weight control, and reduction in salt intake in population-based control of high BP.[14]

The United States National High Blood Pressure Education Program Coordinating Committee has recommended weight loss, dietary sodium reduction, increased physical activity; potassium supplementation and modification of whole diets are six approaches which are efficient for the primary prevention of hypertension.[15].

Physical activity is required to lower blood pressure in hypertensive patients because it is natural, inexpensive, feasible, and effective means of control for hypertension and also a primary life style measure. The US Preventive Services Task Force (USPSTF) recommends the health care providers to counsel the patients for regular physical activity.[16] In the east part of New Zealand, a randomly controlled trial reported the reduction in BP by an average of 1-2 mm Hg over 12 months by counseling patients for general practice on exercise. The recommended that increasing physical activity and improving quality of life may reduce blood pressure by an average.[17] A meta-analysis including 69 studies demonstrated that, despite the relatively small effects, physically active subjects had better cardiovascular recovery than inactive ones.[18]

Stress

Stress can be defined according to the Medical Subject Headings (MeSH) as, a pathological process resulting from body response to external forces and abnormal states that tend to affect its homeostasis. It consists of daily events that enhance physiological activities and lead to somewhat psychological wear and tear.[19] Psychological stress is a condition when emotional stressors are prevailing. Events of the modernized life such as working conditions and family problems, withdrawal from society, financial planning and quarrels are some factors that can enhance stress.[20] Long term chronic exposure to psychological stress can cause increased blood pressure which can develop as

hypertension.[21] A study of over 3,000 individuals[22] showed that urgency/impatience behavior, and hostility assessed during young adulthood along with depression and anxiety were the strong reasons for developing hypertension after 15 years. Financial strain lead to chronic stress has been reported to predict high blood pressure during three to seven years of follow-up.[23] Total 11,119 cases and 13,648 controls from 52 countries were studied[24] which reported attachment of myocardial infarction (cases) and more frequent periods of stress at home, more severe financial stress and more stressful life events compared with controls.

With reference to myocardial infarction risk, the effect of psychosocial stress was also as important as traditional cardiovascular disease risk factors such as smoking, obesity, diabetes and hypertension. A review of 23 treatment comparisons from 17 trials conducted in patients with raised BP, showed strong effects of meditations on lowering of blood pressure. Despite non-significant results, other anti-stress interventions such as biofeedback, progressive muscle relaxation and stress management training also reported clinically important reductions in blood pressure.[25] Therapies such as these may help patients to reduce the effects of stress by reducing physiologic arousal and restoring autonomic balance, thereby reducing blood pressure.[21] Stress reduction has often been regarded as an important component of the lifestyle changes that might be beneficial in reducing an elevated blood pressure in hypertensive patients.[26]

Working hours

Many disorders and diseases can be considered as an effect of working hours such as chronic fatigue,[27,28] musculoskeletal complaints,[29] mental stress or health,[30-32] dissatisfaction with work,[33] depression,[34] and coronary heart disease.[35,36] As for the association between long working hours and blood pressure, the effect of long working hours on blood pressure is related to the activity of sympathetic nervous system and concentrations of hormones that accompanies psychological stress[37,38] and physical activity.[39] As overtime work is very often accompanied by such stress and physical activity, it is quite obvious to expect an association between long working hours and hypertension. Association of working hours per day with the risk for development of hypertension during five years in hypertension free subjects is shown in table 2.[40] During five years of follow up of 3940 person years were stuided, 336 men developed hypertension above the borderline level. The multivariate adjusted relative risk for hypertension above the borderline level, compared with those who worked < 8.0 hours per day, was 0.91 (95% confidence intervals (CI): 0.69, 1.21) for those who worked 8.0–8.9 hours per day, 0.79 (95% CI: 0.57, 1.08) for those who worked 9.0–9.9 hours per day, 0.63 (95% CI: 0.43, 0.91) for those who worked 10.0–10.9 hours per day, and 0.48 (95% CI: 0.31, 0.74) for those who worked > 11.0 hours per day (p for trend < 0.001). As for the incidence of definite hypertension, 88 men developed definite hypertension during five years of follow up (representing 4531 person years). The respective multivariate adjusted relative risks for definite hypertension, compared with those who worked < 8.0 hours per day, were 0.68 (95% CI: 0.39, 1.18), 0.93 (95% CI: 0.53, 1.65), 0.56 (95% CI: 0.27, 1.17), and 0.33 (95% CI: 0.11, 0.95) (p for trend = 0.045).[40]

Table 2. Correlation of working hours per day and the risk of hypertension.

	Working hours per day					
	<8.0	8.0-8.9	9.0-9.9	10.0-10.9	>11.0	p for trend*
Hypertension above the borderline level						
Cases	113	92	61	41	29	
Person years	1022	969	695	645	610	
Rate per 1000 person years	110.6	94.9	87.8	63.6	47.6	
Age adjusted relative risk	1.00	0.86	0.81	0.60	0.45	<0.001
(95 % CI)	(Reference)	(0.66, 1.14)	(0.60, 1.11)	(0.42, 0.87)	(0.30, 0.68)	
Multivariate adjusted relative risk	1.00	0.91	0.79	0.63	0.48	<0.001
(95 % CI)	(Reference)	(0.69, 1.21)	(0.57, 1.08)	(0.43, 0.91)	(0.31, 0.74)	
Definite hypertension						
Cases	31	23	20	10	4	
Person years	1221	1160	782	711	658	
Rate per 1000 person years	25.4	19.8	25.6	14.1	6.1	
Age adjusted relative risk	1.00	0.78	1.03	0.57	0.25	0.010
(95% CI)	(Reference)	(0.45, 1.34)	(0.58, 1.81)	(0.28, 1.18)	(0.09, 0.70)	
Multivariate adjusted relative risk	1.00	0.68	0.93	0.56	0.33	0.045
(95% CI)	(Reference)	(0.39, 1.18)	(0.53, 1.65)	(0.27, 1.17)	(0.11, 0.95)	

Salt intake

It is well known that consumption of salt-rich diet lead to elevation of blood pressure in healthy individuals and is also responsible for making body vulnerable for cardiovascular events, intake of salt in food is generally not within the safe limit (5 g = 87 mmol per day) in developed as well as underdeveloped countries .[41] Even a moderate reduction in salt intake in the general population would be able to have an impact on health and it would reverse 8.5 million cardio-vascular related deaths in the world within a time interval of 10 years.[42] WHO have made a conclusion in a large meta analysis, that the management of cardiovascular diseases is having 11 % part in the total health expenditure in the world.[43]

The involvement of salt in developing hypertension is supported by the study of eight different randomized controlled trials of moderate dietary salt restriction, one observational review of a randomized controlled trial (TOHP Stage II) and one case-control study[44] including 2605 participants. The results gave evidence a reduction in systolic and diastolic blood pressure and urinary sodium excretion when the salt intake was reduced. The data in these 10 trials suggest that if we reduce consumption of salt in daily life, it will help us to maintain the blood pressure and help patients on anti-hypertensive therapy to leave or less use of medication without losing control on blood pressure. Other than blood pressure, studies also show the effects of low salt consumption on protein output of urine,[45] pulse wave velocity,[46] and other measures of vascular activities, namely aortic pulse wave velocity and augmentation index,[47] heart rate variability,[48] carotid artery compliance in the middle aged to older men and women,[49] and variability and consistency of individual systolic blood pressure responses.[50, 51]

There are many strong evidences which support the role of salt intake in causing hypertension. The normal salt ingestion in most countries lies between 9 and 12 g day^{-1}.[52]

In Latin American and the Caribbean countries, after year 2000, its value exceeds 9 g day^{-1}.[53] It is about 40 times higher than the amount our ancestors consumed during several million years of their development. This high increase in salt ingestion is relatively recent in evolutionary terms. Physiological systems also face challenge when this amount of salt is excreted through kidneys which causes a gradual rise in BP[54,55] and body become vulnerable to CVD and kidney diseases. An update on the evidences related to the role of salt intake to BP and cardiovascular diseases has been published. The report also provides a brief update on salt reduction programs being carried out in several countries, particularly in the Americas.[56]

Treatment

As recommended by Joint National Committee 7 of WHO, a practical approach regarding this is to continue to involve lifestyle modifications (non pharmacological treatment). If it does not give the expected results, then pharmacological therapy should be introduced.[57] These therapies work only in the case of sustained hypertension, they are not meant for resistant hypertension.

Non-pharmacological

Modification in the lifestyle is the key process to prevent the onset of hypertension and is necessary therapy for those who are suffering from hypertension.[58] Lifestyle modifications should be introduced, whenever appropriate, in all patients, including those who require drug treatment. The main goal is to lower BP, to control cardiovascular risk factors and to reduce the number or the doses of antihypertensive drugs to a minimum level.[59]

These modifications include weight reduction in overweight or obese patients, physical activity, controlled sodium intake, the adoption of the Dietary Approaches to Stop Hypertension (DASH) diet, controlled alcohol consumption, and reduction in smoking. According to these guidelines, patients whose SBP (Systolic BP) and DBP (Diastolic BP) falls between 130 and 139 mmHg and 80 and 89 mmHg, respectively, should modify their lifestyle to control BP but the effect of this therapy should be observed for maximum of 3 months. If it is not working then the patient should move towards pharmacological treatment.[57]

Dietary modification

DASH-trial proved reductions in BP of 11.4/5.5 mmHg in persons having hypertension on a diet rich in fruits, vegetables, and low-fat dairy products, compared with those people who were on a so-called "usual American diet". Dietary salt intake and weight were kept constant.[60] Another two clinical trials, one with a comprehensive food plan that supplied the recommended dietary allowances of all major nutrients and the other with a diet rich in fruits, vegetables, and low-fat dairy products and reduction in saturated and total fat produced reductions in BP comparable to or greater than those usually seen with monotherapy for stage 1 hypertension.[61, 62] Dietary salt intake has a linear association with blood pressure. Reduced sodium intake to approximately 100 mmol day^{-1} can prevent the development of hypertension.[63]

Weight loss and physical activity

Overweight (body mass index >25 kg/m^2) has been seen in epidemiologic studies to be an important risk factor for higher blood pressure, and there seems to be a linear relation between body weight and blood pressure.[64] Clinical trials have shown that weight loss, specially when combined with dietary sodium restriction, lowers blood pressure in hypertensive and also in normotensive patients. The Hypertension Prevention Trial showed that a 4 % reduction in body weight over 3 years was associated with a 2.4 mmHg reduction in SBP and a 1.8 mmHg reduction in DBP.[63] Increasing aerobic physical activity such as brisk walking, jogging, swimming or bicycling has been shown to lower BP. A meta-analysis of 54 randomized controlled trials showed a net reduction of 3.8 mmHg in SBP and 2.6 mmHg in DBP in individuals performing aerobic exercises, compared to controls.[65]

Pharmacological treatment

As blood pressure increases, it become more difficult to control it at the target level through life style modifications alone and treatment with antihypertensive drugs becomes necessary. WHO guidelines also recommend the use of antihypertensive drugs in patients with grade 1 hypertension at low or moderate cardiovascular risk, that is, when BP is between 140 and 159 mmHg SBP and/or 90 and 99 mmHg DBP, provided nonpharmacological treatment has proved unsuccessful. So, in these conditions the patient should move towards pharmacological treatment.

Diuretics

The steady introduction of newer agents and their heavy promotion by the industry made physicians switch away from use of diuretics as first line agents in the treatment of mild to moderate hypertension but then also thiazide type of diuretics offer better reduction of blood pressure with lesser incidence of coronary revascularization and heart failure as compared to other drugs like CCB, ACEI or ARB.[66] The evidence from the SHEP study emphasizes the value of a low-dose thiazide-type drug as initial therapy for isolated systolic hypertension in older patients.[67] Clinical trial data also indicate that diuretics are generally well tolerated.[66-68]

β-Blockers

These drugs decrease cardiac output and the slowing of heart rate and was originally thought to be of clinical importance, particularly in hypertensive patients with tachycardia. But, at the same time, peripheral resistance is increased slightly and sodium reabsorption by the kidney is increased. The ability of β-blockers to inhibit activity of the RAS by reducing the release of renin from the juxtaglomerular cells of the kidney may contribute to their blood pressure lowering effects, especially in patients with medium or high levels of plasma renin activity.[69] Over time, they became widely accepted for the treatment of hypertension, and one of the reasons for the acceptance of this drug class by clinicians was that these agents appeared to be better tolerated than many of the drugs previously available for treating hypertension.[70]

Angiotensin-converting enzyme Inhibitors, angiotensin receptor antagonists and renin inhibitors

Inhibitors of the renin-angiotensin system (RAS), including ACE-inhibitors, ARBs and now direct rennin inhibitor (DRI) are commonly used in the treatment of hypertension.[71] ACE-inhibitors modulate blood pressure by inhibiting ACE mediated conversion of angiotensin I to angiotensin II. ARBs modulate blood pressure by inhibiting the activation of the AT1 receptor by angiotensin II.[72] Aliskiren, a direct renin inhibitor, is the first of a new class of antihypertensive drugs that block the RAS further upstream. Its antihypertensive effect, safety, and tolerability are comparable with ARBs and ACE inhibitors, however, its long-term data is awaited.[73]

Calcium channel blockers

CCBs which include both dihydropyridines (DHPs) e.g., nifedipine and amlodipine and non-dihydropyridines, like verapamil and diltiazem, are among the most widely prescribed agents for the management of essential hypertension. Several large outcome risk trials and comprehensive meta-analyses have found that CCBs reduce the cardiovascular morbidity and mortality associated with uncontrolled hypertension, including stroke.[74] Conditions favoring the choice of a DHP CCB for hypertension include: advanced age, isolated systolic hypertension, angina pectoris, peripheral vascular disease, carotid atherosclerosis, and pregnancy. Diltiazem or verapamil is considered for use in patients with angina pectoris or supraventricular tachycardia.

Alpha-1 receptor antagonist

A1-adrenergic blocking drugs are effective in reducing blood pressure and do so in a fashion comparable to most other antihypertensive drug classes.[75] Initially, for many years α1-adrenergic antagonists had been considered suitable initial drugs for uncomplicated early-stage hypertension. But guidelines including the European Society of Hypertension/European Society of Cardiology and the authors of the JNC 7 no longer include α1-adrenergic antagonists as initial agents for the treatment of hypertension.[57,59,76]

TRPV1 antagonists

Transient Receptor Potential Vanilloid Receptor type 1 is the latest site for the antihypertensive action. The endocannabinoid, anandamide, can have depressor effects and its production is upregulated in certain pathophysiological states.[77] TRPV1 receptor has been implicated in the hypotensive effects of anandamide.[78-80] Oleamide (*cis*-9 10 octadecenoamide) is a fatty acid primary amide, which was originally derived from sleep-deprived cats and shares structural similarities with anandamide.[81]

Conclusion

After reviewing the literature, it is concluded that hypertension is one of the biggest challenge in the present scenario. Each and every country of the world is in the grip of the disease irrespective of the status of its development. The disease is having prevalent in every kind of population. Now there is a need to make people aware regarding the enormity of the disease and the ways to prevent it. Patient should be given first the nonpharmacological treatment and then they should move towards the pharmacological treatment, if necessary. Life style of the people is the main cause of hypertension and it need to be modified. The world is developing, everything is going in a forward direction so we need to move our health in a forward direction.

References

[1]Kearney, P. M., Whelton, M., Reynolds, K., Whelton, P. K., He, J., *J. Hypertens.*, **2004**, *22(1)*, 1-9. https://doi.org/10.1097/00004872-200401000-00003

[2]World Health Report 2002. Reducing risks, promoting healthy life. Geneva, Switzerland: World Health Organization, **2002**. http://www.who.int/whr/2002.

[3]Booth, F. W., Gordon, S. E., Carlson, C. J., Hamilton, M. T., *J. Appl. Physiol.*, **2000**, *88(2)*, 774-787.

[4]Luft, F. C., Molecular J. Hypertens. **1998**, 16, 1871–1878. https://doi.org/10.1097/00004872-199816121-00004

[5]INTERSALT Co-operative Research Group, *J. Hypertens.*, **1988**, *6(Suppl 4)*, S584–S586. https://doi.org/10.1097/00004872-198812040-00183

[6]Sever, P. S., Poulter, N. R., *J. Hypertens.*, **1989**, *7(Suppl 1)*, S9–S12. https://doi.org/10.1097/00004872-198902001-00004

[7]Booth, F. W., Gordon, S. E., Carlson, C. J., Hamilton, M. T., *J. Appl. Physiol.*, **2000**, *88(2)*, 774-787.

[8]Fagard, R. H., Cornelissen, V. A., *Eur. J. Cardiov. Prev. R.*, **2007**, *14*, 12-17. https://doi.org/10.1097/HJR.0b013e3280128bbb

[9]Hagberg, J. M., Park, J. J., Brown, M. D., *Sports Med.*, **2000**, *30*, 193-206. https://doi.org/10.2165/00007256-200030030-00004

[10]Halm, J., Amoako, E., *Ethnic Dis.*, **2008**, *18(3)*, 278-282.

[11]Padilla, J., Wallace, J. P., Park, S., *Med. Sci. Sport Exer.*, **200**5, *37(8)*, 1264-1275. https://doi.org/10.1249/01.mss.0000175079.23850.95

[12]Dickinson, H. O., Mason, J. M., Nicolson, D. J., *J. Hypertens.*, **2006**, *24(2)*, 215-233. https://doi.org/10.1097/01.hjh.0000199800.72563.26

[13]Bacon, S. L., Sherwood, A., Hinderliter, A., Blumenthal, J. A., *Sports Med.*, **2004**, *34(5)*, 307-316. https://doi.org/10.2165/00007256-200434050-00003

[14]Liu, L., Kanda, T., Sagara, M., *Hypertens. Res.*, **2001**, *24*, 145-151. https://doi.org/10.1291/hypres.24.145

[15]Chobanian, A. V., Bakris, G. L., Black, H. R., *Hypertension*, **2003**, *42(6)*, 1206-1252. https://doi.org/10.1161/01.HYP.0000107251.49515.c2

[16]U.S. Preventive Services Task Force, *Behavioral Counseling in Primary Care to Promote Physical Activity*, Agency for Healthcare Research and Quality, Rockville, MD, **2002**.

[17]Elley, C. R., Kersen, N., Arroll, B., Robinson, E., *BMJ,* **2003**, *326*, 793-798. https://doi.org/10.1136/bmj.326.7393.793

[18]Schuler, J. L., O'Brien, W. H., *Psychophysiology* , **1997**, *34*, 649-659. https://doi.org/10.1111/j.1469-8986.1997.tb02141.x

[19]McEwen, B. S., *Physiol. Rev.*, **2007**, *87*, 873-904. https://doi.org/10.1152/physrev.00041.2006

[20]*Stress and the Heart: Psychosocial Pathways to Coronary Heart Disease,* Eds S. A Stansfeld, M. G Marmot, BMJ 2002; https://doi.org/10.1136/bmj.324.7330.176a

[21]Linden, W., Moseley, J. V., *Appl. Psychophys. Biof.*, **2006**, *31*, 51-63. https://doi.org/10.1007/s10484-006-9004-8

[22]Yan, L. L., Liu, K., Matthews, K. A., Daviglus, M. L., Ferguson, T. F., Kiefe, C. I., *JAMA,* **2003**, *290*, 2138-2148. https://doi.org/10.1001/jama.290.16.2138

[23]Steptoe, A., Brydon, L., Kunz-Ebrecht, S., *Psychosom. Med.*, **2005**, *67*, 2817-2120.

https://doi.org/10.1097/01.psy.0000156932.96261.d2

[24]Rosengren, A., Hawken, S., Ounpuu, S., Sliwa, K., Zubaid, M., Almahmeed, W. A., *Lancet*, **2004**, *364*, 953-962. https://doi.org/10.1016/S0140-6736(04)17019-0

[25]Maxwell, V. R., Schneider, R. H., Ndich, S. I., Gaylord-King, C., Salerno, J. W., Anderson, J. W., *Curr. Hypertens. Rep.*, **2007**, *9*, 520-528. https://doi.org/10.1007/s11906-007-0094-3

[26]Patel, C., North, W. R., *Lancet*, **1975**, *2*, 93–95. https://doi.org/10.1016/S0140-6736(75)90002-1

[27]Ono, Y., Watanabe, S., Kaneko, S., *J. Hum. Ergol. (Tokyo)*, **1991**, *20*, 155–164.

[28]Proctor, S. P., White, R. F., Robins, T. G., *Scand. J. Work Env. Health,* **1996**, *22*, 124–132. https://doi.org/10.5271/sjweh.120

[29]Waersted, M., Westgaard, R. H., *Ergonomics*, **1991**, *34*, 265–276. https://doi.org/10.1080/00140139108967312

[30]Cooper, C. L., Davidson, M. J., Robinson, P., *J. Occup. Med.*, **1982**, *24*, 30–36. https://doi.org/10.1097/00043764-198209000-00009

[31]Richardsen, A. M., Burke, R. J., *Soc. Sci. Med*., **1991**, *33*, 1179–1187. https://doi.org/10.1016/0277-9536(91)90234-4

[32]Cooper, C. L., Roden, J., *Soc. Sci. Med*., **1985**, *21*, 747–751. https://doi.org/10.1016/0277-9536(85)90122-4

[33]Hurrel, J. J., Lindström, K., *Scand. J. Work Env. Healt*., **1992**, *18 (suppl 2)*, S11–S13. https://doi.org/10.5271/sjweh.1613

[34]Watanabe, S., Torii, J., Shinkai, S., *Environ. Res*., **1993**, *61*, 258–265. https://doi.org/10.1006/enrs.1993.1070

[35]Russek, H. I., Zohnman, B. L., *Am. J. Med. Sci*., **1958**, *235*, 266–275. https://doi.org/10.1097/00000441-195803000-00003

[36]Buell, P., Breslow, L., *J. Chron. Diseases*., **1960**, *11*, 615–626. https://doi.org/10.1016/0021-9681(60)90060-6

[37]Kageyama, T., Nishikido, N., Kobayashi., *Lancet*, **1997**, *350*, 639. https://doi.org/10.1016/S0140-6736(05)63328-4

[38]Rissler, A., *Ergonomics*, **1978**, *20*, 13–16.

[39]Watson, R. D., Hamilton, C. A., Reid, J. L., *Hypertension*, **1979**, *1*, 341–346. https://doi.org/10.1161/01.HYP.1.4.341

[40]Nakanishi, N., Yoshida, H., Nagano, K., Kawashimo, H., Nakamura, K., Tatara, K., *J. Epidemiol. Commun. H*., **2001**, *55*, 316-322. https://doi.org/10.1136/jech.55.5.316

[41]World Health Organization, *Sodium, chlorides and conductivity in drinking water*, EURO reports and studies, No. 2. WHO Regional Office for Europe, Copenhagen, Denmark, **1979**.

[42]Asaria, P., Chisholm, D., Mathers, C., Ezzati, M., Beaglehole, R., *Lancet*, **2007**, *370*, 2044-2053. https://doi.org/10.1016/S0140-6736(07)61698-5

[43]Australia's Health: *The 10th biennial heath report of the Australian Institute of Health and Welfare*. Health Expenditure, Canberra, Australia, **2005**.

[44]Kojuri, J., Rahimi, R., *BMC Cardiovasc. Disor*., **2007**, *7*, 34.

[45]Pauline, S. A., Markandu, N. D., Sagnella, G. A., He, F. J., MacGregor, G. A., *Hypertension*, **2005**, *46*, 308-312. https://doi.org/10.1161/01.HYP.0000172662.12480.7f

[46]He, F. J., MacGregor, G. A., *J. Hum. Hypertens*. **2009**, *23*, 363-384. https://doi.org/10.1038/jhh.2008.144

[47]Dickinson, K. M., Keogh, J. B., Clifton, P. M., *Am. J. Clin. Nutr*., **2009**, *89*, 485- 490. https://doi.org/10.3945/ajcn.2008.26856

[48]Mäkelä, P., Vahlberg, T., Kantola, I., Vesalainen, R., Jula, A., *Am. J. Hypertens*., **2008**, *21*, 1183-1187. https://doi.org/10.1038/ajh.2008.272

[49]Gates, P. E., Tanaka, H., Hiatt, W. R., Seals, D. R., *Hypertension*, **2004**, *44*, 35-41. https://doi.org/10.1161/01.HYP.0000132767.74476.64

[50]Obarzanek, E., Michael, A. P., William, M. V., Thomas, J. M., Frank, M. S., Lawrence, J. A., Laura, P. S., Marlene, M. M., Jeffrey, A. C., *Hypertension*, **2003**, *42*, 459-467. https://doi.org/10.1161/01.HYP.0000091267.39066.72

[51]Lala, M. A., Nazar, M. J, Bojrenu, M., Lala H., *Endocrin. Metab. Synd*., **2015**, *4*, 2-6. https://doi.org/10.4172/2161-1017.1000175

[52]Brown, I. J., Tzoulaki, I., Candeias, V., Elliott, P., *Int. J. Epidemiol*., **2009**, *38*, 791–813. https://doi.org/10.1093/ije/dyp139

[53]Legetic, B., Campbell, N., *J. Health. Commun*., **2011**, *16 (Suppl 2)*, 37–48. https://doi.org/10.1080/10810730.2011.601227

[54]He, F. J., MacGregor, G. A., *Prog. Cardiovasc. Dis*., **2010**, *52*, 363–382. https://doi.org/10.1016/j.pcad.2009.12.006

[55]Intersalt Cooperative Research Group, *BMJ,* **1988**, *297*, 319–328. https://doi.org/10.1136/bmj.297.6644.319

[56]He, F. J., Campbell, N. R. C., MacGregor, G. A., *Rev. Panam. Salud. Publ*., **2012**, *32(4)*, 293–300. https://doi.org/10.1590/S1020-49892012001000008

[57]Seventh Report of the Joint National Committee on Prevention, Detection, Evaluation, and Treatment of High Blood Pressure. Hypertension, **2003**, *42*, 1206–1252. https://doi.org/10.1161/01.HYP.0000107251.49515.c2

[58]Hackam, D. G., Khan, N. A., Hemmelgarn, B. R., Rabkin, S. W, Touyz, R. M., Campbell, N. R. , Padwal, R., Campbell, T. S., Lindsay, M. P., Hill, M. D., Quinn, R. R., Mahon, J. L., Herman, R. J., Schiffrin, E. L., Ruzicka, M., Larochelle, P., Feldman, R. D., Lebel, M., Poirier, L., Arnold, J. M., Moe, G. W., Howlett, J. G., Trudeau, L., Bacon, S. L., Petrella, R. J., Milot, A., Stone, J. A., Drouin, D., Boulanger, J. M., Sharma, M., Hamet, P., Fodor, G., Dresser, G. K., Carruthers, S. G., Pylypchuk, G., Burgess, E. D., Burns, K. D., Vallée, M., Prasad, G. V., Gilbert, R. E., Leiter, L. A., Jones, C., Ogilvie, R. I., Woo, V., McFarlane, P. A., Hegele, R. A., Tobe, S. W., *Can. J. Cardiol*., **2010**, *26*, 249–258. https://doi.org/10.1016/S0828-282X(10)70379-2

[59]Mancia, G., DeBacker, G., Dominiczak, A., Cifkova, R., Fagard, R., Germano, G., Grassi, G., Heagerty, A. M., Kjeldsen, S. E., Laurent, S., Narkiewicz, K., Ruilope, L., Rynkiewicz, A., Schmieder, R. E., Boudier, H. A., Zanchetti, A., Vahanian, A., Camm, J., DeCaterina, R., Dean, V., Dickstein, K., Filippatos, G., Funck-Brentano, C., Hellemans, I., Kristensen, S. D. , McGregor, K., Sechtem, U., Silber, S., Tendera, M., Widimsky, P., Zamorano, J. L., Erdine, S., Kiowski, W., Agabiti-Rosei, E., Ambrosioni, E., Lindholm, L. H., Viigimaa, M., Adamopoulos, S., Agabiti-Rosei, E., Ambrosioni, E., Bertomeu, V., Clement, D., Erdine, S., Farsang, C., Gaita, D., Lip, G., Mallion, J. M., Manolis, A. J., Nilsson, P. M., O'Brien, E., Ponikowski, P., Redon, J., Ruschitzka, F., Tamargo, J., vanZwieten, P., Waeber, B., Williams B., *J. Hypertens*., **2007**, *25*, 1105–1187. https://doi.org/10.1097/HJH.0b013e3281fc975a

[60]Carretero, O. A., Oparil, S., *Circulation*, **2000**, *101*, 446–453. https://doi.org/10.1161/01.CIR.101.4.446

[61]McCarron, D. A., Oparil, S., Chait, A., Haynes, R. B., Kris-Etherton, P., Stern, J. S., Resnick, L. M., Clark, S., Morris, C. D., Hatton, D. C., Metz, J. A., McMahon, M., Holcomb, S., Snyder, G. W., Pi-Sunyer, F. X., *Arch. Intern. Med*., **1997**, *157*, 169–177. https://doi.org/10.1001/archinte.1997.00440230041006

[62]Svetkey, L. P., Simons-Morton, D., Vollmer, W. M., Appel, L. J., Conlin, P. R., Ryan, D. H., Ard, J., Kennedy, B. M., *Arch. Intern. Med*., **1999**, *159*, 285–293. https://doi.org/10.1001/archinte.159.3.285

[63]Trials of Hypertension Prevention Collaborative Research Group, Effects of weight loss and sodium reduction intervention on blood pressure and hypertension incidence in overweight people with high-normal blood pressure: the Trials of Hypertension Prevention, Phase II. Arch. Intern. Med., **1997**, 157, 657–67. https://doi.org/10.1001/archinte.1997.00440270105009

[64]Doll, S., Paccaud, F., Bovet, P., Burnier, M., Wietlisbach, V., *Int. J. Obes. Relat. Metab. Disord*., **2002**, *26*, 48–57. https://doi.org/10.1038/sj.ijo.0801854

[65]Whelton, S. P., Chin, A., Xin, X., He, J., *Ann. Intern. Med*., **2002**, *136*, 493–503. https://doi.org/10.7326/0003-4819-136-7-200204020-00006

[66]ALLHAT Collaborative Research Group. *JAMA*, **2002**, *288*, 2981–2997. https://doi.org/10.1001/jama.288.23.2981

[67]Kostis, J. B., Wilson, A. C., Freudenberger, R. S., Cosgrove, N. M., Pressel, S. L., Davis, B. R., *Am. J. Cardiol.*, **2005**, *95*, 29–35. https://doi.org/10.1016/j.amjcard.2004.08.059

[68]Materson, B. J., Reda, D. J., Cushman, W. C., Massie, B. M., Freis, E. D., Kochar, M. S., Hamburger, R. J., Fye, C., Lakshman, R., Gottdiener, J., Ramirez, E. A. and Henderson, W. G., *New Engl. J. Med.*, **1993**, *328*, 914–921. https://doi.org/10.1056/NEJM199304013281303

[69]Buhler, F. R., Laragh, J. H., Baer, L. Vaughan, E. D., Jr, Brunner, H. R., *N. Engl. J. Med.*, **1972**, *287*, 1209–1214.

[70]Weber, M. A. Bakris, G. L., Giles, T. D., Messerli, F. H., *J. Clin. Hypertens.*, **2008**, *10*, 234–238. https://doi.org/10.1111/j.1751-7176.2008.07843.x

[71]Mann, J. F. E., Hilgers, K. F., Renin-angiotensin system inhibition in the treatment of hypertension, Eds., Bakris, G. L., Kaplan N. Kluwer, 2**010**., http://www.uptodate.com/patients/content/topic.

[72]Ram, C. V. S., *Am. J. Med.*, **2008**, *121*, 656–663. https://doi.org/10.1016/j.amjmed.2008.02.038

[73]Gradman, A. H., Schmieder, R. E., Lins, R. L. Nussberger, J., Chiang, Y., Bedigian, M. P., *Circulation*, **2005**, *111*, 1012–1018. https://doi.org/10.1161/01.CIR.0000156466.02908.ED

[74]Basile, J., *J. Clin. Hypertens.*, **2004**, *6*, 621–631. https://doi.org/10.1111/j.1524-6175.2004.03683.x

[75]Sica, D. A., *J. Clin. Hypertens. (Greenwich)*, **2005**, *7*, 757–762. https://doi.org/10.1111/j.1524-6175.2005.05300.x

[76]Iqbal, M., *Indian J. Clin. Med.*, **2011**, *2*, 1–17.

[77]Ho, W. S. V., Gardiner, S. M., *Br. J. Pharmacol.*, **2009**, *156*, 94–104. https://doi.org/10.1111/j.1476-5381.2008.00034.x

[78]Batkai, S., Pacher, P., Osei-Hyiaman, D., Radaeva, S., Liu, J., Harvey-White, J., Offertaler, L., Mackie, K., Rudd, M. A., Bukoski, R. D., Kunos, G., *Circulation*, **2004**, *110*, 1996–2002. https://doi.org/10.1161/01.CIR.0000143230.23252.D2

[79]Lake, K. D., Martin, B. R., Kunos, G., Varga, K., *Hypertension*, **1997**, *29*, 1204–1210. https://doi.org/10.1161/01.HYP.29.5.1204

[80]Wang, Y. P., Kaminski, N. E., Wang, D. H., *J. Pharmacol. Exp. Ther.*, **2007**, *321*, 763–769. https://doi.org/10.1124/jpet.106.112904

[81]Cravatt, B. F., Prosperogarcia, O., Siuzdak, G., Gilula, N. B., Henriksen, S. J., Boger, D. L., Lerner, R. A., *Science*, **1995**, *268*, 1506–1509. https://doi.org/10.1126/science.7770779

COMPARATIVE QUANTIFICATION OF ESCIN FROM DIFFERENT PRODUCTS

Andreia Corciova[a]* and Bianca Ivanescu[b]

The paper aimed to quantify the saponins expressed in escin, the major bioactive constituent of Aesculus hippocastanum, from five different pharmaceutical formulations: two types of tablets, and one type of gel, tincture, and glycerol-hydroalcoholic extract. The products are part of over the counter drugs and dietary supplements categories. Two spectrophotometric methods were used to quantify the escin, after separation from the other active ingredients and excipients. The first method, calibration curve method, is based on the reaction between the oxidized triterpenoid saponins and vanillin and records the absorbance at 560 nm. The limit of detection, limit of quantification, and the RSD values were calculated. The second method is based on the molar absorptivity of escin. Both methods have proved to be suitable for the determination of escin in different products.

* Corresponding Authors
    Fax: +40.232.211.820
    E-Mail: acorciova@yahoo.com
[a] "Grigore T. Popa" University of Medicine and Pharmacy Iasi, Faculty of Pharmacy, Department of Drugs Analysis, 16 Universitatii Street, 700115 Iasi, Romania
[b] "Grigore T. Popa" University of Medicine and Pharmacy Iasi, Faculty of Pharmacy, Department of Pharmaceutical Botany, 16 Universitatii Street, 700115 Iasi, Romania

Introduction

Saponins are secondary metabolites of plants with important pharmacological properties, like antibacterial,[1-3] cytotoxic,[3,4] immunostimulant,[5] antidiabetic,[6] anti-inflammatory and antiulcerogenic,[7] antioxidant[8] etc. Saponins are amphiphilic compounds and tend to form mixed aggregates in solution, making their analysis difficult.[9] For saponins analysis, the literature provides several types of methods, among including spectrophotometric methods,[10] TLC,[11,12] HPLC (with different detection methods: UV, MS, ELSD),[13-17] gas chromatography[18] and capillary electrophoresis[19].

Escin is a complex mixture of triterpenoid saponin glycosides, which is mainly found in *Aesculus hippocastanum* (horse-chestnut).[20] The mixture consists of α-escin and mainly β-escin isomers.[21] The actions of escin reported in various studies are anti-inflammatory,[21] anti-edematous,[21] venotonic,[21,22] anti-cancer,[20,23] and antiallergic[24] properties. Spectrophotometric methods,[25] TLC,[26,27] HPLC,[28,29] etc. can be used for analysis of escin.

The purpose of this paper was to determine the escin by fast, simple, cheap spectrophotometric methods that are easily available to most laboratories. The samples taken for testing included horse-chestnut extract in combination with flavonoids like diosmin, rutin, hesperidin, or with acerola fruit extract (*Malpighia glabra*), butcher's broom (*Ruscus aculeatus*), common bilberry (*Vaccinium myrtillus*), centella (*Centella asiatica*) and vitamin C. The product package provides their utilization especially for: restoring and maintaining the tonus of the vascular walls, the functionality and elasticity of the veins, the capillary resistance and permeability, the vascular elasticity and blood circulation of the legs, and for relief of leg heaviness.

Experimental

Materials

Escin, standard substance, was supplied from Merck (Germany). All the reagents used were analytical grade reagents. The products for testing, dietary suppliments and over the counter drugs, were purchased from pharmacy and herbal stores and they consisted of two products in the form of coated tablets, sample 1 comprising of dried horse-chestnut extract 250 mg/per unit expressed in 50 mg/tablet escin, butcher's broom extract ((*Ruscus aculeatus*), common bilberry (*Vaccinium myrtillus*), centella (*Centella asiatica*), vitamin C, hesperidin and sample 2 comprising of dried horse-chestnut extract 200 mg/tablet, micronized diosmin, rutin trihydrate, acerola fruit extract (*Malpighia glabra*). Sample 3 was gel type consisting of *Aesculus hippocastanum* extract, *Ruscus aculeatus* extract, *Centella asiatica* extract and *Vaccinium myrtillus* extract. Sample 4 was of tincture type, an extract from horse-chestnut seeds (20 g %) in 70% (v / v) ethanol. Sample 5 was a glycerol-hydroalcohol extract of fresh horse-chestnut sprouts (45 % ethanol) (1.5 mL unit).

A Jasco V 530 double beam UV-Vis spectrophotometer with a scan range of 400-800 nm was used.

Sample Processing

For the Sample 1 and 2, prior to analysis, 20 tablets were weighed, and their average mass was calculated, after which they were crushed into a fine homogenised powder. Further, some quality parameters were tested i.e., disintegration time and friability, according to European Pharmacopoeia.[30]

By performing the disintegration test in water, no tablet must disaggregate for 30 min. After that, the operation was repeated, replacing water with 0.1 M hydrochloric acid and monitoring the time for tablet disintegration. Each determination was repeated on five tablets and the mean value of the determinations was calculated. For the friability test, because the analyzed tablets had an individual mass greater than 0.65 g, 10 tablets were used. The determinations were repeated twice and the average of the results was calculated.

Preparation of Solutions

To a quantity of powder corresponding to one tablet, 30 mL of 70 % (v/v) ethanol was added and the mixture was extracted by magnetic stirring for 60 min at 50 ^{0}C. The extract was filtered through Whatman paper in a 50 mL volumetric flask, the filter was washed several times with ethanol and the flask was filled to the mark. Dilutions suitable for determination were made.

For sample 3, to a specific weighed quantity of gel, 50 mL of 70 % (v/v) ethanol was added. The mixture was stirred for 60 minutes at 50 ^{0}C. The extract was filtered in a 50 mL volumetric flask, washing the filter several times and filling the flask to the mark. Dilutions suitable for determination were made. The analyses of samples 4 and 5 were made after suitable dilutions with 70% (v/v) ethanol.

Methods

The quantitative analysis of saponins expressed in escin was carried out by UV-Vis spectrophotometry using the calibration curve method and the molar absorptivity method.

In the first procedure, the samples were treated with 8 % vanillin (alcoholic solution) and 72 % H_2SO_4 after which the mixture was incubated at 70 ^{0}C for 10 minutes. After a rapidly cooling on ice to room temperature, the absorbance of the solutions was measured at 560 nm. From the stock standard solution (0.1 g %), the standard scale solutions were prepared in the range 1-10 mg/L.[31] In the second procedure, the samples were treated with Folin-Ciocalteu reagent (1:10 dilution), after which 7.5 % Na_2CO_3 solution was added. The intensity of the blue color obtained was measured at 760 nm after a reaction time of 2 h.[32] For both methods the determinations were made in triplicate, within 3 consecutive days.

Results and discussion

The quality parameters (disintegration time, friability, average weight) for the samples 1 and 2 are presented in table 1.

Table 1. Quality parameters for the analysed tablets

Samples	Disintegration time (min) average ± SD	Friability g % average ± SD	Average weight (g)
Sample 1	29.65 ± 0.43	0.4095 ± 0.0017	1.3663
Sample 2	14.77 ± 0.48	0.2790 ± 0.0011	1.0540

According to the European Pharmacopoeia, the coated tablets should not disintegrate in water for at most 30 min but must disaggregate in 0.1 mol hydrochloric acid in 30 min. No tablet has disaggregated in water. As can be seen from the data obtained, all analyzed samples are included in the specifications limits of the pharmacopoeia for coated tablets, obtaining a range of 28.22 - 29.08 for sample 1, and

an interval of 14.29 - 15.25 for sample 2. If we should make a hierarchy based on the time of active substance release from the tablets and the availability of the substance for absorption resulting in a faster action, the quickest release of the active substance is obtained in the case of Sample2 as compared to Sample 1.

According to European Pharmacopoeia, regarding the friability parameter, the maximum mass loss considered acceptable is 1% of the mass of the tablets to be determined. As can be seen from table 1, all the tablets under analysis complied with the limits.

The basic principle of the first method is the reaction between oxidized triterpenoid saponins using sulfuric acid as an oxidizing agent and vanillin. In order to determine the total saponins expressed in escin in the analyzed samples, the calibration curve was design by plotting the mean values of absorbances of escin standard solutions versus concentrations. The statistical parameters for the analysis were presented in table 2.

Table 2. Statistical data for escin determination

Statistical parameters	Values
Correlation Coefficient (r^2)	0.9992
Standard error	0.0101
Intercept	0.6622
Slope	0.1105
Limit of detection	0.3041
Limit of quantification	0.9214

The calibration curve has a very good linearity in the range of analysis. The system precision was determined using a 5 mg L^{-1} solution, in 6 replicates. The SD (standard deviation of the mean) and % RSD (relative standard deviation) were calculated (Table 3).

Table 3. Experimental data for precision of the system

No.	Absorbance
1.	1.2012
2.	1.1998
3.	1.2218
4.	1.2107
5.	1.1967
6.	1.2028
Average	1.2055
SD	0.0092
% RSD	0.7678

RSD was 0.7678 %, being lower than 2 %, the value proposed by the European standards, so we can say that the system is precise.[33] Accuracy of the method was investigated by using three concentration levels, in triplicate. In table 4 are presented the experimental data of three consecutive days.

The recovery of the determination in three consecutive days was in the range of 97 – 100.6 % and the RSD values in the range 0.1149 – 0.9830 %. The RSD values were lower than 5 %, so the method is accurate.[33]

Table 4. Experimental data for the accuracy of the method.

Theoretical conc. mg L^{-1}	Day 1			Day 2		Day 3	
	Average calculated conc.	% Recovery	Average calculated conc.	% Recovery	Average calculated conc.	% Recovery	
2.5	2.51	100.4	2.47	98.8	2.49	99.6	
5	5.03	100.6	4.85	97.0	4.99	99.8	
7.5	7.53	100.4	7.39	98.5	7.49	99.8	
Average		100.46	Average	98.1	Average	99.73	
SD		0.1154	SD	0.9643	SD	0.1154	
% RSD		0.1149	% RSD	0.9830	% RSD	0.1157	

Table 5. Escin mg tablet^{-1} in sample 1.

Stated concentration	Method 1			Method 2		
	Day 1	Day 2	Day 3	Day 1	Day 2	Day 3
50 mg tablet^{-1}	51.12	50.87	50.78	51.01	48.97	49.78
	51.60	49.23	50.84	50.98	49.35	48.99
	51.43	49.87	50.91	50.24	49.86	50.10
Average ± SD/day	51.38 ± 0.24	49.99 ± 0.82	50.84 ± 0.06	50.74 ± 0.43	49.39 ± 0.44	49.62 ± 0.57
Average ± SD/sample	50.73 ± 0.7			49.91 ± 0.72		

Table 6. Escin mg tablet^{-1} in sample 2.

Stated Concentration	Method 1			Method 2		
	Day 1	Day 2	Day 3	Day 1	Day 2	Day 3
Not stated	39.48	38.50	39.72	38.94	38.10	38.89
	39.56	38.27	39.61	38.87	38.77	38.01
	39.87	38.19	38.48	38.25	38.12	38.23
Average ± SD/day	39.63 ± 0.2	38.32 ± 0.16	39.27± 0.68	38.68 ± 0.37	38.33 ± 0.38	38.37 ± 0.45
Average ± SD/sample	39.07± 0.67			38.46 ± 0.19		

Table 7. Escin mg 100 g^{-1} gel in sample 3.

Stated Concentration	Method 1			Method 2		
	Day 1	Day 2	Day 3	Day 1	Day 2	Day 3
Not stated	698.73	695.67	696.28	691.67	686.28	687.67
	697.45	695.82	696.55	691.82	686.55	687.25
	697.23	695.32	697.27	691.32	686.27	687.32
Average ± SD/day	697.80 ± 0.81	695.60 ± 0.25	696.70 ± 0.51	691.60 ± 0.25	686.36 ± 0.15	687.41 ± 0.22
Average ± SD/sample	696.70 ± 1.1			688.45 ± 2.77		

Table 8. Escin mg 100 g^{-1} tincture in sample 4.

Stated Concentration	Method 1			Method 2		
	Day 1	Day 2	Day 3	Day 1	Day 2	Day 3
Not stated	368.67	367.25	368.25	366.23	366.79	367.74
	367.26	368.01	368.15	367.76	368.27	367.10
	369.10	368.54	368.92	368.10	367.75	366.98
Average ± SD/day	368.34 ± 0.96	367.93 ± 0.64	368.44 ± 0.41	367.36 ± 0.99	367.60 ± 0.75	367.27 ± 0.40
Average ± SD/sample	368.23 ± 0.27			367.41 ± 0.17		

When applying the validated method to the analyzed samples, the total saponins value was expressed in mg escin/tablet and the values are shown in table 5 for sample1 and table 6 for sample 2. For the 3amples 3 and 4, the total saponins value was expressed in mg escin/100 g sample and the values are shown in table 7 and 8. For sample 5, the results are presented in table 9, expressed in mg escin/unit (1.5 mL).

Table 9. Escin mg/unit glycerol-hydroalcoholic extract in sample 5.

Stated Concentration	Method 1			Method 2		
	Day 1	Day 2	Day 3	Day 1	Day 2	Day 3
Not stated	0.2218	0.2035	0.2156	0.2226	0.2110	0.2232
	0.2305	0.2189	0.2333	0.2145	0.2045	0.2024
	0.2018	0.2301	0.2006	0.1958	0.2232	0.2115
Average ± SD/day	0.2180 ± 0.014	0.2175 ± 0.013	0.2165 ± 0.016	0.2109 ± 0.013	0.2129 ± 0.01	0.2123 ± 0.01
Average ± SD/sample	0.2173 ± 0.007			0.2120 ± 0.001		

The proposed spectrophotometric method is based on the reduction of phosphomolybdotungstic acid from the Folin-Ciocalteu reagent by escin, in the presence of sodium carbonate, to obtain a blue product. The molar absorptivity method was applied for calculation, knowing from the literature that for escin $\varepsilon = 1.0439 \times 10^4$ Lmol^{-1}cm^{-1}.[32] The results are presented for each sample in tables 3-7.

According to the leaflet, Sample 1 contains 250 mg of horse-chestnut extract/unit, corresponding to an escin content of 50 mg/tablet. If we consider a deviation according to Romanian Pharmacopoeia, Compressi Monograph, this would be ± 7. 5%,[34] which means 46.25-53.75 mg escin/tablet. If we consider a deviation according to European Pharmacopoeia,[33] this would be ± 5 %, which means 47.5-52.5 mg escin/tablet. Our results meet both national and European requirements.

According to the leaflet, the analyzed tablets from sample 2 contain 200 mg of horse-chestnut/tablet extract but the amount of escin mg/tablet is not specified. If we take into account the first analyzed product, we can consider that the 200 mg extract contains 40 mg escin/tablet, implicitly a 37-43 mg escin/tablet range according to Romanian Pharmacopoeia and 38-42 mg escin/tablet range according to European Pharmacopoeia. In this case also, we can consider that the results comply with both national and European requirements.

On samples 3, 4 and 5, the quantity of escin is not specified in the leaflet, so no comparison can be made with the declared quantity. But, we noted that between the two methods of analysis used, the differences are insignificant.

Conclusions

We analyzed five products in the over the counter and dietary supplements categories by two spectrophotometric methods using calibration curve and molar absorptivity methods. The methods were simple, easy to use and cheap. In the case of products that have the concentration stated on the label, the results comply with the limits imposed by regulations. For products that did not have the concentration specified on the label, a comparison could not be made. Thus, we draw attention to the need to include the concentration of active substances on the product label, even if they are part of the category of supplements.

References

[1] Mostafa, A., Sudisha, J., El-Sayed, M., Ito, S. I., Ikeda, T., Yamauchi, N., Shigyo, M., *Phytochem. Lett.*, **2013**, *6*, 274–280. https://doi.org/10.1016/j.phytol.2013.03.001.

[2] Teshima, Y., Ikeda, T., Imada, K., Sasaki, K., El-Sayed, M. A., Shigyo, M., Tanaka,S., Ito, S., *J. Agric. Food Chem.*, **2013**, *61*, 7440–7445. https://doi: 10.1021/jf401720q.

[3] Fouedjou, R.T., Teponno, R.B., Quassinti, L., Bramucci, M., Petrelli, D., Vitali, L.A., Fiorini, D., Tapondjou, L.A., Barboni, L., *Phytochem. Lett.* **2014**, *7*, 62–68. https://doi.org/10.1016/j.phytol.2013.10.001.

[4] Cheng, T. C., Lu, J. F., Wang, J. S., Lin, L. J., Kuo, H. I., Chen, B. H., *J. Agric. Food Chem.*, **2011**, *59*, 11319–11329. https://doi: 10.1021/jf2018758.

[5] Verza, S. G., Silveira, F., Cibulski, S., Kaiser, S., Ferreira, F., Gosmann, G., Roethe, P. M., Ortega, G. G., *J. Agric. Food Chem.*, **2012**, *60*, 3113–3118. https://doi: 10.1021/jf205010c.

[6] Joseph, B., Jini, D., *Asian Pac. J. Trop. Dis.*, **2013**, *3*, 93–102. https://doi.org/10.1016/S2222-1808(13)60052-3.

[7] Adão, C. R., da Silva, B. P., Parente, J. P., *Fitoterapia*, **2011**, *82*, 1175–1180. https://doi: 10.1016/j.fitote.2011.08.003.

[8] Dini, I., Tenore, G. C., Dini, A., *Food Chem.*, **2009**, *113*, 411–419.

[9] Balsevich, J. J., Bishop G. G., Deibert L. K., *Phytochem. Anal.*, **2009**, *20*, 38-49. https://doi: 10.1002/pca.1095.

[10] Aksu Dönmez, O., Bozdoğan, A., Kunt, G.. *Monatsh. Chem.*, **2006**,*137*, 1163–1168. https://doi: 10.1007/s00706-006-0520-2.

[11] Avula, B., Wang, Y. H., Rumalla, C. S., Ali, Z., Smillie, T. J., Khan, I. A., *J. Pharm. Biomed. Anal.*, **2011**, *56*, 895–903. https://doi: 10.1016/j.jpba.2011.07.028.

[12] Dolowy, M., Pyka-Pajak, A., Filip, K., Zagrodzka, J., *Curr. Issues Pharm. Med. Sci.*, 2015, *28*, 186-191. https://doi.org/10.1515/cipms-2015-0069.

[13] Lian, X. Y., Zhang, Z., *J. Pharm. Biomed. Anal.*, **2013**, *75*, 41–46. https://doi: 10.1016/j.jpba.2012.11.007.

[14] Ling, J., Liu, L., Wang, Y., Li, Z., Liu, R., Li, Q., Wang, Y., Yang, b., Chen, X., Bi, K., *J. Pharm. Biomed. Anal.*, **2011**, *55*, 259–264. https://doi: 10.1016/j.jpba.2011.01.030.

[15] Chai, X. Y., Li, S. L., Li, P., *J. Chromat. A*, **2005**, *1070*, 43–48. https://doi.org/10.1016/j.chroma.2005.02.031.

[16] Foubert, K., Cuyckens, F., Vleeschouwer, K., Theunis, M., Vlietinck, A., Pieters, L., Apers, S., *Talanta*, **2010**, *81*, 1258–1263. https://doi: 10.1016/j.talanta.2010.02.018.

[17] Ji, S., Wang, Q., Qiao, X., Guo, H. C., Yang, Y. F., Bo, T., Xiang, C., Guo, D. A., Ye, M., *J. Pharm. Biomed. Anal.*, **2014**, *90*, 15–26. https://doi: 10.1016/j.jpba.2013.11.021.

[18] Oleszek, W. A., *J. Chromatogr. A,* **2002**, *967*, 147-162.

[19]Dutra, L.S., Leite M. N., Brandão M. A. F., Almeida P. A., Vaz F. A. S, Oliveira M. A. L., *Phytochem. Anal.,* **2013**, *24*, 513-519. https://doi:10.1002/pca.2425.

[20]Zhou, X., Fu, F., Li, Z., Dong, Q., He, J., Wang C., *Planta Med.,* **2009**,*75*, 1580-1585. https://doi:10.1124/jpet.110.165498.

[21]Sirtori, C.R., *Pharmacol. Res.,* **2001**, *44*, 183-193.

[22]Kahn, S. R., *ACP J. Club*, **2006**, *145*, 20. https://doi:10.7326/ACPJC-2006-145-1-020.

[23]Man, S., *Fitoterapia*, **2010**, *81*, 703-714. https://doi: 10.1016/j.fitote.2010.06.004.

[24]Lindner, I., Meier, C., Url, A., Unger, H., Grassauer, A., Prieschl-Grassauer, E., Doerfler, P., *BMC Immunol.* **2010**, *21*, 11-24, 2010. https://doi: 10.1186/1471-2172-11-24.

[25]Acar, A. M., Paksoy, S., *Pharmazie*, **1993**, *48*, 65-66.

[26]Apers, S., Naessens, T., Pieters, L., Vlietinck, A., *J. Chromatogr.,* A. **2006**, *1112,* 165-170. . https://doi:10.1016/j.chroma.2005.10.069.

[27]Costantini, A., *Il Farmaco,* **2013**, *54*, 728-732.

[28]Zhang, M., Wu, X., Cui, X., Gao, F., Zhang, C., Yang, Y., Gu, J., *Chromatographia,* **2011**, *744*, 243-250. https://10.1007/s10337-011-2053-z.

[29]De Almeida, P., Alves, M. C., Polonini, H. C., Dutra, L. S., Leite, M. N., Raposo, N. B., Ferreira, A. O., Brandão, M. A. F., *Lat. Am. J. Pharm.* **2013**, *32,* 1082-1087.

[30]European Pharmacopoeia 8.0, Chapter 2.9.6 Uniformity of content of single-dose preparations, **2014**, 298.

[31]Nguyen, V. T., Bowyer, M. C., Vuong, Q. V., van Altena, I. A., Scarlett, C. J., *J. Ind. Crop.,***2015**, *67,* 192-200.

[32]Murthy N. E. N. K., Syed A. A., *Nat. Prod.,* **2007**, *3*, 77-80.

[33]ICH, ICH Harmonised Tripartite Guideline – Validation of Analytical Procedures: Text and Methodology Q2(R1), London, **2005**, Current Step 4 version.

[34]Romanian Pharmacopoeia 10th edition, Bucuresti: Editura Medicala, **1993**, 284.

URIDINE AS PHOTOCHEMICAL ACTINOMETER: APPLICATION TO LED-UV FLOW REACTORS

Franco Cataldo[a]*

Keywords: actinometry; uridine; UV-LED; flow reactors; photochemistry.

Two LED-UV based photochemical flow reactors have been compared. One was a commercially available LED-UV flow reactor designed for water disinfection or sterilization and the other one was a home-made LED-UV flow reactor designed for analogous purposes. The photochemical performances of two mentioned flow reactors working both at about 275 nm were evaluated using uridine actinometry through the determination of the pseudo-first order kinetics rate constant of uridine photolysis and through the measurement of the incident light I absorbed by the actinometer solution. From these data, the energy released to the solution by the LED-UV sources was determined. Furthermore, a third LED-UV reactor working at 360 nm was evaluated with uridine actinometer. As expected in the latter case uridine was not photolyzed and the reactor was found unsuitable for water disinfection.

* Corresponding Authors
     E-Mail: franco.cataldo@fastwebnet.it
[a]   Actinium Chemical Research Institute, Via Casilina 1626A, 00133 Rome, Italy

Introduction

The consolidated technology of laboratory photochemical reactors is based on the application of low-pressure mercury lamps submerged in a batch reactor where the reaction mixture to be irradiated is kept in the gap between the quartz lamp walls and the glass walls of the reactor.[1,2] This scheme was also adapted to the batch-wise production of chemicals on an industrial scale or the batch-wise wastewater treatment.[3] For continuous processes, photochemical flow reactors are designed around submerged mercury lamps.[2] Other types of advanced design is already applied in the case of photochemical flow reactors.[4] Low-pressure mercury lamps are characterized by relatively low cost and long duty and an almost monochromatic emission at 253.7 nm.[1,2] Drawbacks in the mercury lamps regard their fragility, the release of mercury into the environment in case of accidental breaking or in case of uncontrolled disposal of exhausted lamps. Furthermore, the silica walls of the mercury lamps show a tendency to darken with the continuous use.[1,2] Medium and high-pressure mercury lamps are instead characterized by a polychromatic emission and large part of the input energy is lost in the visible where most of the photochemical reactions do not occur.[1,2] Therefore, the application of these lamps is limited. Alternatives to mercury-based lamps involve xenon-arc lamps and excimer lamps.[2] However, the former has little emission in the UV while the excimer lamps are interesting with monochromatic radiation in the UV-C or also the vacuum-UV (i.e. λ< 190 nm). The excimer lamp technology, although promising, remains a complex, expensive and not fully reliable technology and is relegated to niche applications, although the improvements are coming fast in this field also.[2,5,6]

A solid alternative to the mercury lamp is represented by the LED-UV (Light Emitting Diodes in the UV). These devices are essentially solid-state semiconductor-based systems which, when appropriately designed and electrically powered, are able to transform electric current in photons.[7]

Commercially-diffused LEDs are able to emit light in the visible and are characterized by a very long life of the order of 25000-100000 h, against only 1500-8000 h of mercury vapor lamps.[2,7,8-10] In addition, LEDs are very low energy-consuming systems. For example, a common 4000 Lumen visible light source requires 300 W from a classic incandescent bulb with tungsten filament, about 100-200 W with modern compact fluorescence lamps and only 40 W from a LED source.[9,10] In addition, the LEDs are compact, resistant to shock and vibrations and therefore far superior to mercury vapor lamps even because their emission intensity can be modulated within certain limits by the current intensity, a possibility which is not applicable to the traditional mercury vapor lamps. Despite the wide diffusion of LED light sources for visible lighting, the LED sources which are able to emit in the UV have become available in the market only very recently. These LED-UV sources are based on semiconductor materials made of gallium-aluminum nitrides or gallium-indium-aluminum nitrides, through which it is possible to approach or reach the wavelengths normally emitted by low-pressure mercury vapor sources, the UV-C, which is the wavelength range commonly used for photochemical reactions and water disinfection.[7-10]

More in detail, low-pressure mercury vapor lamps emit almost exclusively about 254 nm and it is not practically possible to change the position of the emission line due to an electronic mercury transition. Instead, LED-UV sources can be suitably configured to operate in the desired wavelength in the UV. For example, for sterilization or disinfection of water, it has been established that the most desirable wavelength is the one where the maximum absorption of nucleotides (DNA and RNA components) is located, at about 260 nm.[2,10] However, the inactivation of bacteria and viruses also requires the irradiation of proteins and enzymes that are present, for example, in cell membranes, in the external coating of certain viruses, or act as enzymatic repair from radiation damage.[2,10] The absorption maximum of the proteins in solution is at about 280 nm and it was demonstrated that the spectrum of action for maximum bactericidal activity on the *S. aureus* micro-organism shows a maximum of efficiency at about 260-275 nm, an intermediate wavelength between maximum absorption of nucleotides and proteins.[2,10] Other authors come up with

similar conclusions on the bactericidal action of UV light on *E. coli*, indicating the range between 265 and 275 nm as the most effective in sterilization or disinfection of water.[11] Furthermore, the LED-UV technology allows even the choice of most suitable LED-UV for irradiating any organic substance to convert it photochemically. Therefore, to work up to 240 nm, it is suggested to select UV-LEDs of the AlGaInN type available in various versions.[8-10] For irradiation to 235 nm, there are available LED-UV based on a suitably doped diamond. [8-10] To irradiate up to 215 nm are available LED-UV based on boron nitride. [8-10] Finally, to reach 210 nm, LED- UV based on aluminum nitride can be used. [8-10]

As explained in the experimental section, in this study two different LED-UV based reactors were used. The first one was a commercially available flow reactor from Aquisense Technologies with diodes emitting in the range comprised between 265 and 285 nm, a range suitable for water disinfection and sterilization. Furthermore, a home-made reactor was designed and built using three LED-UV emitting at 275 nm with 10 mW power each. To test the photochemical efficiency of these two photochemical reactors, use was made of uridine actinometer.[12,13] The UV irradiation of a dilute solution of uridine affords practically a single photoproduct, the photohydrate of uridine as shown in scheme 1. The uridine photoproduct does not absorb light at 260 nm (in contrast to the parent molecule) and is stable for very long time in aqueous solution at pH = 7 and 20 °C.[14]
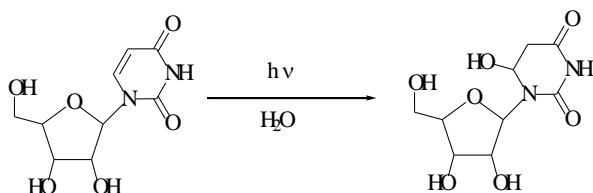
Scheme 1. Formation of uridine photohydrate on irradiation of uridine with UV light.

Flow photochemistry was thoroughly reviewed in recent times.[16-18] The increasing availability of LED-UV has propelled their application in flow photochemistry of small and even micro-reactors.[16-18] Furthermore, the LED-UV technology has also found application in water disinfection.[19-20] What is lacking or is remained behind in this flourishing field is the simple evaluation of the photochemical efficiency of these LED-UV based photochemical reactors. A need that was highlighted in a recent paper.[21] Consequently, in the present paper, the uridine actinometer was employed in the evaluation of the photochemical efficiency of two LED-UV reactors, one of them was commercially available and purchased fully assembled while the other was assembled in a simple building scheme in our laboratory.

Experimental

Materials and equipment

Uridine was purchased from Sigma-Aldrich. A commercial photochemical reactor for water disinfection was purchased from Aquisense Technologies, model

PearlAqua 6D with the emission of the LED-UV in the UV-C range (265-285 nm). This lamp is working with water flow rate of 1.8 L min^{-1}. The input power is 12 V (DC) and the power consumption 8 W. Lamp life is granted for >10000 h. Another commercial photochemical reactor was purchased from Novaquashop.com. The reactor was made of PMMA and it was equipped with an LED-UVA lamp powered at 3W and emitting at 360 nm.[22]

To construct the home-made LED-UV photochemical reactor, working in the UV-C range, commercial LED-UV were purchased from LG-Innotek. The selected LED-UV are of type 8686 emitting at 275 nm with 10 mW power each. The typical electric current used for these diodes was 111 mA with a radiant flux of 1.1 a.u. each. We used 3 LED-UV diodes 10mW each, mounted on three adjacent faces inside a polished aluminum cube. Polite aluminum has been chosen as the ultimate reflection material for ultraviolet radiation.[2] On the fourth face of the cubic reactor a UV photodiode was mounted to detect the amount of light emitted by the diodes to check and confirm their service. Under normal operating conditions at 111 mA, the photodiode gave an indicative signal of about 200 Lux. Initially, inside the cubic reactor along with three LED-UV and a photodiode, a spherical quartz reactor having a volume of 1.26 ml equipped with inlet and outlet piping was inserted. It was fed with distilled water at a rate of 23 mL min^{-1}.

Later, the quartz reactor was replaced by perfluoropolymer piping (Teflon-FEP) which is transparent to UV radiation and which overcomes the fragility of the quartz reactor. Thus, the Teflon-FEP piping was installed in order to be irradiated by the three adjacent LED-UV diodes. UV-LEDs are not in contact with the substances or water to be irradiated because they are made to flow into perfluoropolymer pipes which are known to be highly inert from the chemical and health point of view, eliminating corrosion and dirt problems This facilitates the maintenance of the reactor for the rapid replacement of perfluoropolymer pipes or the external UV-LEDs.

Uridine irradiation in the Aquisense Technologies reactor (UV-C at about 275 nm)

A uridine solution in distilled water (50.0 mg L^{-1}) was loaded in the photochemical reactor and in the pipes connecting to the peristaltic pump and an expansion vessel. A total volume of 122 ml of the uridine solution was used. At the beginning of the irradiation 62 ml of the uridine solution was loaded into the expansion vessel and other 60 ml into the pipes and in the reactor. The uridine solution was circulated from the expansion vessel to the reactor and back to the expansion vessel using a peristaltic pump working at 30 mL min^{-1}. Periodically a sample of the uridine solution was collected and checked spectrophotometrically for its absorbance at about 262 nm. In this run, the LED-UV irradiation was prolonged for 90 min. A decay of the uridine absorbance at 262 nm was treated according to pseudo-first chemical kinetics law, so that a photolysis rate constant could be determined (see the Results and Discussion section). The irradiation was repeated thrice with freshly prepared uridine solution and similar photolysis rate constant values were obtained.

Uridine irradiation in the home-made photochemical reactor (UV-C at 275 nm)

The home-made reactor was used directly in the configuration with Teflon-FEP pipes also in the UV-irradiation chamber. A total volume of about 100 ml of uridine solution in distilled water (48.8 mg L^{-1}) was loaded into the pipes, the reactor, and the expansion vessel. The uridine solution was circulated in the system through the use of a peristaltic pump working at 30 mL min^{-1}. Also, in this case, the irradiated uridine solution was periodically sampled and checked spectrophotometrically for its absorbance at 262 nm. The absorbance decay as the function of the irradiation time was treated according to the pseudo-first order kinetics law, determining the photolysis rate constant.

Uridine irradiation in the Aquashop reactor (UV-A at about 360 nm)

The photochemical reactor, the circuit, and the expansion vessel were loaded with 150 ml of uridine solution in distilled water (1.9 mg L^{-1}). The solution was pumped in the circuit through the reactor at 30 mL min^{-1} using a peristaltic pump. Periodically the uridine solution was sampled and checked spectrophotometrically. However, even after 4 h irradiation, no change in the uridine concentration was detected. This result was expected since the uridine is not absorbing at 360 nm and therefore the uridine photolysis was not achieved.

Results and Discussion

Uridine photolysis with the Aquisense Technologies LED-UV reactor (UV-C at about 275 nm)

Uridine is characterized by an absorption maximum at about 262 nm in neutral water as shown in figure 1. To photolyze uridine, it is necessary that the UV light source used emits in the wavelengths corresponding to its absorption maximum. The commercial Aquisense Technologies LED-UV reactor employed in the present work is reported by specification to emit in the range comprised between 265 and 285 nm. As shown in figure 1, the LED-UV irradiation of the uridine solution causes a reduction in the intensity of the absorption band at 262 nm as a function of the irradiation time at the flow rate of 30 mL min^{-1}. In these conditions, the reaction, shown in scheme 1, occurs with the disappearance of the uridine and the formation of the photolysis reaction product uridine photohydrate which does not absorb a at 262 nm.[12-14] The uridine absorbance data taken from figure 1 followed the pseudo-first order kinetics law (Figure 2), with a rate constant of 3.55×10^{-4} s^{-1}.

The change of uridine optical density during the UV irradiation allows the calculation of the incident light I, in photons cm^{-2} s^{-1}, absorbed by the actinometer solution using the following equation.[14]

$$I = 6.02 \times 10^{20} \, (\xi\psi t)^{-1} \log[(10^{A0}-1)(10^{At}-1)^{-1}] \qquad (1)$$

where

ξ is the molar extinction coefficient of uridine ≈ 8000 M^{-1} cm^{-1} and

ψ the quantum yield of uridine photohydration is 2.16×10^{-2}, with

t the irradiation time in s.[12,14]

A_0 and A_t are the absorbances measured at 262 nm of the uridine solution at the beginning and the end of the UV irradiation.

In a series of different irradiation experiments with the Aquisense Technologies LED-UV reactor, I = 1.1-3.2 × 10^{15} photons cm^{-2} s^{-1} was determined.
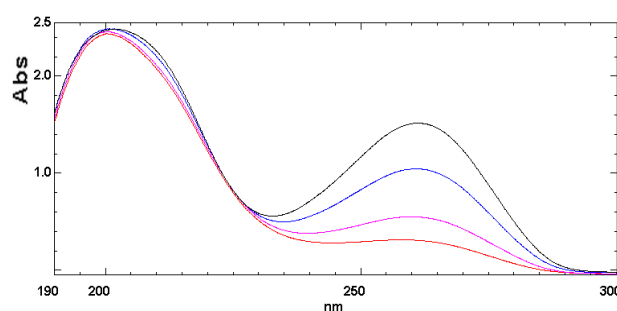
Figure 1. Electronic absorption spectra of uridine solution in distilled water irradiated with the LED-UV.
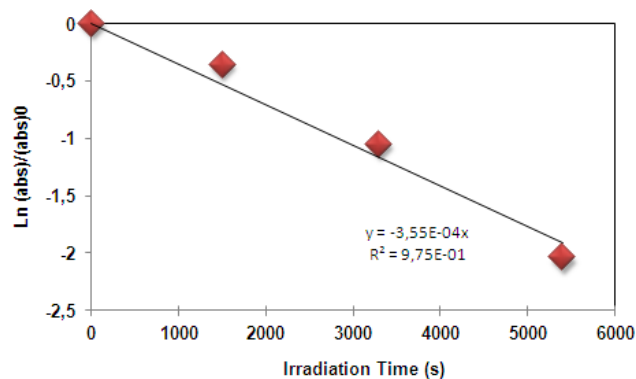
Figure 2. Pseudo-first order plot of photolysis of uridine.

Since the energy of a single photon at 275 nm is given by eqn. (2), eqn. (3) gives the amount of energy transported by the incident light beam emitted by the LED-UV lamp and delivered on the uridine solution in mJ cm^{-2} s^{-1}. The β value was found in the range of 1.0 and 2.3 mJ cm^{-2} s^{-1}.

$$E = h\nu = hc\lambda^{-1} = 7.23 \times 10^{-19} \text{ J} \qquad (2)$$

$$E \times I = \beta \qquad (3)$$

Uridine photolysis in the home-made photochemical LED-UV reactor (UV-C at 275 nm)

Uridine solution irradiated in the home-made LED-UV photochemical reactor working at 275 nm at the flow rate of 30 mL min^{-1} gives a response similar to that already observed in figure 1, with the gradual disappearance of the absorption band at 262 nm. Treating the absorbance data according to the pseudo first order chemical kinetics law leads to the linear graph of figure 3.

From the slope of the mentioned graph, the kinetic rate constant k = 2.17 × 10^{-5} s^{-1} was determined for the uridine photolysis in the home-made LED-UV reactor. The *k* value for uridine photolysis measured on the home-made reactor is just one order of magnitude lower than that measured on the commercial LED-UV reactor (2.17 × 10^{-5} s^{-1} vs. 3.55 × 10^{-4} s^{-1} respectively).
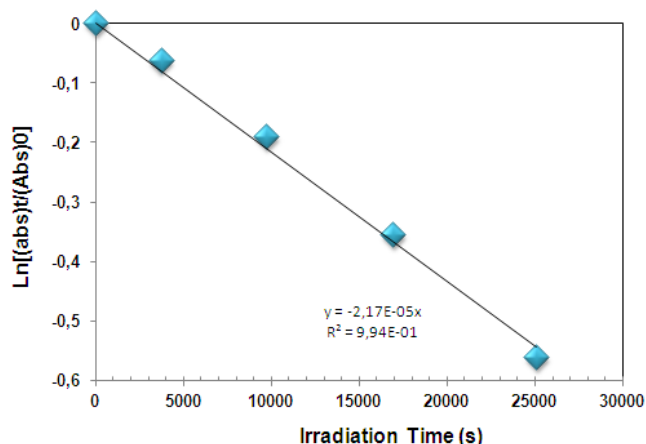
Figure 3. Pseudo-first order kinetics plot of uridine photolysis in the home-made LED-UV reactor.

Substituting in Eqn. (1) the appropriate values for the home-made LED-UV reactor, the incident light absorbed by uridine is: $I \approx 1.18 \times 10^{14}$ photons cm^{-2} s^{-1} which is again one order of magnitude lower than the *I* value found in similar conditions on the commercial LED-UV reactor from Aquisense Technologies. Using to the *I* value measured on the home-made reactor the eqns. (2) and (3) yield β = 8.55 × 10^{-2} mJ cm^{-2} which should be compared to the range of 1.0 and 2.3 mJ cm^{-2} s^{-1} measured on the commercial LED-UV reactor. Thus, the latter reactor is able to transfer to the actinometer from about 12 to 27 times more energy than the home-made reactor build with only 3 LED-UV diodes each having 10 mW power.

Comparative aspects between the two LED-UV reactors (UV-C at 275 nm)

Apart the number of UV-LED installed and the individual power from each LED which is unknown in the case of the commercial Aquisense Technologies LED-UV reactor and which is limited to 30 mW in the case of the LED-UV home-made reactor, another crucial aspect regards the materials through which the actinometer solution was irradiated. The chemical nature of the pipes used in the commercial reactor remains unknown although it is reasonable to assume that a perfluoroelastomer-based material was used.
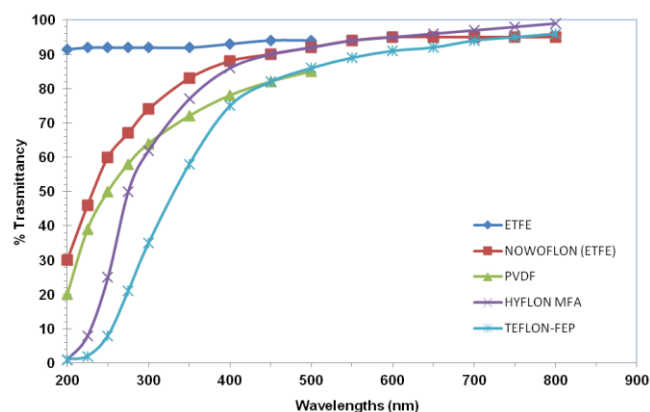
Figure 4. UV-light transmittance of a series of commercially available perfluoroelastomers employed in pipes of photochemical flow reactors at the same thickness.

As already discussed, in the home-made reactor also the pipes in the irradiation chamber were made by Teflon-FEP (a terpolymer made by tetrafluoroethylene, ethylene, and propylene. From figure 4, it is evident that the Teflon-FEP is not the best material for photochemical reactors since at 262 nm it ensures only 13% transmittance of the UV-C light. All the other materials considered in figure 4 show a much better transmittance with the best material being the ETFE, a copolymer of ethylene and perfluoroethyelene. Thus, one of the reasons of the best performance of the commercial reactor from Aquisense Technologies may be due not only to the number of individual LED-UV installed but also by the most judicious selection of the most appropriate material for the irradiation segment of the reactor.

Turning back to the home-made LED-UV reactor, figure 5 shows the selection criteria of the available materials for the irradiation chamber. As reported in the experimental section, initially use was made of quartz which however is fragile but the most transparent to the UV light at about 270 nm. Afterward, quartz was replaced by Teflon-FEP because it is more transparent than PDMS at 270 nm, although less transparent than quartz, as shown in figure 5. However, Teflon-FEP is characterized by an outstanding chemical resistance as well as resistance to UV irradiation. Even after prolonged UV irradiation at 254 nm in air and for a week, the Teflon-FEP did not show any sign of oxidation in its FT-IR spectrum.[23]
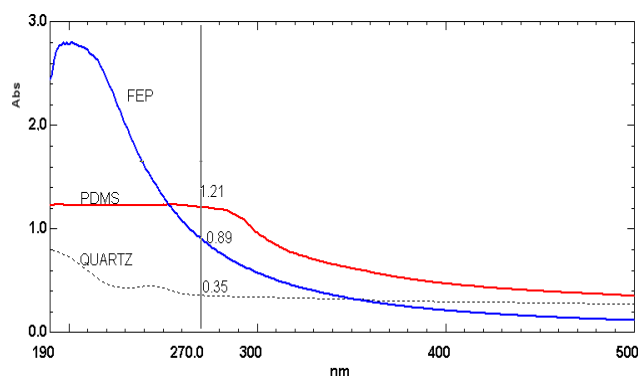
Figure 5. The UV-light absorbance of quartz (black dotted line), polydimethylsiloxane (PDMS, red line) and Teflon-FEP (blue line).

Uridine photolysis in the Aquashop reactor (UV-A at about 360 nm)

The absorption spectrum of uridine is completely free from any significant absorption in the UV-A range and specifically at 360 nm. Consequently, the LED-UV-A reactor is not able to cause the photolysis of uridine as expected and found experimentally. This part of the study represents a "blank" or a reference to the actinometric work with the LED-UV reactors working at about 275 nm. Furthermore, the light emitted by the LED-UV-A diode is a very narrow line at 360 nm.[22]. Therefore, the commercial reactor from Aquashop is not emitting photons in the spectral range suitable for water disinfection and sterilization, i.e. in the 265-280 nm spectral range.[2, 10,11]

Conclusions

Uridine as a chemical actinometer is useful for the determination of the number of photons or the energy released by a UV light source provided that the emission is comprised between 250 to 285 nm.[12] Despite its simple use in the neutral aqueous solution, it is seldom used.[13] When uridine is irradiated with the UV-C light source, it is transformed into a photohydrate as shown in scheme 1, which does not absorb anymore in the spectral range comprised between 250 and 285 nm. In the present work uridine, actinometry was successfully employed in the evaluation of the irradiation efficiency of two LED-UV photochemical reactors both working at about 275 nm. One of them was a commercially available LED-UV reactor from Aquisense Technologies while the other one was a home-made photochemical reactor designed to work with only three 10 mW diodes. It was found that the pseudo-first order kinetics rate constant for the uridine photolysis was one order of magnitude larger for the commercially available LED-UV reactor from Aquisense Technologies concerning the home-made LED-UV reactor. Accordingly, also the energy delivered to the uridine solution by the light sources in the two reactors was found from 12 to 27 times larger for the commercially available LED-UV reactor from Aquisense Technologies. It can be concluded that both the photochemical flow reactors equipped with UV-LED are effective tools in water disinfection and sterilization, with their light emission at 275 nm, although the commercially available reactor from Aquisense Technologies outperforms the home-made reactor. Uridine actinometer does not work with another LED-UV reactor which instead emits light in the UV-A spectral region i.e. at 360 nm. In this latter case, uridine is not photolyzed by the monochromatic light at 360 nm since it does not absorb at this wavelength.

Since also bacteria and viruses do not absorb at 360 nm, it appears obvious that the LED-UV reactor working at 360 nm is not suitable for water disinfection or sterilization.

References

[1]Weissberger, A. (Ed.) *"Techniques of Organic Chemistry"* Vol. 2, 2nd Ed., Wiley-Interscience, New York, **1956**, p.257-381.

[2]Oppenlander, T. *"Photochemical Purification of Water and Air*," Wiley-VCH, Weinheim, **2003**. DOI: 10.1002/9783527610884

[3]Cataldo, F. *"Process for the purification of landfill leachate wastewater by active charcoal and photo-ozonolysis."* U.S. Patent Application No. 14/356,881, **2014**.

[4]Schiavello, M. *"Photoelectrochemistry, Photocatalysis and Photoreactors"*, Springer, Berlin, **1985**, p. 527-547. DOI: 10.1007/9789401577250

[5]Lomaev, M. I., Sosnin, E. A., Tarasenko, V. F. *Chem. Eng. Technol.* **2016**, *39*, 39. DOI: 10.1002/ceat.201500229

[6]Lomaev, M. I., Sosnin, E. A., Tarasenko, V. F. *Progr. Quantum Electron.* **2012**, *36*, 51. DOI: https://doi.org/10.1016/j.pquantelec.2012.03.003

[7]Tamulaitis, G. *Lithuanian J. Phys.* **2011**, *51*, 177.

[8]Wikipedia, *"Light Emitting Diode"* https://en.wikipedia.org/wiki/Light-emitting_diode

[9]Wikipedia, *"Lumen"* https://en.wikipedia.org/wiki/Lumen_(unit),

[10]Cataldo, F. *"Photochemical reactors for photochemical wastewater treatments"* Italian Patent Demand No UB2015A005719, filed June 30th, **2015**.

[11]Vermeulen, N., et al., *Biotechnol. Bioeng.* **2008**, *99*, 550-556. DOI: 10.1002/bit.21611

[12]Kuhn, H. J., Braslavsky, S. E., Schmidt, R. *Pure Appl. Chem.* **2004**, *76*, 2105. **DOI:** https://doi.org/10.1351/pac200476122105

[13]Zhang, J. Y., Boyd, I. W., Esrom, H. *Appl. Surf. Sci.* **1997**, *109*, 482. **DOI:**https://doi.org/10.1016/S0169-4332(96)00789-1

[14]Cohn, W.E., Moldave, K. (Eds) *"Progress in Nucleic Acids Research and Molecular Biology"* Vol. 37, Academic Press, San Diego, **1989**, Chapter 1.

[15]Oelgemöller, M., Shvydkiv, O. *Molecules*, **2011**, *16*, 7522-7550. DOI:10.3390/molecules16097522

[16]Knowles, J. P., Elliott, L. D., Booker-Milburn, K. I. *Beilstein J. Org. Chem.*. **2012**, *8*, 2025. DOI: 10.3762/bjoc.8.229

[17]Gilmore, K., Seeberger, P. H. *Chem. Record*, 2014, *14*, 410-418. DOI: 10.1002/tcr.201402035

ONE POT SYNTHESIS AND BIOLOGICAL EVALUATION OF PYRANOPYRAZOLES IN AQUEOUS MEDIUM

Priya M. Khandare,[a] Rajita D. Ingale,[a] Aparna S. Taware,[a] Suresh U. Shisodia,[b] Shankar S. Pawar,[c] Laszlo Kotai,[d] Rajendra P. Pawar[a]*

A simple and green one pot protocol for the synthesis of pyranopyrazoles using ultrasonication waves in aqueous medium has been developed. Advantages of this method are it provides operational simplicity and environment-friendly green approach.

*Corresponding Authors
E-mail: rppawar@yahoo.com rajitaingle@yahoo.in
[a]   Department of Chemistry, Deogiri College, Station Road, Aurangabad, Maharashtra- 431005, India
[b]   Department of Polymer Science and Engineering Division, CSIR-National Chemical Laboratory, Dr. Homi Bhabha Road, Pune – 411008, Maharashtra, India
[c]   Department of Chemistry, Ferguson, College, Pune, Maharashtra- 411004, India
[d]   Research Centre for Natural Sciences, Hungarian Academy of Sciences, P. O. Box 17, HU-1525, Budapest, Hungary

Introduction

Multicomponent reactions (MCRs) are known as efficient tools for the generation of complex heterocyclic bioactive compounds useful in organic and medicinal chemistry, in which three or more reactants react to give final product in a one-pot procedure.[1] The first multicomponent reaction was described in 1850 by Strecker, and later many such reactions have been reported in the literature.[2] This attracted attention of industrial and academic researchers.[3]

Water is the safest and abundant substance in nature, and almost all compounds are sparingly soluble in water. Hence it is referred as a benign 'Universal Solvent'.[4] The search for alternative reaction media to replace volatile, flammable and often toxic organic solvents is an important objective in the development of the green chemical process.[5] Hence organic synthesis in an aqueous medium is preferred from environmental as well as from the economical point of view.

Pyrano pyrazole is a fused heterocyclic compound, which adds functional diversity to the molecule and provides fruitful area to study the bioactivity. Pyranopyrazoles were first obtained in 1973 by the reaction between 3-methyl-1-phenylpyrazolin-5-one and tetracyano ethylene.[6] Pyranopyrazole scaffold has shown bioactivity such as anticoagulant, spasmolytic, hypnotic, diuretic,[7] insecticidal,[8] anti-inflammatory,[9] anticancer,[10] antibacterial and antifungal[11], as well as antimicrobial.[12] Owing to the biological importance, scientists have developed several methodologies for the synthesis of pyranopyrazoles by using different catalysts such as piperidene,[13] DBSA,[14] PTSA,[15] [Sipim]HSO4,[16] citric acid,[17] β-cyclodextrin,[18] NH4Cl,[19]

ZrO2-NPs,[20] PS-PTSA,[21] thiamine hydrochloride.[4] But still, these methods have certain limitations like use of harsh reaction conditions, low yield of products, use of volatile organic solvents, etc. Recently ultrasound irradiation has been used in organic synthesis.

In continuation of our efforts to the ecofriendly synthetic approach towards synthesis of bioactive heterocyclic compounds, herein we wish to report one pot four component synthesis of pyranopyrazoles by the reaction of aromatic aldehyde, malononitrile, ethyl acetoacetate, hydrazine hydrate using lanthanum (III) nitrate as a catalyst[22] in aqueous medium under ultrasound irradiation method in short time.
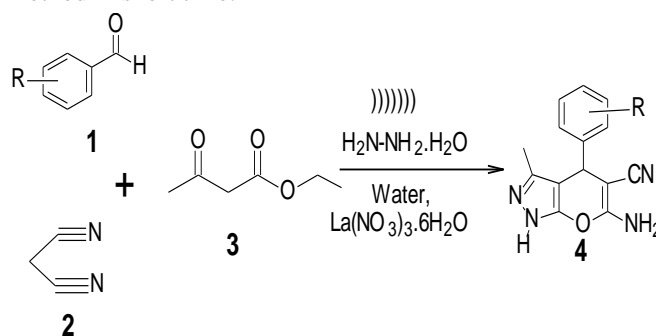
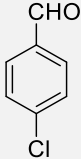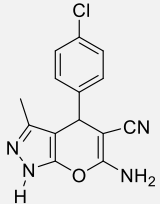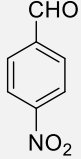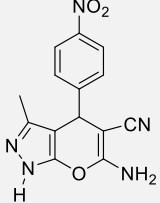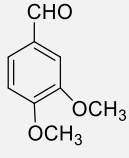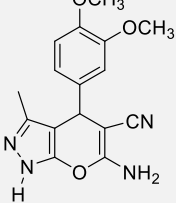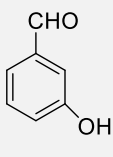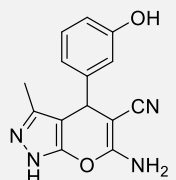**Scheme 1.** General synthetic route to prepare compounds 4.
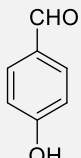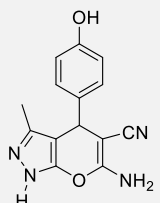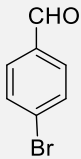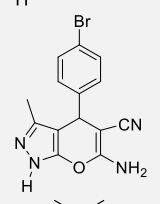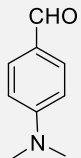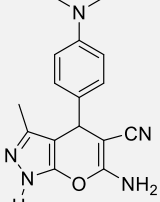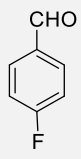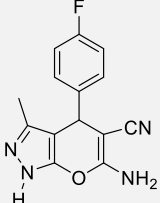
Experimental

All reagents and chemicals were of analytical grade and used without further purification. Sonication was performed in ultrasonic cleaner with a frequency of 25 KHz and nominal power 250 W. The reaction temperature was controlled by addition or removal of water from ultrasonic bath.
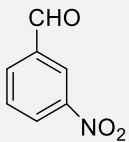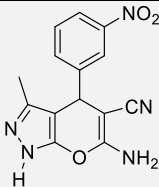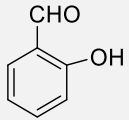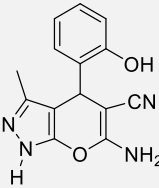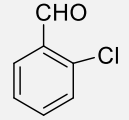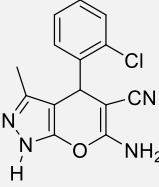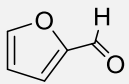
General procedure for the synthesis of substituted pyranopyrazoles

In 100 mL round bottom flask substituted benzaldehyde (1 mol), malononitrile (1.1 mol), ethyl acetoacetate (1 mol), hydrazine hydrate (1 mol) and La(NO3)3.6H2O (10 % mol) were taken in 20 mL water as a green solvent.

Table 1. Synthesis of pyranopyrazole derivatives

Sr. No.	Benzaldehyde	Product	Time, min	Yield, %	M.P., °C found	M.P., °C lit.(ref.)
1			30	77.13	174	175[9]
2			30	85.41	193	195[9]
3			45	94.22	220-222	222-224[10]
4			30	70.61	178	177[9]
5			45	75.37	224-225	225-227[10]
6			30	83.58	169-170	169-171[10]
7			40	57.05	190-191	188-190[10]
8			30	67.46		-

9	CHO, NO_2	(3-nitrophenyl pyranopyrazole)	45	73.41	190-192	190-192[10]
10	CHO, OH	(2-hydroxyphenyl pyranopyrazole)	30	64.72	208-210	208-210[10]
11	CHO, Cl	(2-chlorophenyl pyranopyrazole)	40	65.75	144-146	144-146[10]
12	furan-CHO	(furyl pyranopyrazole)	45	62.82	174-176	176-178 [10]

The resulting reaction mixture was sonicated for a period as indicated in Table 1. The progress of reaction was monitored by using TLC. After completion of reaction, the solid product obtained was filtered, washed with water and recrystallized from ethanol to afford the pure product. All the products were confirmed by comparing their melting points, IR and ^{1}H NMR data with literature data.

Spectral data of compound 8.

6-Amino-3-methyl-4-(4-nitrophenyl)-2, 4-dihydropyrano [2,3-c] pyrazole-5-carbonitrile (2). Brown solid. IR (KBr): ν 3373.50, 3450.32, 2191.13, 1932.67, 854.47, ^{1}H NMR : (200 MHz, CDCl$_3$) δ 8.27 (s, 1H, NH), 7.43-7.47 (dd, 2H, arom), 8.17 (s, 2H, NH_2), 8.21 (s, 2H, NH_2), 1.56 (s, 3H, CH_3), 7.55 (s, 3H, arom).

Results and discussion

To optimize the reaction conditions, we have carried out the model reaction of 4-hydroxybenzaldehyde, ethyl acetoacetate, hydrazine hydrate, and lanthanum (III) nitrate as a catalyst by using water or ethanol as a solvent or without solvent, at room temperature, reflux and by using ultrasound irradiations. Results obtained are presented in Table 2. High yields were obtained by using ultrasonication method and utilizing water as a green solvent in short time.

In order to understand amount of catalyst to obtain maximum yield we have carried out model reaction with different amount of catalyst (Table 3) and found that 10 mol % of catalyst is sufficient, further increasing the amount of catalyst does not affect the yield.

Table 2. Effect of various solvent on synthesis of compound **3.**

Entry	Solvent	Temperature, ^{0}C/)))))))	Time, min	Yield, %
1	H_2O	r.t.	360	85
2	H_2O	Reflux	240	83
3	H_2O	)))))))	45	94
4	EtOH	r.t	378	70
5	EtOH	reflux	300	67
6	EtOH	)))))))	50	80
7	Without Solvent	r.t	420	40
8	Without Solvent	reflux	480	45
9	Without Solvent	)))))))	120	35

Table 3. Effect of catalyst, on the synthesis of pyranopyrazole 3 by ultrasonification

Entry	Amount of La(NO_3)$_3$.6H_2O, mol %	Yield, %
1	No catalyst	8
2	5	40
3	10	94
4	20	94
5	30	92

Mechanism

The possible mechanism for this reaction is, malononitrile and benzaldehyde through Knoevenagel condensation produces ylidene malononitrile and hydrazine on reaction with ethyl acetoacetate produces pyrazolone. These ylidenemalononitrile and pyrazolone together produce our desired product through Michael addition.

Antifungal activity

Antifungal activity of synthesized compounds has been screened against fungal species *A. niger* and *Phytophthora* using drug streptomycin as a standard. Agar well diffusion method is used for screening purpose. Observations were recorded after 72 h, and the zone of inhibition was measured in mm The antifungal activity is comparable with Streptomycin against *A. niger and Phytophthora megasperma* at a concentration of 10 mg/ml of DMF solvent.
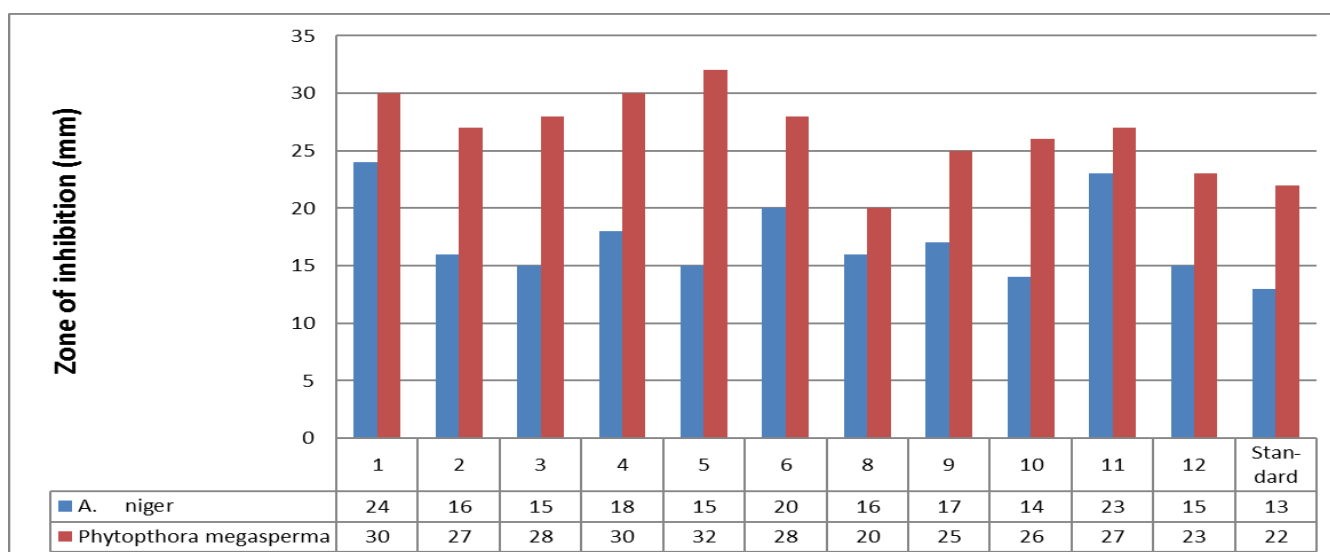
It was observed that all the synthesized compounds showed good antifungal activity against fungal species *A. niger* and *Phytophthora megasperma* as compared to standard drug streptomycin.

Compounds **1**, **4**, **6**, **11** shown excellent activity against *A. niger* whereas compounds **1**, **3**, **4**, **5**, **6,** have shown excellent activity against *Phytophthora* species, Other compound shown good to moderate biological activity.

Table 4. Zone of inhibition in mm of synthesized pyranopyrazole derivatives

Compound	*A.niger*	*Phytophthora megasperma*
1	24	30
2	16	27
3	15	28
4	18	30
5	15	32
6	20	28
8	16	20
9	17	25
10	14	26
11	23	27
12	15	23
Standard	**13**	**22**

Table 5. Graphical Zone of inhibition in mm of synthesized pyranopyrazole derivatives

	1	2	3	4	5	6	8	9	10	11	12	Standard
A. niger	24	16	15	18	15	20	16	17	14	23	15	13
Phytopthora megasperma	30	27	28	30	32	28	20	25	26	27	23	22

Conclusion

In conclusion, we have achieved pyranopyrazole synthesis by one pot multicomponent procedure using green synthetic protocol under ultrasound irradiation technique, using water as a green solvent and $La(NO_3)_3.6H_2O$ as a catalyst. Striking features of this method are short reaction time, easy work up procedure, water solvent, use of ultrasound waves, atom economy.

Acknowledgement

References

[1]Domling, A., Ugi, I., *Angew. Chem., Int. Ed. Engl.* **2000**, *39*, 3168. https://doi.org/10.1002/1521-3773(20000915)39:18<3168::AID-ANIE3168>3.0.CO;2-U

[2]Pawar, B., Jadhav, S. D., Patil, B. M., Shejwal, R. V., Patil S., *Arch. Appl. Sci. Res.,* **2014**, *6,* 150-158.

[3]Davood, A., Khatami, S. M., Razieh, N. Y., *J. Chem. Sci.* **2014**, *126, 95*-101. https://doi.org/10.1007/s12039-013-0548-x

[4]Nikam, M. D., Mahajan, P., Chate, A. V., Dabhade, S. K., Gill, C. H., *J. Chil. Chem. Soc.* **2015**, *60*, 2847. https://doi.org/10.4067/S0717-97072015000100016

[5]Khurana, J. M., Nand, B., Kumar, S., *Synth Commun*, **2011**, *41*, 405-410. https://doi.org/10.1080/00397910903576669

[6]Junek, H., Aigner, H., Chem. Ber. **1973**, 106, 914-921. https://doi.org/10.1002/cber.19731060323

[7]Ahluwalia, V. K., Dahiya, A., Indian, V., *Indian J. Chem., B: Org. Chem. Incl. Med. Chem.*, **1997**, *36*, 88.

[8]Ismil, Z. H., Aly, G. M., El-Degwi, M. S., *Egypt. J. Biotechnol*, **2003**, 13, 73-82.

[9]Zaki, M. E. A, Soliman, H. A., Rashad, A. E., *Z. Naturforsch. C.*, **2006**, 61, 1-5. https://doi.org/10.1515/znc-2006-1-201

[10]Wang, J. L., Liu, D., Zheng, Z. J., Shan, S., Han, X., Srinivasula, S. M., Croce, C. M., Alnemri, E. S., Huang, Z., *Proc. Natl. Acad. Sci. U. S. A.*, **2009**, *97*, 7124. https://doi.org/10.1073/pnas.97.13.7124

[11]Katariya, L. K., Kharadi, G. J., *IJPRS*, **2014**, *3*, 627-637.

[12]Dawane, B. S., Yemul, O. S., Chobe, S. S., Mandawad, G. G., Kamble1, R. D., Shinde, A. V., Kale, M. P., Hurne1, A. O., Pawde, M. A:, Desai, N. P., Salgare, R. R., Patil, M. B., Mundhe S. N. and Chavan, S. R., *Der Pharma Chemica*, **2011**, *3*, 300-305.

[13]Bekington, M., Hormi M., Rohman, Md. R., Rajbangshi, M., Kharkongor, I., Laoo, B. M., Iadeishisha, Kharbangar, Kshair, B., *Org. Prep. Pro.* I, **2013**, 45, 253-303.

[14]Jin, T. S., Zhao, R. Q., Li, T. S., *ARKIVOC*, xi **2006**, 176-182.

[15]Heravi, M. M., Javanmardi, N., Oskooie, H. A., Baghernejad, B., *GUJ Sci.,* **2011**, *24*, 227-231.

[16]Nikam, K., Piran, A., *Green Sustain. Chem.*, **2013**, 3, 1-8.

[17]Pawar, P. B., Patil, B. M., Shejwalb, Patil, S., *Arch. Appl. Sci. Res.*, **2014**, *6,* 150-158.

[18]Kanagraj K., Pitchumani K., *Tetrahedron Lett.* , **2010**, *51*, 3312-3316. https://doi.org/10.1016/j.tetlet.2010.04.087

[19]Pagore, V. P., Rupnar, B. D., Tekale, S. U., Pawar, R. P., *Der Pharma Chemica*, **2015**, *7*, 312-317.

[20]Saha, A., Payra, S., Bannerjee, S., *Green Chem.*, **2015**, *17*, 2859. https://doi.org/10.1039/C4GC02420F

[21]Chaudhari, M. A., Gujar, J. B., Kawade, D. S., Jogdand, N. R., Shingare, M. S., *Cogent Chem.*, **2015**, *1*, 1063830.

[22]Pandule, S. S., Shisodia, S. U., Patil, M. R., Chabukswar, V. V., *Eur. Chem. Bull.,* **2015**, *4*, 364-367. DOI: 10.17628/ecb.2017.6.365-375

SYNTHESIS, CHARACTERIZATION AND CATALYTIC ACTIVITY OF TUNGSTOCOBALTATE-PILLARED ZnAl-LAYERED DOUBLE HYDROXIDE

Bhabani S. Mohanta[a], Rita Das[b]* and Nigamananda Das[c]

Tungstocobalate, $(Co^{III}W_{12}O_{40})^{5-}$, intercalated ZnAl-layered double hydroxide (ZnAl-CoW$_{12}$) was prepared via rehydration of calcined ZnAl-LDH under nitrogen atmosphere. Characterization by chemical analysis together with powder XRD, FT-IR, TG-DTA and UV-VIS DRS provided evidence of intercalation of $Co^{III}W_{12}O_{40}^{5-}$ (58 wt. %) in the interlayer of LDH. The catalytic activity of ZnAl-CoW$_{12}$ was evaluated for hydrogen peroxide mediated decolourisarion of methyl orange and oxidation of benzaldehyde to benzoic acid under varying reaction conditions. ZnAl-CoW$_{12}$ was found effective for both the reactions and stable under the experimental conditions for repetitive use without any noticeable decrease in activity.

* Corresponding Authors
    Phone: +91-9437380056
    E-Mail: dasrita66@rediffmail.com
[a]   Department of Chemistry, North Orissa University, Baripada 757 001, Odisha, India
[b] Department of Chemistry, Rama Devi Women's University, Bhubaneswar 751 022, Odisha, India
[c] Department of Chemistry, Utkal University, Bhubaneswar 751 004, Odisha, India

Introduction

Polyoxometallates (POMs) constitute a potentially important class of inorganic materials because of their unique properties like structural stability and catalytic efficiency for various organic transformations in homo- and heterogeneous media.[1-3] POMs are known to activate H$_2$O$_2$ and subsequently oxidize several organic molecules.[1-8] The oxidizing ability can be systematically controlled by changing the constituent atoms of polyanion structure.[4,8] However, their low surface area and thermal stability in addition to high solubility in aqueous medium limit their utility in many catalytic applications.[9,10] In order to avoid the loss of POMs in reaction medium and increase the surface area for widening their practical applications, POMs are often supported on different solid supports like silica, alumina, resin, clays, zeolites and molecular sieves.[9-15]

Layered double hydroxides (LDHs) is another important class of inorganic layered compounds offering support for hosting a variety of catalytically active anionic species in the interlayer space of metal hydroxide layers.[16] Among them, the POMs are found to be a potentially interesting class of guests for LDHs to develop oxidation catalysts or catalyst precursors for several reactions of chemical and environmental importance.[16-18] A variety of structurally different iso- and heteropolyoxometallates with varying metal have been intercalated in the interlayer of LDHs and their catalytic properties have been studied by several workers.[12,19-24]

The present work pertains to intercalation of a catalytically active POM having strong oxidizing ability of Co^{III} ion, $[CoW_{12}O_{40}]^{5-}$ (CoW$_{12}$),[14,26] in the interlayer of ZnAl-layered double hydroxide (ZnAl-LDH), characterization of resulted intercalated sample by various physicochemical methods and evaluation of its catalytic activity for oxidative decolourisation methyl orange (MO) and oxidation benzaldehyde to benzoic acid as the model reactions.

Experimental

Synthesis of materials

ZnAl-LDH (molar ratio of Zn/Al = 3) was prepared by coprecipitation of mixed aqueous solutions of Zn(NO$_3$)$_2$.7H$_2$O and Al(NO$_3$)$_3$.9H$_2$O at ambient temperature under low supersaturating conditions (pH ~ 10).[26] The synthesized sample was calcined at 450 °C for 5 h in air to yield ZnAl-mixed oxide, ZnAl(O). The potassium salt of tunstocobaltate, K$_5$[Co^{III}W$_{12}$O$_{40}$].20H$_2$O, was synthesized following the reported method[25,27] and its purity was checked by spectral analysis.

(CoW$_{12}$) ion was intercalated in the interlayer LDH through rehydration of calcined LDH in presence desired amount of aqueous solution of K$_5$[Co^{III}W$_{12}$O$_{40}$].20H$_2$O. In typical lot a weighed amount of ZnAl(O) was dispersed in 50 mL of aqueous solution of K$_5$[Co^{III}W$_{12}$O$_{40}$] (0.52 g) and the pH was adjusted to *ca.* 6.5 with dilute HNO$_3$ solution. The mixture was then stirred under N$_2$ atmosphere for ~ 4 h. By this time the initial green colour of the solution was changed to colourless indicating almost complete intercalation of tunstocobaltate ion in the LDH interlayer. The resulting solid was separated by centrifugation, washed several times with water and finally with ethanol. The isolated solid was dried at 60°C for 8 h in vacuum. The CoW$_{12}$ intercalated sample was denoted as ZnAl-CoW$_{12}$.

Characterizations

The Zn, Al, Co and W contents in the samples were determined by ICP (Varian Liberty series2). Carbon and nitrogen was analysed by Euro EA Vector elemental

analyser. Powder X-ray diffraction patterns were recorded in a Rigaku (Miniflex II) X-ray diffractometer at a scanning speed of 2°(2θ)/min using Ni filtered CoK$_\alpha$ (30 kV, 15 mA) radiation source. Thermogravimetric measurements in argon atmosphere were performed on a Shimadzu DTG 60 Thermal analyser at a heating rate of 10 °C min^{-1}. FT-IR spectra in KBr phase were recorded on a Shimadzu IR Affinity-1 spectrophotometer averaging 45 scans with a nominal resolution of 4 cm^{-1} to improve signal to noise ratio. The UV-Visible diffuse reflectance spectra were recorded on a Varian UV-Visible spectrophotometer using BaSO$_4$ white standard.

Catalytic activity

The catalytic activity of ZnAl-CoW$_{12}$ was evaluated for oxidative decolourisation of a methyl orange and oxidation of benzaldehyde. Stock solution (500 μM) of methyl orange was prepared by dissolving accurately weighed solid methyl orange (Mecrk, GR) in deionized distilled water and was diluted to desired concentration as and when required. H$_2$O$_2$ (30 % w/v, Merck) and benzaldehyde (Merck, GR) was used as received.

For decolourisation of study, 50 mL of MO at desired concentration along with appropriate amounts of H$_2$O$_2$ and ZnAl-CoW$_{12}$ in a 100 mL conical flask were mechanically shaken in thermostated water bath shaker at 30±0.2 °C. The initial pH of the reaction mixture was adjusted to 6.0±0.2 by addition of 0.1 M NaOH/HCl solution. At regular intervals, the reaction mixture was withdrawn, centrifuged and measured the absorbance at 464 nm (ε = 2.68×10^4 M^{-1} cm^{-1}) to evaluate the concentration of residual MO. In aqueous solution, MO is almost completely dimerised above 2×10^{-4} M and undergoes further aggregation at millimolar and higher concentrations[29]. Hence, the concentration of MO was kept < 1×10^{-4} M where the Beer–Lambert law is obeyed. All the experiments were carried at pH above the pK$_a$ value of MO (~3.4) in order to avoid any further colour change due to pH variation. The reaction parameters such as time of reaction, catalyst amount and initial concentrations of MO and H$_2$O$_2$ were varied to optimize the parameters.
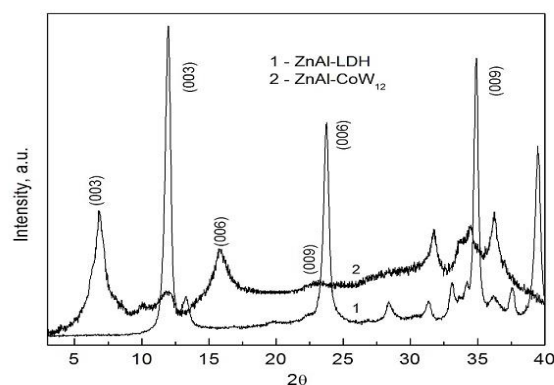
The oxidation of benzaldehyde was carried out by a similar procedure adopted in a previous study.[14] The reaction mixture containing ZnAl-CoW$_{12}$, benzaldehyde and 30 wt. % H$_2$O$_2$ in a 100 mL flask was heated under stirring condition to initiate the reaction. The reaction time, temperature and amounts of H$_2$O$_2$ and catalyst were varied to optimize the reaction parameters. The formation of benzoic acid is evident from its isolation by similar method described earlier[14] and characterized by FT-IR spectral analysis and melting point measurement. The yield of benzoic acid was calculated from the weight of the final white crystals.

Results and Discussion

Characterizations of ZnAl-CoW$_{12}$

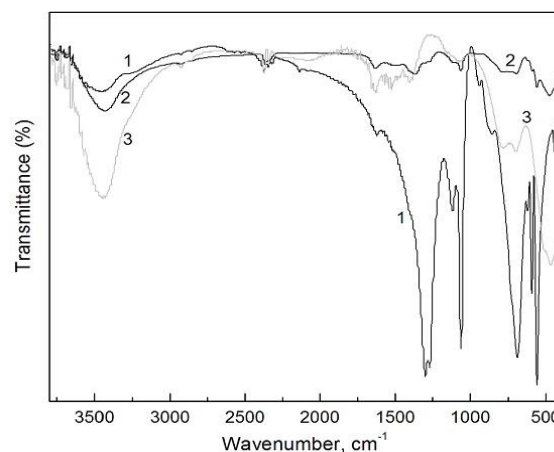The addition of ZnAl(O) to the green solution of K$_5$[Co^{III}W$_{12}$O$_{40}$].20H$_2$O followed by stirring under N$_2$ atmosphere for 4 h results almost colourless solution

indicating complete intercalation of CoW$_{12}$ in the interlayer of regenerated ZnAl-LDH to yield ZnAl-CoW$_{12}$. The molecular formulae of ZnAl-LDH (carbonate form) and CoW$_{12}$ intercalated LDH (ZnAl-CoW$_{12}$), derived from the chemical analyses, are tentatively represented as [Zn$_{0.74}$Al$_{0.26}$(OH)$_2$](CO$_3$)$_{0.146}$ and [Zn$_{0.73}$Al$_{0.27}$(OH)$_2$] (CoW$_{12}$O$_{40}$)$_{0.045}$(CO$_3$)$_{0.012}$, respectively indicating all the residual positive charge of brucite like layer is not compensated by CoW$_{12}$ ion and about 16.6% of total positive charge is balanced by CO$_3$$^{2-}$/OH$^-$ ions. The wt. % of CoW$_{12}$ in ZnAl-CoW$_{12}$ is ~ 56.2 which is ~ 12% lower than that reported (68.7 wt.%) in the case of corresponding MgAl-CoW$_{12}$ sample.[14] This is primarily due to higher residual positive charge in brucite like layer of MgAl-LDH (Mg/Al = 2) sample, used for intercalation, than ZnAl-LDH (Zn/Al ≈ 3).
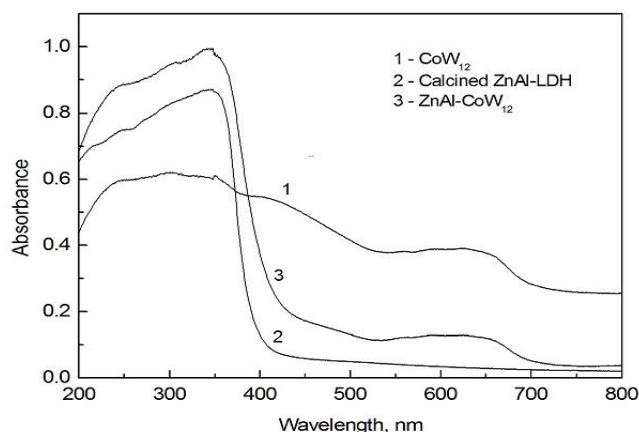

Figure 1. Powder XRD patterns of ZnAl-LDH and ZnAl-CoW$_{12}$.

The powder XRD patterns of ZnAl-CoW$_{12}$ along with ZnAl-LDH are presented in figure 1. The appearance of some new peaks in ZnAl-CoW$_{12}$ and shifting of reflections (003, 006, 009) to lower 2θ values indicate the intercalation of CoW$_{12}$ in the interlayer. The basal spacing, derived from 2θ values, is increased from 7.38 Å to 12.96 Å. Assuming the hydroxide layer thickness of ZnAl-LDH to be 4.8 Å and size of the Keggin ion 10.2 Å, as estimated from crystallographic data for a Keggin ion salt,[14] this increase of basal spacing is quite reasonable. A decrease of crystallinity of ZnAl-CoW$_{12}$ is also evident from its broadened low intensity diffraction peaks.
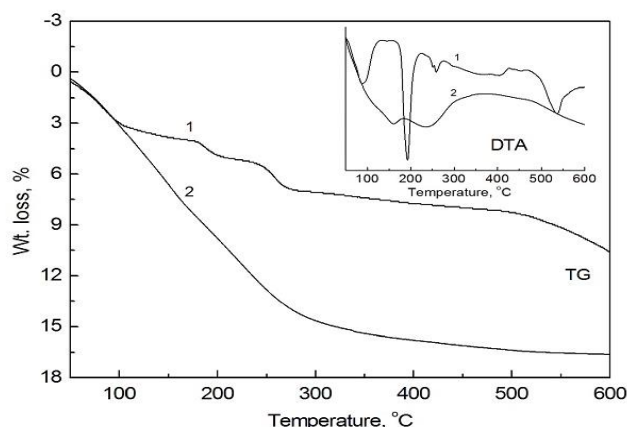

Figure 2. FT-IR spectra of calcined ZnAl-LDH (1), CoW$_{12}$ only (2) and ZnAl-CoW$_{12}$ (3).

The IR spectra of ZnAl-CoW$_{12}$ along with K$_5$[Co^{III}W$_{12}$O$_{40}$] and Zn(Al)O are presented in figure 2. The Keggin-type structure of [CoW$_{12}$O$_{40}$]$^{5-}$ anion consists of one centrally located CoO$_4$ which is caged by 12 octahedral WO$_6$ units linked to one another by the neighbouring oxygen atoms. In general, the asymmetric stretching of the different kinds of W–O bonds is observed in the following spectral regions: W–O$_d$ bonds (1000–900 cm^{-1}), W–O$_b$–W bridges (800–900 cm^{-1}), W–O$_c$–W bridges (700–800 cm^{-1}). The K$_5$[Co^{III}W$_{12}$O$_{40}$]. 20H$_2$O displayed four characteristic bands at 955, 883, 698 and 445 cm^{-1} attributing to ν_{as}(W–O$_d$); ν_{as}(W–O$_b$–W), ν_{as}(W–O$_c$–W), ν_{as}(Co–O$_a$) or δ(O–Co–O)[19,30] and are very much similar to those reported previously.[14,15] The bands at 3520 and 1640 cm^{-1} are attributed to the stretching and bending vibrations of O–H and H–O–H bonds. The band positions, although of lower intensities, in the spectra of ZnAl-CoW$_{12}$ are similar to that of K$_5$[Co^{III}W$_{12}$O$_{40}$] providing further evidence of intercalation of [CoW$_{12}$O$_{40}$]$^{5-}$ ions in the interlayer of ZnAl-LDH. After the exchange, the bands due to W–O and Co–O stretching modes are still recorded (938, 885 752 and 440 cm^{-1}), together with other band at 648 cm^{-1} due to the transitional modes of the LDH.

Figure 3. UV-Vis DRS ZnAl-LDH (calcined), ZnAl-CoW$_{12}$ and CoW$_{12}$.

Figure 4. TG and DTA curves of CoW$_{12}$ (1) and ZnAl-CoW$_{12}$ (2) at heating rate 10°C under N$_2$ atmosphere.
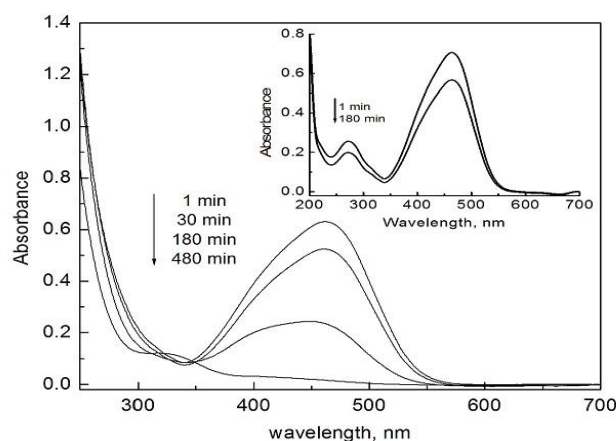
More evidence in favour of intercalation of CoW$_{12}$ in the interlayer of LDH is obtained from UV-Vis DRS (Figure 3). The characteristics peaks of CoW$_{12}$ and ZnAl-LDH are also appeared in the case of ZnAl-CoW$_{12}$ indicating the intercalation of CoW$_{12}$ in the interlayer of ZnAl-LDH. The

TG-DTA curves of CoW$_{12}$ and uncalcined ZnAl-CoW$_{12}$ are presented in figure 4. It is seen that ZnAl-CoW$_{12}$ exhibits a continuous weight loss up to 600 °C with two distinct endothermic peaks centered at ~ 160 and 245 °C in the DTA profile. A hump like endothermic peak observed at ~ 120 °C is presumably due to the loss of surface-adsorbed water. The peaks at 160 and 245 °C are attributed to the removal of interlayer water followed by collapse of the layered structure.[14] The weight loss beyond 300 °C is resulted from both the dehydroxylation of ZnAl–LDH layers and the decomposition of CoW$_{12}$ to expel the produced water molecules. The neat complex also exhibits multi stage weight losses with two major endothermic peaks at 90 and 190 ºC.

Catalytic activity of ZnAl-CoW$_{12}$

Oxidative decolourisation of methyl orange (MO)

Preliminary observation indicates practically no change in the absorbance of MO over a period of 3 h in presence of H$_2$O$_2$ (0.05 M) indicating there is no decolourisation of MO by H$_2$O$_2$ alone. As MO exists in anionic form at pH > 4.0, decolourisation due to ion exchange or adsorption of a small amount of MO in the interlayer or surface of ZnAl-CoW$_{12}$, respectively, cannot be ruled out. A typical experiment, with ZnAl-CoW$_{12}$ (0.5 g l^{-1}) and MO (35 µM) and without addition of H$_2$O$_{2,}$, shows (Figure 5, inset) a decrease in absorbance over the entire range of spectrum. The amount of MO decolourised due to ion exchange/adsorption on ZnAl-CoW$_{12}$, estimated using the absorbance values of MO at 275 and 464 nm, is found to be ~ 14 %. In presence of both H$_2$O$_2$ and ZnAl-CoW$_{12}$, the MO peak at 275 nm is not observed (Figure 5) due to high absorbance of H$_2$O$_2$ at < 300 nm. However, the absorbance of MO at 464 nm is progressively decreased with time and reached to almost zero in ~ 8 h. Interestingly the MO peak at 275 nm is reappeared when the concentration of H$_2$O$_2$ is decreased with the progress of reaction.


Figure 5. Successive spectral scan of MO (35 µM) with time in presence of ZnAl-CoW$_{12}$ (0.5 g/l) and H$_2$O$_2$ (0.05 M). (Inset) in presence of ZnAl-CoW$_{12}$ (0.5 g/l) only.

As more than 80 % of MO is decolourised within 300 min of reaction, all further decolourisation experiments for determination rate constant and optimization of other parameters were carried out keeping the time of reaction

time fixed at 300 min. The time course percentage of MO decolourised in the presence and absence of H_2O_2 is presented in figure 6. It is seen that the decolourisation of MO is strongly catalysed in presence of both H_2O_2 and catalytic amount of ZnAl-CoW$_{12}$ and more than 80 % MO (35 µM) is decolourised against 14 % decolourisation in the absence of H_2O_2. The decolourisation data up to 300 min are subjected to non-linear least square fitting (eqn. 1).

$$C_t = (C_0 - C_\infty)\ e^{(-kt)} + C_\infty \qquad (1)$$

where C_0, C_t and C_∞ are the concentrations of MO at the beginning, time 't' and the end, respectively and k is the rate constant. The first-order rate constants, derived from least square fittings ($R^2 = 0.99$), are found to be 0.357 ± 0.070 and 0.433 ± 0.051 h^{-1} for 35 and 60 µM MO concentrations, respectively under identical conditions.
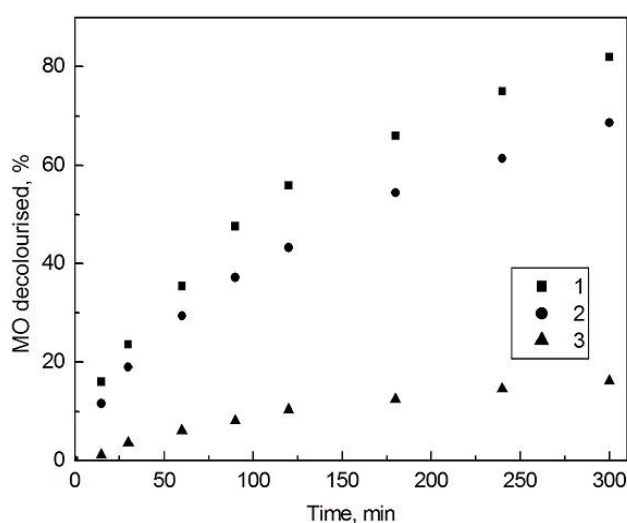
Figure 6. Time course of MO decolourisation in presence of ZnAl-CoW$_{12}$ (0.5 g/l) and [H_2O_2] = 0.02 M at varying MO concentrations: (1) 35 µM, (2) 60 µM and MO decolourisation (35 µM) by ZnAl-CoW$_{12}$ (0.5 g/l) without H_2O_2.

Table 1. Effect of catalyst amount and initial dye concentration on decolourisation of MO.

[H_2O_2], M	ZnAl-CoW$_{12}$, g L^{-1}	MO decolourization, %
0.02	0.20	34.5
0.02	0.50	66.3
0.02	1.00	88.0
0.02	1.50	98.4
0.05	0.50	76.5
0.10	0.50	87.2
0.015	0.50	90.9
0.20	0.50	93.4

[MO] 35 µM, reaction time 300 min, temperature 30±0.2 ºC.

The effect of initial H_2O_2 concentration (0.02 to 0.20 M), keeping the dye and catalyst amounts fixed, is presented in Table 1. It is seen that the percentage of decolourisation increases non-linearly with increase of initial concentration of H_2O_2. The decrease of oxidation activity of H_2O_2 at higher concentration is most likely due to increase of catalysed H_2O_2 decomposition at higher concentration. The

effect of catalyst amount on overall MO decolourisation, keeping all other parameters fixed, is also presented in Table 1. The decolourisation is progressively increased due to availability of more active component for catalysis and sites for adsorption/ion exchange. In order to see the efficiency of ZnAl-CoW$_{12}$ for repetitive use, the reactant solution was charged with desired amount of MO and H_2O_2 after every 5 h to maintain the same initial MO (35 µM) and H_2O_2 (0.05 M) concentrations. In the first round, 76.1 % of 35 µM MO is decolourised in 5 h at initial pH ~ 6.0 and ZnAl-CoW$_{12}$ dose of 0.50 g L^{-1}. In the second round with a fresh load of MO and H_2O_2, to maintain the same initial concentrations, 64.1% of MO is decolourised. In third and fourth cycles, the percentage of MO decolourisation are 62.6 and 61.3, respectively. Significant decrease of decolourisation in second cycle is primarily due to significant decrease of MO intercalation in the interlayer region of ZnAl-CoW$_{12}$. As expected, this decrease is marginal from second to third or subsequent cycles. The above results indicate that the catalytic system (ZnAl-CoW$_{12}$ + H_2O_2) has potential for repetitive use without any noticeable decrease in decolourisation activity for organic dyes like MO. Analyses of reactant solution after each catalytic run by Atomic absorption spectroscopy (AAS) do not show any detectable cobalt content in the solution indicating the CoW$_{12}$ in the interlayer is quite stable and the LDH is proved to be a suitable host for heterogenisation of catalytically active species like CoW$_{12}$. The catalytic activity of ZnAl-CoW$_{12}$ can be further extended for decolourisation of other organic dyes.

Oxidation of benzaldehyde

The catalytic efficiency of ZnAl-CoW$_{12}$ was also assessed for hydrogen peroxide mediated oxidation of benzaldehyde to benzoic acid. The results obtained under varying reaction temperature, amount of catalyst, volume of H_2O_2 and reaction time is presented in Figure 7a-d. At first the reaction was carried out for 1.0 h to optimize the other parameters like reaction temperature, amount of catalyst and H_2O_2. It is evident from Figure 7a that the conversion of benzaldehyde (10.2 mL, 89.7 mM) with a fixed dose of catalyst (0.1 g) and H_2O_2 (20 mL of 30%) increases with increasing temperature, reaches to a maximum value at ~ 80-90°C and then decreases marginally on further increase of temperature. On variation of H_2O_2 (10-40 mL), keeping the other parameters constant, the activity (Figure 7b) is found increase up to 20 mL and there after practically remains constant on further increase of H_2O_2. The results of variation of amount of ZnAl-CoW$_{12}$ in the range (0.05 to 0.2 g) again shows (Figure 7c) an increasing trend up to 0.1 g catalyst dose but decreases at higher dose of catalyst presumably due to partial decomposition of H_2O_2 by catalyst causing a decrease in its concentration. Keeping the reaction temperature, catalyst dose and H_2O_2 volume fixed at 90 ºC, 0.1 g and 20 mL, respectively, the reaction time was optimized. The variation of reaction time in between 1-6 h shows that the conversion of benzaldehyde increases with increase of time, reaches to a maximum value in ~ 4 h. Further increase in time course of reaction does not lead to any increase in conversion of benzaldehyde. Under these optimize set of conditions (benzaldehyde, 10.2 mL; H_2O_2, 20 mL; ZnAl-CoW$_{12}$, 0.10 g; Reaction temperature, 90 ºC and reaction time, 4 h), the conversion of benzaldehyde is found to be ~ 86.6 %.
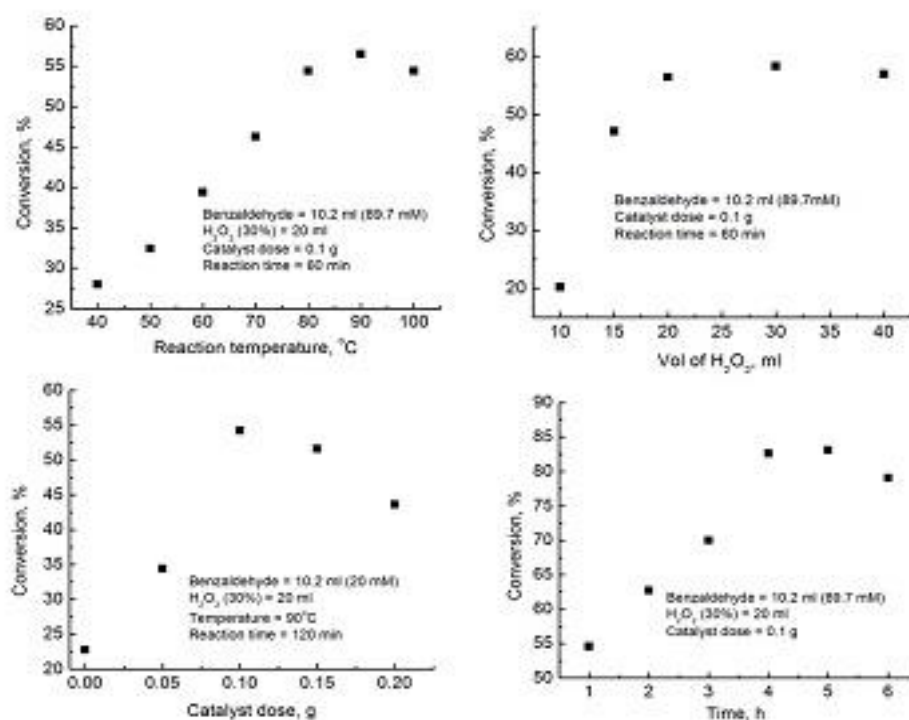
Figure 7. Effect of (a) reaction temperature (40–100 ºC) and (b) H_2O_2 amount (10–40 ml) on the oxidation of benzaldehyde. Effect of (c) catalyst amount (0.05–0.2 g) and (d) reaction time (1–6 h) on the oxidation of benzaldehyde.

This values is lower than that reported (98.8%) for the same reaction using MgAl-CoW$_{12}$ as the catalyst primarily due to intercalation of relatively higher amount of CoW$_{12}$ in the interlayer of MgAl-LDH (68.7 wt. %) as against 56.2 wt. % in the present case.[14] It is worth noting that the conversion of benzaldehyde under identical conditions with either ZnAl-CO$_3$ (0.1 g) or equivalent amount (0.58 g) of neat CoW$_{12}$ in presence of H_2O_2 (20 mL 30 %) is only 27 % and 48 %, respectively. Similarly, the conversion of benzaldehyde (10.2 mL) by H_2O_2 (20 mL) and without ZnAl-CoW$_{12}$ is only 30.5 %. While with ZnAl-CoW$_{12}$ (0.10 g) alone without H_2O_2, the conversion of benzaldehyde is less than 5 %. The above observation shows that there is a significant improvement in the catalytic activity of CoW$_{12}$ when intercalated in the interlayer of ZnAl-LDH. Moreover, the loss of CoW$_{12}$ after the reaction can be avoided.
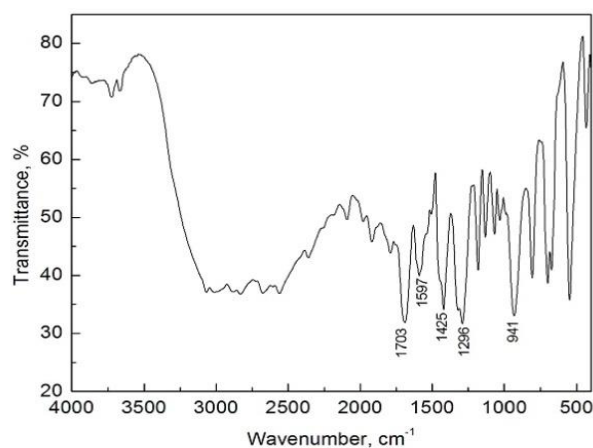
Figure 8. FT-IR spectra of oxidation product of benzaldehyde.

The formation of benzoic acid as the oxidation product of benzaldehyde is evident from melting point measurement (122–124 °C) and FT-IR spectra (Figure 8). The bands at 1703 and 1296 cm^{-1} are attributed to >C=O and − OH group, respectively. The absorption bands in between 900-1100 cm^{-1} are attributed to the benzene ring or to the carbon-oxygen bond of the acid grouping.

Conclusions

A catalytically active polyoxometallate (Co^{III}W$_{12}$O$_{40}^{5-}$) was successfully intercalated in the interlayer of ZnAl-LDH through rehydration of its calcined product at ambient temperature under N$_2$ atmosphere. Physicochemical characterization by various methods indicated the intercalation of Co^{III}W$_{12}$O$_{40}^{5-}$ in the interlayer region of LDH. The intercalated material was found active for oxidative decolourisation of methyl orange as well as conversion of benzaldehyde to benzoic acid in presence of H_2O_2.

References

[1]Mizuno, N., Yamaguchi, K. Kamata, K., *Coord. Chem. Rev.*, **2012**, *249*, 1944. https://doi.org/10.1016/j.ccr.2004.11.019

[2]Okuhara, T., Mizuno, N., Misono, M., *Appl. Catal. A*, **2001**, *222*, 63. https://doi.org/10.1016/S0926-860X(01)00830-4

[3]Ingle, R. H., Kala Raj, N. K., Manikandan, P., *J. Mol. Catal. A*, **2007**, *262*, 52. https://doi.org/10.1016/j.molcata.2006.08.050

[4]Zhou, Y., Chen, G., Long, Z., Wang, J., *RSC Adv.*, **2014**, *4 (79)*, 42092-42113.

[5]Heravi, M. M., Bakhtiari, K., Javadi, N. M., Bamoharram, F. F., Sedai, M., Oskooie, H. A., *J. Mol. Catal. A*, **2007**, *264*, 50 and references therein. https://doi.org/10.1016/j.molcata.2006.09.004

[6]da Silva Rocha, K. A., Kozhevnikov, I. V., Gusevskaya, E. V., *Appl. Catal. A*, **2007**, *294***,** 106. https://doi.org/10.1016/j.apcata.2005.07.031

[7]Jin, H., Wu, Q., Zhang, P., Pang, W., *Solid State Ionics*, **2005**, *7*, 333.

[8]Nowi´nska, K., Fórmaniak, R., Kaleta, W., Wacław, A., *Appl. Catal. A*, **2003**, *256*, 115. https://doi.org/10.1016/S0926-860X(03)00393-4

[9]Manyar, H. G., Chaure, G. S. & Kumar, A., *J. Mol. Catal. A*, **2006**, *243***,** 244. https://doi.org/10.1016/j.molcata.2005.09.036

[10]Thanasilp, S., Schwank, J. W., Meeyoo, V., Pengpanich, S., Hunsom, M., *J. Mol. Catal. A*, **2013**, *380*, 49-56. https://doi.org/10.1016/j.molcata.2013.09.023

[11]Palomeque, J., Figueras, F., Gelbard, G., *Appl. Catal. A.*, **2006**, *300*, 100. https://doi.org/10.1016/j.apcata.2005.10.037

[12]Liu, Y., Murata, K., Hanaoka, T., Inaba, M., Sakanishi, K., *J. Catal.*, **2007**, *248*, 277. https://doi.org/10.1016/j.jcat.2007.03.025

[13]Briand, L. E., Baronetti, G. T., Thomasa, H. J., *Appl. Catal. A*, **2003**, *256*, 37-50. https://doi.org/10.1016/S0926-860X(03)00387-9

[14]Wei, X., Fu, Y., Xu, L., Li, F., Bi, B., Liu, X., *J. Solid State Chem.*, **2008**, *181*,1292. https://doi.org/10.1016/j.jssc.2008.02.030

[15]Wu, Q., Sang, X., Shao, F., Pang, W., *Mater. Chem. Phys.*, **2005**, *92*,16. https://doi.org/10.1016/j.matchemphys.2004.07.026

[16]Rives, V., Ulibari, M. A., *Coord. Chem. Rev.*, **1999**, *181*, 61. https://doi.org/10.1016/S0010-8545(98)00216-1

[17]Mizuno, N., Yamaguchi, K., Kamata, K., *Coord. Chem. Rev.*, **2005**, *249*, 1944. https://doi.org/10.1016/j.ccr.2004.11.019

[18]Kwon, T., Pinnavaia, T. J., *J. Mol. Catal. A*, **1992**, *74*, 23. https://doi.org/10.1016/0304-5102(92)80220-B

[19]Omwoma, S., Chen, W., Song, Y.-F., Coord. Chem. Rev., **2014**, *258-259*, 58-71. https://doi.org/10.1016/j.ccr.2013.08.039

[20]Kai Liu, K., Xu, Y., Yao, Z., Miras, Song, Y.-F., *ChemCatChem.*, 2016, *8(5)*, 929-937. https://doi.org/10.1002/cctc.201501365

[21]Watanabe, Y., Yamamoto, K., Tatsumi, T., *J. Mol. Catal. A*, **1999,** *145*, 281. https://doi.org/10.1016/S1381-1169(99)00012-6

[22]Carriazo, D., Martin, C., Rives, V., Eur *J. Inorg. Chem.*, **2006**, 4608. https://doi.org/10.1002/ejic.200600580

[23]Sousa, F. L., Pillnger, M., Ferreira, R. A. S., Granadeiro, C. M., Cavaleiro, A. M. V., Rocha, J., Carlos, L. D., Trindade, T., Nogueira, H. I. S., *Eur. J. Inorg. Chem.*, **2006**, 726. https://doi.org/10.1002/ejic.200500518

[24]Guo, Y. H., Li, D. F., Wu, C. W., Wang, E. B., Zou, Y. C., Ding, H., Feng, S. H., *Micropor. Mesopor. Mater.*, **2002**, *56*, 153. https://doi.org/10.1016/S1387-1811(02)00481-X

[25]Baker, L. C. W., McCutcheon, T. P., *J. Am. Chem. Soc.*, **1956**, *78*, 4503. https://doi.org/10.1021/ja01599a001

[26]Sahu, R., Mohanta, B. S., Das, N. N., *J. Phys. Chem. Solids*, **2013,** *74*, 1263. https://doi.org/10.1016/j.jpcs.2013.04.002

[27]Walmsley, F., *J. Chem. Edu.*, **1992,** *69*, 936. https://doi.org/10.1021/ed069p936

[28]Gould, D. M., Spiro, M., Griffith, W. P., *J. Mol. Catal. A*, **2002**, *186*, 69. https://doi.org/10.1016/S1381-1169(02)00136-X

[29]Uchida, S., Mizuno, N., *J. Am. Chem. Soc.*, **2004**, *126*, 1602. https://doi.org/10.1021/ja038063f

ISOLATION OF ETHYL CINNAMATE AND A SUBSTITUTED FLUORENE FROM *PYCNANTHUS ANGOLENSIS* (WELW.) WARB

Olawale H. Oladimeji [a]* and Ngozi O. Onu[a]

Before now, two compounds namely, 3-ethoxy-3,7-dimethyl-1,6-octadiene (ethyl linalool) and 1,2-benzenedicarboxylic acid diethyl ester (diethyl phthalate) have been isolated from the ethyl acetate fraction of *Pycnanthus angolensis* by column chromatography. In this study, the preparative thin-layer chromatography (p-TLC) of two previously obtained residues was carried out. The chemical and biological properties of the compounds obtained there from were evaluated. This exercise led to two isolates (**NG-1b** and **NG-3b)** whose identities have been revealed to be ethyl cinnamate (cinnamic acid, ethyl ester) and 9-oximino-2,7-diethoxy fluorene (2,7-diethoxy-9H-fluoren-9-one oxime) respectively using the MS and IR spectral techniques. The compounds were surprisingly strongly bacteriostatic against *Escherichia coli* but recorded no activity against *Staphylococcus aureus* and *Candida albicans*.

* Corresponding Authors
   Tel.: +2347038916740, +2348180035112, +2348173486285
   E-Mail: wale430@yahoo.co.uk,
   hakeemoladmeji@uniuyo.edu.ng
[a]   Department of Pharmaceutical & Medicinal Chemistry,
   Faculty of Pharmacy, University of Uyo, Uyo, Nigeria.

Introduction

Pycnanthus angolensis (Welw.) Warb. is synonymous with *P. kombo, Myristica angolensis* (Welw.) and *Myristica kombo* (Baill.) amongst many others. Apart from its diverse uses in traditional medical practice, the plant is also employed in economic ventures such as fuel and paper pulp, candle, plywood, timber, furniture making and construction associated with paneling, siding, roof shingles and framing.[1] In a previous study two compounds namely, 3-ethoxy-3,7-dimethyl-1,6-octadiene (ethyl linalool) and 1,2-benzene-dicarboxylic acid diethyl ester (diethyl phthalate) from ethyl acetate fraction by column chromatography were obtained.[2] Preparative thin-layer chromatographic(p-TLC) study has been carried out on two of obtained residues which showed multi-component TLC profiles with the aim of isolating more compounds from the plant. The antimicrobial potential of obtained compounds was also evaluated.

Experimental

Preparation of plates

Glass plates (20 x 20 cm) were washed in detergent solution, rinsed with water and air-dried. Silica gel (Sigma-Aldrich, USA) was treated with $CaSO_4$ (Bond Chemicals, Nigeria) which served as a binding agent. The slurry obtained there from was vigorously shaken, thereby making it homogenous and free flowing. A thickness of 0.5 mm of the slurry was uniformly applied across the glass plates and allowed to set for 24 h. The coated plates were then activated in a laboratory oven (Gallenkamp, England) at 60 ^{0}C for at least 10 h prior to use.

Isolation

NG-1 (light brown, 78 mg) and **NG**-3 (deep brown, 46 mg) were separately dissolved in a little methanol and applied across the coated silica plates using a micro Pasteur Pipette (Simax, India) 1 cm above the bottom edge of the plates and then allowed to dry. Afterwards, the plates were separately developed in toluene:acetone:water (40:80:4) inside large chromatographic glass tanks (Pyrex, USA). The obtained chromatograms showed appreciably distinct layers which were carefully scrapped, separately filtered with methanol and concentrated in vacuo in a rotary evaporator (R205D, Shensung BS & T, China). The apparently pure sub-fractions were monitored on commercial silica plates in toluene:acetone:water (10:20:1) and acetone:ethyl acetate (35:65) using $FeCl_3/CH_3OH$ and vanillin-H_2SO_4 as spray reagents. Further TLC evaluations indicated a spot in **NG-1b** (yellow oil; R_f (0.48); 37 mg) and **NG-3b** (pale brown compound; R_f (0.31), 18 mg).

Structural elucidation

The mass spectra of the compounds were obtained on Kratos MS 80 (Germany) while the IR analyses were done on Shimadzu FTIR 8400S (Japan). The refractive index was obtained using WAY-15 Abberefractometer (England). The refractometer was initially zeroed and the refractive index measured at the wavelength (λ) of Na-D line (589.3 nm) and 20 ^{0}C.

Antimicrobial screening

The micro-organisms used in this study were limited to three *viz*: one Gram (+), Gram (-) and a fungus. *Staphylococcus aureus* (ATCC 21824), *Escherichia coli* (ATCC 23523) and *Candida albicans* (NCYC 106) were

clinically isolated from specimens of diarrheal stool, abscesses, necrotizing fascitis, urine and wounds obtained from the Medical Laboratory, University of Uyo Health Centre, Uyo. The clinical isolates were collected in sterile bottles, identified and typed by convectional biochemical tests.[3, 4] These clinical microbes were then refrigerated at -5 ^{0}C at the Microbiology and Parasitology Unit, Faculty of Pharmacy prior to use. The media and plates were sterilized in an autoclave at 121°C for 15 min. The hole-in-plate agar diffusion method was used observing standard procedure with Nutrient Agar-CM003, Mueller-Hinton-CM037 (Biotech Limited, Ipswich, England) and Sabouraud Dextrose Agar (Biomark, India) for the bacteria and fungus respectively. The inoculum of each microorganism was introduced into each petri dish (Pyrex, England). Cylindrical plugs were removed from the agar plates by means of a sterile cork borer (Simax, India) to produce wells with a diameter of approximately 5 mm. The wells were equidistant from each other and away from the edge of the plate.[5, 6] Concentrations of 20 mg mL-^{1} of crude extract, 10 mg mL-^{1} of ethyl acetate fraction, 2 mg mL-^{1}of **NG-1b** and **NG-3b** were introduced into the wells. Also, different concentrations of 10 μg mL-^{1} Streptomycin (Orange Drugs, Nigeria), 1 mg mL-^{1} of nystatin (Gemini Drugs, Nigeria) and deionized water was introduced into separate wells as positive and negative controls respectively.[7] The experiments were carried out in triplicates. The plates were labelled on the underside and left at room temperature for 2 h to allow for diffusion. The plates were then incubated at 37± 2 ^{0}C for 24 to 48 h. Zones of inhibition were measured with the aid of a ruler.

Results and Discussion

Spectroscopic data

NG-1b: $C_{11}H_{12}O_2$, yellow oil, R_f = 0.48, $[n]_D^{20}$ = 1.5583. MS [ES$^+$-MS] *m/z* 177 [M+H]$^+$ (100.00 %), 176 [M]$^+$ (0.70 %), 161 [M-CH$_3$]$^+$ (11.29 %), 147 [M-C$_2$H$_5$]$^+$ (83.34 %), 131[M-OC$_2$H$_5$]$^+$(54.40 %), 122[M-C$_2$H$_2$-CO]$^+$ (5.61%), 99 [M-C$_6$H$_5$]$^+$ (75.94 %) and 54 [M-C$_6$H$_5$-OC$_2$H$_5$]$^+$. IR [FTIR] cm^{-1}: 785, 873 (alkyl substitution), 1072 (-C-O-C), 1616 (Ar-C=C), 1637 (exocyclic-C=C) and1712 (-C=O).
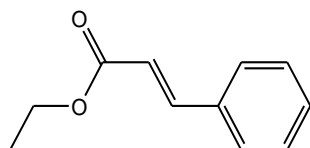

NG-1B

Figure 1. Ethyl cinnamate.

NG-3b:$C_{17}H_{17}NO_3$, pale brown compound, R_f = 0.31. MS [ES$^+$-MS] *m/z* 283[M]$^+$ (1.26 %), 266[M-OH]$^+$ (1.07 %), 254[M-C$_2$H$_5$]$^+$(24.70 %), 238[M-OC$_2$H$_5$]$^+$ (1.53 %), 226 [M-2C$_2$H$_5$+1]$^+$ (32.36 %), 210 [M-OC$_2$H$_5$-C$_2$H$_5$+1]$^+$ (5.23 %), 198 [M-2OC$_2$H$_5$+5]$^+$ (2.36%), 181 [M-C$_6$H$_5$-O-9]$^+$ (7.81 %), 163 [M-2OC$_2$H$_5$-OH-N+1]$^+$ (5.21 %), 149 [M-2OC$_2$H$_5$-OH-N-13]$^+$ (12.46 %), 129 [M-C$_6$H$_5$-OC$_2$H$_5$-OH-N-1]$^+$ (4.15 %), 115[M-C$_6$H$_5$-OC$_2$H$_5$-CH$_3$-OH-N]$^+$ (9. 36 %), 101 [M-C$_6$H$_5$-OC$_2$H$_5$-C$_2$H$_5$-OH-N]$^+$ (8.28 %), 94 [M-C$_6$H$_5$-OC$_2$H$_5$-C$_2$H$_5$-

OH-N-7]$^+$ (21.45 %), 81 [M-2C$_6$H$_5$-OC$_2$H$_5$-13]$^+$ (27.15 %), 58[M-2C$_6$H$_5$-OC$_2$H$_5$-OH-N-5]$^+$ (100 %) and 55 [M-2C$_6$H$_5$-OC$_2$H$_5$-OH-N-8]$^+$ (32.75 %). IR [FTIR] cm^{-1} 756, 758, 856, 859 (alkyl substitution), 1047, 1048 (-C-O-C), 1606, 1609 Ar (-C=C), 2219 (-C=N) and 3471 (-CN-OH).

The determination of a physical constants such as the refractive index is used in the qualitative and quantitative analyses of substances. It is also employed to confirm the purity, identity, the integrity of compounds and as well as monitor the progress of reactions. **NG-1b** was isolated as an oily substance with a fruity fragrance. Consequently, the refractive index of **NG-1b** was determined at the wavelength (λ) of Na-D light (589.3 nm) and at 20 ^{0}C. The refractive index of a substance is an indication of the number, type of atoms and chemical groups (species) in the substance. Each atom or group in the substance contributes to its refractivity which adds eventually to the refractive index of the substance.**NG-1b** recorded a refractive index of 1.5583which is consistent with the literature value of 1.5880. However, the refractive index of **NG-3b** could not be unambiguously determined because of small sample size.
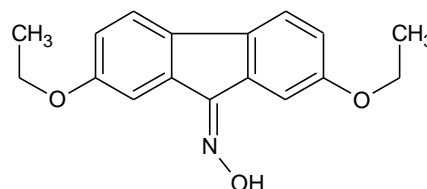
NG-3b

Figure 2. 2,7-Diethoxy-9*H*-fluoren-9-one oxime.

The identities of the compounds were established by a combination of spectroscopic techniques as shown above. The obtained data were compared with those in the library data of organic compounds. Furthermore, these data were found to be consistent with those reported in the literature.[8-11] Consequently, **NG-1b** and**NG-3b** have been revealed to be ethyl cinnamate (cinnamic acid, ethyl ester) and 9-oximino-2, 7-diethoxy fluorene (2, 7-diethoxy-9H-fluoren-9-one oxime) respectively as presented in 1igures1 and 2. Due to the nature of the matrices, many fragmented ions appeared in the mass spectra of the compounds. In the MS of **NG-1b**, those that are easily identifiable include [M]$^+$ at *m/z* 176 (0.70 %) while fragments at 161 (11.29 %) and 147 (83.34 %) represent the removal of methyl and ethyl units respectively from molecular ion. Furthermore, peaks at 131 (54.40 %) and 99 (75.94 %) correspond to the excisions of ethoxy and phenyl groups from **NG-1b** while the peak at 77 (100 %) (base peak) indicates the addition of a proton to the molecule. The FTIR spectrum of **NG-1b** shows diagnostic stretchings at 785, 873, 1072, 1616, 1637 and 1712 cm^{-1} indicating alkyl substitutions, ether linkage, aromatic C=C, exocyclic -C=C and C=O absorptions respectively. The mass spectrum of **NG-3b** shows very elaborate fragmentations in its matrix. The molecular ion can readily be identified at *m/z* 283 (1.26 %) while the ion at 266 (1.07 %) indicates a loss of a hydroxyl group. The fragments at 254 and 226 correspond to the excision of ethyl units from the [M]$^+$. The peaks at 198 (2.36 %), 163 (5.21 %) and 149 (12.46 %) represent the successive losses of two ethoxy and an oximino group respectively from the matrix.

Table 1. Antimicrobial screening of crude extract, ethyl acetate fraction, **NG-1b** and *NG-3b* at different concentrations on test microbes in water.

Test microbe	CE 20 mg mL^{-1}	ET 10 mg mL^{-1}	NG-1b 2 mg mL^{-1}	NG-3b 2 mg mL^{-1}	Deionized water	SP 10 µg mL^{-1}	NY 1 mg mL^{-1}
S. aureus (ATCC 21824)	5	5	5	5	5	24	5
E. coli (ATCC 23523)	5	5.5	13.5	18	5	30	5
C. albicans (NCYC 106)	5	5	5	5	5	5	27

The zone diameter recorded is zone of inhibition + size of cup (zone of inhibition +5)mm, CE = Crude ethanolic extract; ET = Ethyl acetate fraction, SP =Streptomycin, NY =Nystatin, NCYC = National Collection of Yeast Cultures, UK, ATCC = American Type Culture Collection**,** Washington, DC, USA.

Ions at 181 (7.81 %), 101 (8. 28 %) and 94 (21.45 %) shows the removal of phenyl and phenyl, ethoxy, ethyl and oximino moieties respectively from **NG-3b**. The most abundant ion (base peak) at 58 (100 %) and the fragment at 55 (32.75 %) indicate the excision of phenyl, ethoxy and oximino from the matrix.

The IR spectrum of the compound shows absorptions at 756, 758, 856, 859, 1047, 1048, 1606, 1609, 2219 and 3471 cm^{-1} which represent alkyl substitutions, ether linkage, aromatic C=C, -C=N and –OH absorptions, respectively.

It is pertinent to note that the isolation of **NG-1b** could be due to the partial esterification of cinnamic acid in ethanol during extraction. Also, **NG-1b** has been reportedly isolated from the rhizomes of *Kaempfera galanga* (L.).

This compound has been found to inhibit monoamine oxidase and possesses vasorelaxation activity.[8-10] However, a closer examination of the chemical structure of **NG-3b** shows a carbazole-like skeleton which has been found in studies to be important biogenetic precursors in phytochemistry.[12] Furthermore, this compound has been obtained from *Lepidium sativum* using GC-MS, and FTIR spectrometry.[11]

Antimicrobial tests

The spectrum of microbes employed in these tests was narrow, encompassing one each of Gram positive (*S. aureus*) and Gram negative (*E. coli*) bacterial strains and a fungus (*C. albicans*). The results displayed in table 1 show that the crude extract, ethyl acetate fraction, **NG-1b** and **NG-3b** were inactive against S. *aureus* and *C. albicans*. Surprisingly, the two compounds were remarkably bacteriostatic against *E. coli*. However, it is imperative to indicate that **NG-3b** was more suppressive of the bacterium than **NG-1b**. This was unexpected because Gram negative bacteria are well known for their unique resistance to antimicrobial agents. This resistance is believed to be due to the nature of the cell envelope of these organisms which unlike gram positive organisms possess a sophisticated three-layered envelope which does not allow permeation of external agents. Also, both compounds demonstrated no antifungal activity against *C. albicans*. This particular observation was in order because fungal strains especially *Candida* spp. limit the permeation of substances because of their integral structures which are pleomorphic and facultative in nature hence, resembling those of higher plants.[13]

Conclusion

The isolation of these compounds is being reported for the first time from the plant. Hence, NG-1band NG-3bare equally expected to serve as chemotaxonomic markers for this species and the genus, *Pycnanthus* in general. Furthermore, the results of the antimicrobial screening partly lend some justification for the use of this plant especially in the treatment /management of bacterial infections. However, the two compounds will be tested against other bacterial and fungal strains with the aim of obtaining improved activity.

References

[1]Hutchinson, J., Dalziel, J. M., *Flora of West Tropical Africa. Vol. I, Part I,* Crown Agents for Overseas Governments and Administrations, London, **1954.**

[2]Oladimeji, H. O.,Attih, E. E., Onu, N. O., *Eur. Chem. Bull.* **2017,** *6(2),* 76-78. https://doi.org/10.17628/ecb.2017.6.76-78

[3]Gibson, L., Khoury, J., *Lett. Appl. Microbiol.,* **1986,** *3,* 127-129. https://doi.org/10.1111/j.1472-765X.1986.tb01565.x

[4]Murray, P., Baron, E., Pfaller, M., Tenover, F., Yolken, R., *Manual of Clinical Microbiology.* American Society of Microbiology Press, **1995.**

[5]Washington, J., *The Agar Diffusion Method. In: Manual of Clinical Microbiology. 4th ed.,* American Society of Microbiology Press, **1995.**

[6]N.C.C.L.S. *Performance Standard for Antimicrobial Susceptibility Test. 8th edition, Approved Standard,* The Committee, **2003.**

[7]Oladimeji, H. O., Johnson, E. C., *J. Pharm. Biores.,* **2015,** *12(1),* 48-53. https://doi.org/10.4314/jpb.v12i1.7

[8]Noro, T., Miyasa, T., Kuruyagi, M., Ueno, A., Fukushima, S., *Chem. Pharm. Bull.,* **1983,***31(8),* 2708-27011. https://doi.org/10.1248/cpb.31.2708

[9]Wong,K. C., *Flavour & Fragrance J.,* **2006,***7(8),* 253-256.

[10]Othman, R.,*Phytomedicine,* **2006,** *3(1-2),* 61-66. https://doi.org/10.1016/j.phymed.2004.07.004

[11]Hussein, H. M., *Res. J. Pharm.Biol. Chem. Sci.,* **2016,** *7(4),* 2553-2579.

[12]Adebajo, A. C., Aladesanmi, A. J., Reisch, J., *Nat. Prod. Drug Dev.,* Conf. Proc., Ile-Ife,**1998.**

[13]Brown, M. R., *Pharm. J.,* **1975,** *215,* 239-242.

ELEMENTAL SULFUR PRODUCTION IN HYDROMETALLURGY

Fathi Habashi

Elemental sulfur obtained during oxidative leaching of sulfides at low temperature will contain mercury and gold and both can be effectively recovered using sodium sulfide. Other metals go into solution.

* Corresponding Authors:
    E-mail: Fathi.Habashi@arul.ulaval.ca
[a] Department of Mining, Metallurgical, and Materials
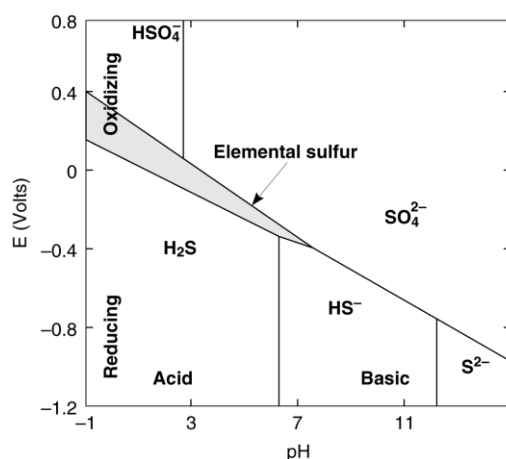   Engineering, Laval University, Quebec City, Canada

INTRODUCTION

When sulfide minerals are treated in acid medium and in oxidizing atmosphere elemental sulfur forms while the metals goes into solution (Figure 1).[1] There is a narrow region where elemental sulfur can form (Figure 2).
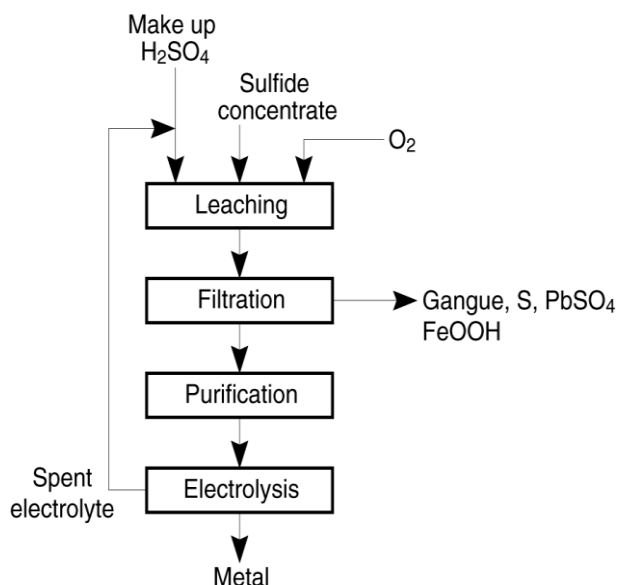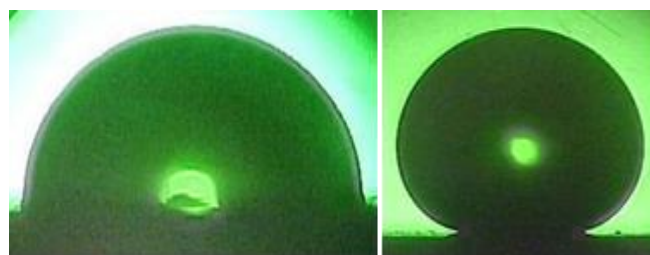

Figure 1. Recovery of metals in sulfide ores below the melting point of sulfur

Figure 2. Formation of elemental sulfur during oxidizing sulfide ores at 100°C


Figure 3. Left: Molten sulfur covers sulfide surface in absence of surface active agent. Right: Molten sulfur does not cover sulfide surface in presence of surface active agent

SPECIAL CASES

Sulfides containing gold

Sulfide ores may contain gold embedded in the sulfide matrix and as a result many gold producers treat such ores at high temperature to liberate gold then treating the residue containing gold by cyanidation to recover gold.[3] It was found that gold will be associated with the sulfur.

This region disappears above 150 °C. Sulfur melts at 119.5 °C and polymerizes at 160 °C. If the treatment is conducted below 150 °C a surface active agent must be present to prevent the molten sulfur from impeding the reaction by forming a protective layer on the sulfide particle (Figure 3).[2]

Jeffrey and Anderson[4] and Anderson and Twidwell[5] found that sulfur formed agglomerates containing all the gold as well as unreacted sulfides. Cyanidation of these agglomerates was not effective in recovering gold but sodium sulfide was. This can be conducted by leaching the agglomerates in sodium hydroxide whereby sodium sulfide was formed:

$$4S^o + 6NaOH \rightarrow 2Na_2S + Na_2S_2O_3 + 3H_2O$$

$$(x-1)S^o + Na_2S \rightarrow Na_2S_X \quad \text{(where x = 2 to 5)}$$
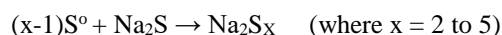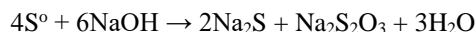
Gold dissolution was the result of leaching by polysulfides and sulfides:

$$2Au + S_2^{2-} + 2S^{2-} \rightarrow 2AuS^- + 2S^{2-}$$
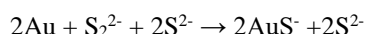
Gold was recovered from solution by including electrowinning, gaseous precipitation, chemical precipitation, cementation, solvent extraction and ion exchange.

Sulfides containing mercury

Jorjani and Ghahreman[6] reported that if mercury is present in the ores the elemental sulfur will contain the mercury and this can be leached by sodium sulfide to free it from mercury by forming insoluble mercury sulfide while elemental sulfur forms soluble polysulfide:

$$Na_2S + (x-1)S^\circ \rightarrow Na_2S_x$$

$$Hg^{2+} + S^{2-} \rightarrow HgS$$
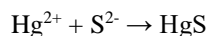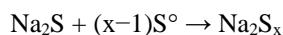
In conclusion, it is obvious therefore that elemental sulfur obtained during oxidative leaching of sulfides will contain mercury and gold and both can be effectively recovered using sodium sulfide.

CONCLUSION

While metals in sulfide ores go in solution as elemental sulfur forms, gold and mercury are embedded in the sulfur and can be recovered by leaching with sodium sulfide provided a surface active agent is present.

REFERENCES

[1]Habashi, F., *A Textbook of Hydrometallurgy*, Métallurgie Extractive Québec, Québec City, Canada **1993**, second edition **1999**. Distributed by Laval University Bookstore, www.zone.ul.ca

[2]Tong L. and Dreisinger, D. "Interfacial Properties of Liquid Sulfur in the Pressure Leaching of Nickel Concentrate". *Miner. Engg., 2009,* 22, 456–461, https://doi.org/10.1016/j.mineng.2008.12.003

[3]Habashi, F. *Gold. History, Metallurgy, Culture*, Métallurgie Extractive Québec, Québec City, Canada **2009**. Distributed by Laval University Bookstore, www.zone.ul.ca

[4]Jeffrey, M. and Anderson, C. G. "A Fundamental Study of the Alkaline Sulfide Leaching of Gold", *European Journal of Mineral Processing and Environmental Protection,* October **2002**

[5]Anderson, C. G. and Twidwell, L. G. "The Alkaline Sulfide Hydrometallurgical Separation, Recovery and Fixation of Tin, Arsenic, Antimony, Mercury, and Gold", pp. 121-131 in *Lead and Zinc 2008,* Southern African Institute of Mining and Metallurgy

[6]Jorjani, E. and Ghahreman, A. "Elemental Sulfur Removal during the Leaching of Copper and Zinc Sulfides, and from the Residues; A Review", *Hydrometallurgy* **2017**, *171*, 333-343 https://doi.org/10.1016/j.hydromet.2017.06.011